

**CHEMICAL FLUSHING FOR NONAQUEOUS PHASE LIQUID
SOLUBILIZATION AND RECOVERY FROM POROUS MEDIA**

by

GÖKÇE AKGÖZE AYDIN

B.S. in Chemical Engineering, Istanbul Technical University, 1998

M.Sc. in Environmental Technology, Boğaziçi University, 2001

**Submitted to the Institute of Environmental Sciences in partial fulfillment of
the requirements for the degree of**

Doctor

of

Philosophy

in

Environmental Technology

Boğaziçi University

2008

**CHEMICAL FLUSHING FOR NAPL SOLUBILIZATION AND
RECOVERY FROM POROUS MEDIA**

APPROVED BY:

Prof. Dr. Günay Kocasoy
(Thesis Supervisor)

Assoc. Prof. Dr. Nadim Copty
(Thesis Supervisor)

Prof. Dr. Orhan Yenigün

Prof. Dr. Ayşen Erdinçler

Assist. Prof. Dr. İrfan Yolcubal

DATE OF APPROVAL: 12/06/2008

ACKNOWLEDGEMENTS

I wish to express my gratitude to my advisors, Dr. Nadim Copty and Prof. Dr Günay Kocasoy, for their guidance, persistence and inspiration throughout the years. I am especially thankful for Dr. Copty's advice and support in making this dissertation possible. He openly shared his knowledge with me and inspired me to work in this research area.

I would also like to acknowledge my Committee Members for sharing their comments with me at different stages of this research.

Obvious thanks go to Berken Ağaoğlu for his help during the experimental stages of the research. I would also like to thank Nihat Akyol for his guidance and assistance in setting up the column for flushing experiments. His contribution, together with Assist. Prof. Dr. İrfan Yolcubal's comments, was a milestone in my research.

Assistance from Marmara University-Chemical Engineering Department was essential in GC analysis. In particular, I wish to extend profound gratitude to Göksun Dizbay and Süleyman Arsu for their indispensable advices with GC applications.

I extend my sincere appreciation to Boğaziçi University - BAP and TÜBİTAK for providing the financial support in this research.

I especially would like to thank to my family who instilled in me a sense of motivation and encouragement and provided their complete support for my thesis. I am also thankful to my son Efe and my husband Ersin for their patience. Through several times of self-evaluation and self-redirection, they have always been very supportive.

Finally, I wish to acknowledge a great many friends and colleagues who made my study enjoyable

ABSTRACT

Contamination of the subsurface by organic compounds in the form of non-aqueous phase liquids (NAPL) is a major threat to groundwater resources. Many of these compounds are characterized by low water solubility and are highly persistent in the subsurface environment. This means that once the NAPL is inadvertently released into the subsurface, it can act as a secondary source of contamination for many decades to come. Furthermore, although the solubility of most of these compounds is low, the aqueous concentrations encountered in the field are sufficiently high to cause significant adverse effects on human health and the environment. The significance of this problem is exasperated by the wide use of NAPLs in the industry and the fact that many of these compounds are classified as known human carcinogens. Therefore, any cleanup effort must not only attempt to clean the dissolved aqueous plume, but should also focus on the recovery of the released NAPL mass.

The remediation of groundwater resources contaminated by NAPL poses a formidable environmental challenge. Currently, there is no known technology that can fully recover the NAPL mass once released into the subsurface. Over the past two decades numerous innovative technologies for the remediation of groundwater with NAPL contamination were developed. One of the most promising is the use of chemical agents, such as cosolvents and surfactants, for the enhanced solubilization, mobilization and removal of NAPL mass.

Nonetheless, despite their potential, these technologies have been shown to be insufficient in many field applications in reaching the desired target efficiencies. This is primarily attributed to the complexity of the subsurface system and that the performance of chemical agents can be affected by the interactions between the subsurface properties and chemical agent formulations.

The two NAPLs considered in this study are toluene and 1,2-dichlorobenzene. These two compounds are two of the most prevalent contaminants in the subsurface due to their established toxicity and their widespread use. Toluene is a major constituent of petroleum

products such as gasoline, while 1,2-dichlorobenzene is widely used as a degreasing agent for metals, leather and wool.

Prior to the application of any in-situ flushing scheme, it is important to understand the phase behaviour of the system, in particular the tendency of the NAPL for enhanced solubilization (increase solubility of the organic phase in the aqueous phase) or partitioning (increase solubility of the aqueous phase in the organic phase). For this purpose a bench scale titration method was used to identify phase compositional changes in the presence of a variety of chemical agents such as alcohols, surfactants and modified sugars. The results of the phase behavior as a function of solution content were presented in the form of ternary phase diagrams which are composed of miscibility curves and tie-lines and are unique in that they show all three components of a reaction system on one plot. The main benefit of the titration based phase change observations was to prepare a quick procedure which enabled rapid evaluation of the effectiveness of different agents for the solubilization and mobilization of NAPLs. Results indicated that the alcohols, in particular ethanol, were effective in solubilizing model NAPLs. However, the effectiveness of alcohols was enhanced when used together with surfactants, provided that the surfactants can be added to the system efficiently.

A computer code was also developed to determine the ternary phase behaviour of the water-NAPL-agent system numerically. The code provides a rapid and inexpensive means for the evaluation of different flushing solutions and how the ternary system would behave at different mole fractions. The program solves a system of nonlinear algebraic equations which represent multiphase equilibrium. Because of the nonlinearity of the system, an iterative solution scheme is used to compute the mole fractions at equilibrium, the tie lines and plait point.

Within the scope of this study, flushing experiments were also conducted in a one-dimensional column packed with sand. The target NAPL was toluene, while the solubilizing agent was ethanol. Ethanol content and the flow rate of the flushing solution were evaluated in terms of toluene recovery from the sandpack. The experiments were also conducted at different temperatures to evaluate the overall system efficiency when thermal enhancements were applied in combination with the ethanol flushing solution. The results

of the column experiments showed that although solubilization was enhanced when the chemical agent content in the flushing solution is increased, equally significant improvements can be achieved with relatively small increases in system temperature. Improved performance was also observed with variable flow regimes that can increase the contact time between the NAPL and the flushing solution.

In summary, this study shows that in-situ flushing is a viable remedial scheme for groundwater contaminated with organic compounds in the form of NAPLs. Yet, significant challenges remain for the successful transfer of this technology to the field. Moreover, it is important to recall that while extraction of the NAPL from the porous medium is the primary focus of this study, in real applications such a scheme would produce large volumes of waste water. Efforts must also focus on methods for the separation and recycling of the NAPL and agent volumes.

ÖZET

Yeraltı sularının NAPL formundaki bileşenlerle kirlenmesi bu değerli kaynakları tehdit etmektedir. Söz konusu bileşenlerin en önemli özelliklerinden biri suda çözünürlüklerinin çok düşük olmasıdır. NAPL bileşenlerinin yanlışlıkla yeraltına sistemine sızması, çözülmüş bileşenlerin yarattığı uzun süreler boyunca etkili olacak ikincil bir kirlilik kaynağı oluşturmaktadır. Bu bileşenlerin suda çözünürlükleri çok düşük olmasına rağmen bu çözünürlük değerleri insan ve çevre sağlığı açısından tehdit oluşturabilecek seviyelerde bulunmaktadır. Kanserojen etkileri bilinmekte olan bu NAPL bileşenlerini içeren kimyasalların endüstride yoğun olarak kullanımı bu tehdidi arttırmaktadır. Bu nedenle kirliliğin giderilmesinde tercih edilen metodun sadece çözülmüş bileşenlerin değil kirliliği yaratan NAPL kaynağının da kontrolü ve uzaklaştırılmasını sağlayabilmesi gerekmektedir.

NAPL bileşenleriyle kirlenmiş olan yeraltı kaynaklarının temizlenmesi zorlu bir çevresel çalışmayı gerektirmektedir. Güncel teknolojilerden hiçbirinin kirlilik kaynağı oluşturan NAPL bileşenlerinin ortamdaki giderimini sağlayamadığı bilinmektedir. Son yirmi yıldır yeraltında NAPL kirliliğinin giderimini sağlamaya yönelik birçok yeni teknoloji geliştirilmiştir. Bu teknolojiler içinde en umut verici olanı kimyasalların çözücü etkisinden yararlanan sistemlerdir. Çözücü ve yüzey aktif maddeleri içeren çözeltilerin kullanıldığı bu sistemlerde etkisi artırılmış çözünürlük, mobilizasyon ve NAPL kaynağının uzaklaştırılması sağlanabilmektedir.

Tüm olumlu etkilerine rağmen, bu teknolojilerin birçok saha çalışmasında hedeflenen verimlere ulaşamadığı görülmüştür. Yeraltı sistemlerinin karmaşık bir yapıya sahip olması ve kimyasalların yüzey özellikleri ile etkileşimleri uygulama verimini düşürmektedir.

Bu çalışmada toluen ve 1,2-diklorobenzen model kirletici olarak kullanılmışlardır. Bu iki bileşenin deneysel çalışmalarla toksisite kanıtlanmıştır ve endüstriyel çalışmalarda sıklıkla kullanılmaktadırlar. Toluen petrol ürünlerinde yüksek miktarlarda bulunan bir bileşendir. 1,2-Diklorobenzen ise metal, deri ve tekstil endüstrilerinde yaygın olarak kullanılmakta olan bir yağ giderme kimyasalıdır.

Kaynakta kirletici bileşenlerin sıvılarla sürüklenmesini hedefleyen her çalışmanın öncesinde sistemin faz davranımını ve özellikle NAPL bileşenlerinin geliştirilmiş çözünme (organik fazın su fazında çözünürlüğünün artması) ve organik faza katılma (su fazını oluşturan bileşenlerin organik fazda çözünürlüğünün artması) yönelimlerinin belirlenmesi gerekmektedir. Çalışmada kirlilik gideriminde etkili olduğu bilinmekte olan kimyasalların (alkol, yüzey aktif madde, modifiye şekerler) varlığında karşılaşılabilecek faz kompozisyonlarındaki değişimlerin belirlenmesi için küçük ölçekte bir titrasyon metodu kullanılmıştır. Faz davranımı deneylerinin sonucunda fazların içeriği üçlü faz diyagramları kullanılarak oluşturulmuştur. Üçlü faz diyagramları çözünürlük eğrisi ve bağlantı çizgilerinden oluşmaktadır ve bu diyagramların en önemli özelliği reaksiyona giren üç bileşenin kompozisyonunu tek veya iki faz oluşturacak şekilde birarada ifade edebilmeleridir. Titrasyon işlemiyle faz değişiminin belirlenmesinin en önemli yararı ise farklı çözücülerin NAPL bileşenlerinin çözünme ve mobilizasyonu üzerindeki etkisinin hızlı bir prosedür dahilinde belirlenebilmesidir. Titrasyon deneylerinde elde edilen sonuçlar özellikle etanol olmak üzere alkollerin model NAPL bileşenlerinin çözünürlüğünü arttırmada etkili olduğunu göstermektedir. Alkollerin çözünürlüğü arttırmada gösterdiği iyileştirme yüzey aktif maddelerle beraber kullanımında daha da artmakta ancak yüzey aktif maddelerin sisteme eklenmesi noktasında yaşanan sorunların azaltılmasına yönelik çalışmaların yapılması gerekmektedir.

Simulasyon yöntemiyle su-NAPL-çözücü içeren üçlü faz diyagramlarının oluşturulmasına yönelik bir bilgisayar program hazırlanmıştır. Bu program ile farklı sürüklenme solüsyonlarının performansının hızlı ve maliyeti düşük bir şekilde değerlendirilebilirliği hedeflenmiş ve simulasyonlarda üçlü bileşenli sistemlerin farklı başlangıç madde içeriklerinde faz davranımları incelenmiştir. Program çok fazlı denge içeren nonlinear cebirsel denklemler sisteminin çözümünü sağlamaktadır. Denklem sisteminin nonlinear olmasından dolayı dengede madde miktarları, bağlantı çizgileri ve tepe kesişim noktası iterasyon kullanılarak düzenlenmiştir.

Bu çalışma kapsamında toprak doldurulmuş cam kolonlarda sürüklenme deneyleri gerçekleştirilmiştir. Bu deneylerde kullanılan model kirletici toluen iken çözücü olarak etanol kullanılmıştır. Toprak kolondan toluene giderimi sürüklenme çözeltisinin içeriği akış hızı değiştirilerek incelenmiştir. Sürüklenme deneyleri ayrıca farklı sıcaklıklarda

tekrarlanmış ve çözücü ile sürüklenme işlemlerinde ısıl iyileştirmelerin sistem verimi üzerine etkisi tartışılmıştır. Kolon deneylerinden elde edilen sonuçlar, sürüklenme çözeltisinde çözücü miktarının artmasıyla çözünürlüğün arttığını göstermiştir. Sistem sıcaklığında nispeten az bir artışın da aynı ölçüde çözünürlüğü arttırdığı görülmüştür. NAPL bileşenleri ile sürüklenme çözeltisi arasındaki temas süresini arttıracak farklı çözelti besleme metodlarının da çözünürlük üzerine olumlu etkisi gözlemlenmiştir.

Sonuç olarak, bu çalışma kirlilik kaynağı oluşturan bileşenlerin kimyasal maddelerle sürüklenmesi işlemlerinin, NAPL formunda organik bileşenlerle kirlenmiş yeraltı sularına uygulanabilir bertaraf alternatiflerinden olduğunu göstermektedir. Bu teknolojinin sahada başarılı bir şekilde kullanılabilmesi için önemli aşamalardan geçmesi gerekmektedir. Bu çalışmanın öncelikli hedefi yeraltından NAPL bileşenlerinin ekstraksiyonu idi. Ancak sahada gerçek uygulamalarda bu işlem sonucunda yüksek hacimlerde atıksu oluşacaktır ve bu atıksu içinden NAPL bileşenlerinin ve çözücü maddelerin ayrıştırılması ve geri kazanımı başka çalışmalarda incelenmelidir.

TABLE OF CONTENTS

	page
ACKNOWLEDGEMENTS	iii
ABSTRACT	iv
ÖZET	vii
TABLE OF CONTENTS	x
LIST OF FIGURES	xv
LIST OF TABLES	xxii
LIST OF SYMBOLS	xxiii
LIST OF ABBREVIATIONS	xxv
1. INTRODUCTION	1
1.1. Problem Statement and Significance	1
1.2. Research Objectives	5
1.3. Thesis Organization	6
2. BACKGROUND AND LITERATURE REVIEW	7
2.1. Organic Contaminants and Non-aqueous Phase Liquid (NAPL) Problem	7
2.1.1. Dense Nonaqueous Phase Liquids (DNAPLs)	8
2.1.2. Light Nonaqueous Phase Liquids (LNAPLs)	10
2.2. Subsurface Characteristics	14
2.3. Mechanisms of Contaminant Fate and Transport in the Subsurface	19
2.4. Pollution Control Techniques	23
2.4.1. Pump-and-treat	25
2.4.2. Chemical Agent Flushing	26

	page
2.4.3. In-situ Chemical Treatment	29
2.4.4. Soil Vapor Extraction	30
2.4.5. Thermal Remediation	31
2.4.6. Permable Reactive Barriers	33
2.4.7. Natural Attenuation and Enhanced Bioremediation	34
2.5. Chemical Agents Used in Enhanced Flushing	35
2.5.1. Alcohols	35
2.5.2. Surfactants	37
2.5.3. Cyclodextrins	42
2.5.4. Humic Substances	44
2.5.5. Polymers	45
2.6. Legal Aspects of NAPL Management in the Subsurface	46
3. TERNARY PHASE DIAGRAMS	48
3.1. Phase Behaviour and Equilibrium	48
3.2. Theory of Ternary Phase Diagrams	49
3.3. Numerical Methods for the Construction of TPDs	51
3.3.1. UNIFAC Model and Activity Coefficients	53
3.3.2. Simulation of Activity Data	56
3.3.3. FORTRAN Programme for Phase Equilibrium Calculations	58
3.3.4. Analysis of the Fortran Derived Data	62
3.4. Experimental Methods for the Construction of TPD's	62
3.4.1. Chemicals	62
3.4.2. Analysis Procedures for the Determination of TPDs	64
3.4.2.1. Cloud point titration	64

	page
3.4.2.2. Gas chromatography analysis	66
3.4.2.3. Determination of the water content	67
3.4.2.4. Determination of the anionic surfactants	68
3.4.2.5. Determination of the HPCD	69
3.4.3. Determination of Other Critical Physical Parameters	70
3.4.3.1. Interfacial tension (IFT)	70
3.4.3.2. Density	72
3.4.3.3. Viscosity	72
3.5. Results and Discussion	73
3.5.1. Titration Results for 1,2-Dichlorobenzene Containing Samples	73
3.5.2. Titration Results for Toluene Containing Samples	79
3.5.3. Density Profiles of Toluene-Ethanol-Water Mixtures	80
3.5.4. Interfacial Tension Profiles of Toluene-Ethanol-Water Mixtures	83
3.5.5. Numerical Ternary Phase Diagram for Toluene-Ethanol-Water System	85
3.6. Conclusions	87
4. ENHANCED CHEMICAL AGENT FLUSHING	89
4.1. Theory and Background Information	89
4.2. Operational Parameters for the Extraction Process	91
4.3. Experimental Set-up	93
4.3.1. Model Aquifer Construction	93
4.3.2. Saturation of the Column	94
4.3.3. Tracer Controls	94

	page
4.3.4. Determination of the Hydraulic Conductivity	96
4.3.5. Contamination of the Sandpack	97
4.3.6. Chemicals Used	97
4.3.7. Sampling	97
4.3.8. Analysis Procedures	98
4.4. Results and Discussion	98
4.4.1. Dissolution Performance of Ethanol Solutions at Low Flow Rate (20 ⁰ C)	99
4.4.1.1. Dissolution performance of 20% ethanol solution at low flow rate (20 ⁰ C)	99
4.4.1.2. Dissolution performance of 40% ethanol solution at low flow rate (20 ⁰ C)	101
4.4.1.3. Dissolution performance of 60% ethanol solution at low flow rate (20 ⁰ C)	103
4.4.1.4. Dissolution performance of 100% ethanol solution at low flow rate (20 ⁰ C)	105
4.4.2. Dissolution Performance of Ethanol Solutions at High Flow Rate	108
4.4.2.1. Dissolution performance of 60% ethanol solution at high flow rate (20 ⁰ C)	108
4.4.2.2. Dissolution performance of 100% ethanol solution at high flow rate (20 ⁰ C)	109
4.4.3. Dissolution Performance of Ethanol Solutions with Intermittent Flow Rate (20 ⁰ C)	112
4.5. Conclusions	114

	page
5. EFFECT OF TEMPERATURE ON THE PERFORMANCE OF CHEMICAL AGENT FLUSHING	122
5.1. Theory	122
5.2. Useful Concepts in Thermal Treatment	125
5.2.1. Boiling Point	125
5.2.2. Henry's Law Constant	127
5.2.3. Octanol-Water Partition (K_{ow}) Coefficient	127
5.3. Remediation at Elevated Temperatures	128
5.4. Experimental Set-up	129
5.5. Results and Discussion	131
5.5.1. Dissolution Performance of 20% Ethanol Solution at 40 ⁰ C (Low Flow Rate)	131
5.5.2. Dissolution Performance of 40% Ethanol Solution at 40 ⁰ C (Low Flow Rate)	132
5.5.3. Dissolution Performance of 60% Ethanol Solution at 40 ⁰ C (Low Flow Rate)	134
5.5.4. Dissolution Performance of 60% Ethanol Solution at 10 ⁰ C (Low Flow Rate)	135
5.6. Conclusions	137
6. FINAL CONCLUSIONS AND RECOMMENDATIONS FOR FUTURE RESEARCHES	140
REFERENCES	144
APPENDIX A - FORTRAN CODE USED FOR THE TERNARY PHASE DATA	164
APPENDIX B - SILTAS SAND 60/70 USED IN THE COLUMN EXPERIMENTS	169

LIST OF FIGURES

	page
Figure 2.1. Simplified conceptual model of a DNAPL release and migration	10
Figure 2.2. Simplified conceptual model of a LNAPL release and migration	13
Figure 2.3. The main concepts and the status of the technologies in remediation activities	26
Figure 2.4. Phase diagram for oil-water-surfactant systems	39
Figure 2.5. Microemulsion systems with respect to the salinity or temperature changes	40
Figure 2.6. Chemical structure of the three main types of cyclodextrins	43
Figure 3.1. Ternary phase diagram	49
Figure 3.2. The UNIFACAL interface	57
Figure 3.3. A sample definition of components in UNIFACAL Software	57
Figure 3.4. A sample input file	58
Figure 3.5. A sample guess file	59
Figure 3.6. Fortran code used in simulations	61
Figure 3.7. A sample output file	62
Figure 3.8. Molecular structure of 1,2-dichlorobenzene	63
Figure 3.9. Molecular structure of toluene	63
Figure 3.10. Molecular structure of Oil-Red-O	64
Figure 3.11. The titration set-up used for the determination of miscibility points	64
Figure 3.12. Gastight macrosyringes	65
Figure 3.13. The basic steps of constructing ternary phase diagrams	65

	page
Figure 3.14. Karl Fisher Titrator	67
Figure 3.15. Molecular structure of SLS	68
Figure 3.16. Molecular structure of Hyamine	68
Figure 3.17. KSV 703 Digital Tensiometer	71
Figure 3.18. The steps of the measurement of interfacial tension with DuNouy Ring	71
Figure 3.19. Miscibility curves for (a) 1,2-dichlorobenzene-ethanol-water system and (b) 1,2-dichlorobenzene- methanol-water system at 20 ⁰ C	74
Figure 3.20. Miscibility curve for 1,2-dichlorobenzene-SLS-water system showing the formation of (a) foam and (b) paste-like mixture at 20 ⁰ C	75
Figure 3.21. Miscibility curve for the 1,2-dichlorobenzene-(ethanol:Tween 80=1)-water system at 20 ⁰ C	76
Figure 3.22. Miscibility curve for (a) 1,2-dichlorobenzene-Triton X 100-water system and (b) 1,2-dichlorobenzene-(ethanol:Triton X 100=1)-water system at 20 ⁰ C	77
Figure 3.23. Miscibility curve for (a) 1,2-dichlorobenzene-HPCD-water system, (b) 1,2-dichlorobenzene-ethanol-(water/HPCD:4) system at 20 ⁰ C	78
Figure 3.24. Miscibility curve for toluene-ethanol-water system at 20 ⁰ C	79
Figure 3.25. Miscibility curve for toluene-Triton X100-water system at 20 ⁰ C	80
Figure 3.26. The density profiles of the aqueous and the NAPL phases in toluene(50%)-water(50%) with varying ethanol additions at 20 ⁰ C	81
Figure 3.27. The measured densities with respect to the mass ratios of the prepared solutions at 20 ⁰ C	82

	page
Figure 3.28. The phase separations of toluene(9)-water(1) with varying ethanol additions at 20 ⁰ C	83
Figure 3.29. The phase separations of toluene(7)-water(3) with varying ethanol additions at 20 ⁰ C	83
Figure 3.30. The interfacial tension profiles of the aqueous and the NAPL phases in toluene(1)-water(1) with varying ethanol additions at 20 ⁰ C	84
Figure 3.31. The measured interfacial tensions (dyne/cm) with respect to the mass ratios of the prepared solutions at 20 ⁰ C	84
Figure 3.32. Numerical ternary phase diagram of toluene-ethanol-water system	86
Figure 4.1. The breakthrough curve of the non-reactive tracer (chloride)	96
Figure 4.2. The formation of channels during flushing with 20% ethanol solution at low flow rate (20 ⁰ C)	100
Figure 4.3. The cumulative toluene removal with 20% ethanol flushing at low flow rate (20 ⁰ C)	100
Figure 4.4. The effluent toluene concentration profiles with 20% ethanol flushing at low flow rate (20 ⁰ C)	100
Figure 4.5. The samples collected during flushing with 40% ethanol solution at low flow rate (20 ⁰ C)	101
Figure 4.6. The cumulative toluene removal with 40% ethanol flushing at low flow rate (20 ⁰ C)	102
Figure 4.7. The effluent toluene concentration profiles with 40% ethanol flushing at low flow rate (20 ⁰ C)	102
Figure 4.8. The movement of the dyed toluene during flushing with 40% ethanol solution at low flow rate (20 ⁰ C)	103

	page
Figure 4.9. The samples collected during flushing with 60% ethanol solution at low flow rate (20 ⁰ C)	104
Figure 4.10. The cumulative toluene removal with 60% ethanol flushing at low flow rate (20 ⁰ C)	104
Figure 4.11. The effluent toluene concentration profiles with 60% ethanol flushing at low flow rate (20 ⁰ C)	104
Figure 4.12. The movement of dyed toluene in the column during flushing with 60% ethanol solution at low flow rate (20 ⁰ C)	105
Figure 4.13. The samples collected during flushing with pure ethanol solution at low flow rate (20 ⁰ C)	106
Figure 4.14. The movement of the dyed toluene during flushing with pure ethanol solution at low flow rate (20 ⁰ C)	106
Figure 4.15. The cumulative toluene removal with 100% ethanol flushing at low flow rate (20 ⁰ C)	107
Figure 4.16. The effluent toluene concentration profiles with 100% ethanol flushing at low flow rate (20 ⁰ C)	107
Figure 4.17. The samples collected during flushing with 60% ethanol solution at high flow rate (20 ⁰ C)	108
Figure 4.18. The cumulative toluene removal with 60% ethanol flushing at high flow rate (20 ⁰ C)	108
Figure 4.19. The effluent toluene concentration profiles with 60% ethanol flushing at high flow rate (20 ⁰ C)	109
Figure 4.20. The samples collected during flushing with pure ethanol solution at high flow rate (20 ⁰ C)	110
Figure 4.21. The accumulation of the free phase toluene at the top of the soil column and in the effluent collection vial	110

	page
Figure 4.22. The cumulative toluene removal with 100% ethanol flushing at high flow rate (20 ⁰ C)	111
Figure 4.23. The effluent toluene concentration profiles with 100% ethanol flushing at high flow rate (20 ⁰ C)	111
Figure 4.24. The movement of the toluene bank during flushing with pure ethanol	112
Figure 4.25. The samples collected during flushing with 40% ethanol solution at intermittent flow rate (20 ⁰ C)	112
Figure 4.26. The cumulative toluene removal with 40% ethanol flushing at intermittent flow rate (20 ⁰ C)	113
Figure 4.27. The effluent toluene concentration profiles with 40% ethanol solution at intermittent flow rate (20 ⁰ C)	114
Figure 4.28. Comparison of the cumulative toluene removal performances of different ethanol solutions at low flow rate (20 ⁰ C)	115
Figure 4.29. Comparison of the effluent toluene concentrations of different ethanol solutions at low flow rate (20 ⁰ C)	116
Figure 4.30. Comparison of the cumulative toluene removal performances of different ethanol solutions at different flow rates (20 ⁰ C)	117
Figure 4.31. Comparison of the effluent toluene concentrations of different ethanol solutions at different flow rates (20 ⁰ C)	118
Figure 4.32. Comparison of the cumulative toluene removal performances of 40% ethanol solutions at different flow rates (20 ⁰ C)	118
Figure 4.33. Comparison of the effluent toluene concentrations of 40% ethanol solutions at different flow rates (20 ⁰ C)	119
Figure 4.34. Comparison of the final toluene removal performances of different ethanol solutions at different flow rates (20 ⁰ C)	119

	page
Figure 4.35. Comparison of the final toluene removal performances of different ethanol solutions at high and low flow rates (20 ⁰ C)	120
Figure 4.36. Comparison of the final toluene removal performances of 40% ethanol solution at low and intermittent flow rates (20 ⁰ C)	121
Figure 5.1. The insulated column (heated)	130
Figure 5.2. The insulated column (cooled)	130
Figure 5.3. The samples collected during flushing with 20% ethanol solution at 40 ⁰ C (low flow rate)	131
Figure 5.4. The cumulative toluene removal with 20% ethanol flushing at 40 ⁰ C (low flow rate)	132
Figure 5.5. The effluent toluene concentration profiles with 20% ethanol flushing at 40 ⁰ C (low flow rate)	132
Figure 5.6. The samples collected during flushing with 40% ethanol solution at 40 ⁰ C (low flow rate)	133
Figure 5.7. The phases of toluene removal with 40% ethanol solution at 40 ⁰ C (low flow rate)	133
Figure 5.8. The cumulative toluene removal with 40% ethanol flushing at 40 ⁰ C (low flow rate)	133
Figure 5.9. The effluent toluene concentration profiles with 40% ethanol flushing at 40 ⁰ C (low flow rate)	134
Figure 5.10. The cumulative toluene removal with 60% ethanol flushing at 40 ⁰ C (low flow rate)	134
Figure 5.11. The effluent toluene concentration profiles with 60% ethanol flushing at 40 ⁰ C (low flow rate)	135
Figure 5.12. The samples collected during flushing with 60% ethanol solution at 40 ⁰ C (low flow rate)	135

	page
Figure 5.13. The cumulative toluene removal with 60% ethanol flushing at 10 ⁰ C (low flow rate)	136
Figure 5.14. The effluent toluene concentration profiles with 60% ethanol flushing at 10 ⁰ C (low flow rate)	136
Figure 5.15. The samples collected during flushing with 60% ethanol solution at 10 ⁰ C (low flow rate)	137
Figure 5.16. Comparison of the cumulative toluene removal performances of different ethanol solutions at different temperatures (low flow rate)	138
Figure 5.17. Comparison of the effluent toluene concentration profiles with different ethanol solutions at different temperatures (low flow rate)	138
Figure 5.18. Comparison of the final toluene removal performances with different ethanol solutions and different temperatures (low flow rate)	139

LIST OF TABLES

	page
Table 2.1. The most common DNAPL types, their uses and sources	9
Table 2.2. The properties of the most common DNAPLs	11
Table 2.3. The properties of the most common LNAPLs	12
Table 2.4. Transport mechanisms in the subsurface	15
Table 2.5. List of equations for micro and macroscale systems and for single and multiphase composition	24
Table 2.6. The properties of the most common alcohols	36
Table 2.7. Properties of some common commercial surfactants	41
Table 2.8. Selected physical properties of cyclodextrin derivatives	42
Table 3.1. Main Groups for UNIFAC calculations	55
Table 3.2. Subgroups for UNIFAC calculations	56
Table 3.3. Fluid properties at room temperature	63
Table 3.4. Density measurements for different initial ratios of toluene and water with varying ethanol contents	82
Table 3.5. Interfacial tension measurements for different initial ratios of toluene and water with varying ethanol contents	85
Table 4.1. 60/70 AFS sand properties	93
Table 4.2. Parameters of the tracer control experiments	95
Table 5.1. The eutectic boiling points of some NAPL mixtures	126

LIST OF SYMBOLS

A	Cross sectional area of the sediment sample	m^2
C	Solute concentration	m/L
D_L	Longitudinal hydrodynamic dispersion coefficient	m^2/d
f_{oc}	Fraction of organic carbon	-
h	Height	m
H_c	Henry's law constant	$L.atm/mole$
k_{ij}	Permeability tensor	m^2
k_r^α	Relative permeability of the phase α	-
k_{eff}	Effective permeability	m^2
K_d	Distribution coefficient	-
K_{oc}	Organic carbon partition coefficient	L/kg
K_{ij}	Hydraulic conductivity tensor	m/h
K_{ow}	Octanol-water partition coefficient	-
L	Length	m
P	Pressure	atm
$P_c(S_w)$	Capillary pressure vs. saturation	-
R	Retardation factor	-
R_k	Surface area of group k in UNIFAC calculations	-
Q_k	Volume for group k in UNIFAC calculations	-
q_i	Flow rate through porous media in direction i	m/h
ρ_b	Dry bulk density of the medium	g/cm^3
S	Solubility	g/L
t	Time	h
V	Volume	m^3
v_{ave}	Average linear groundwater velocity	m/d
v_c	Contaminant velocity	m/d
x_a	Mole fraction of chemical a in solution	-
μ	Chemical potential of a phase	-
γ	Activity coefficient	-
Ψ	Pressure head	m

z	Elevation head	m
θ	Molecular surface area	-
ϕ	Medium porosity	-
η_T	Viscosity at temperature T	cp

LIST OF ABBREVIATIONS

BTEX	Benzene-toluene-ethylbenzene-xylene
CMC	Critical micelle concentration
cp	Centipoise
cSt	Centistokes
DMD	Density modified displacement
DNAPL	Dense nonaqueous phase liquid
GC	Gas chromatograph
HPCD	Hydroxypropyl- β -cyclodextrin
IFT	Interfacial tension
KF	Karl Fisher
LNAPL	Light nonaqueous phase liquid
MS	Mass spectroscopy
MW	Molecular weight
NAPL	Nonaqueous phase liquid
NRTL	Nonrandom two-liquid
PCE	Perchloroethylene
PT	Pump and treat
SDS	Sodium dodecyl sulfate
SG	Specific gravity
STANMOD	Studio of analytical models
SVE	Soil vapour extraction
SVOC	Soil vapour organic carbon
TCE	Trichloroethylene
TNS	Potassium 2-p-toluidynaphthalene-6-sulfonate
TPD	Ternary phase diagram
UNIFAC	Uniquac Functional Group Activity Coefficient
UNIQUAC	Universal quasichemical

1. INTRODUCTION

1.1. Problem Statement and Significance

Water resources are under major stress around the world. Rivers, lakes and aquifers supply fresh water for irrigation, drinking and sanitation, while the oceans provide habitat for many species that have vital roles in the food supply chain (UNEP, 2006). The unabated and rapid expansion of urbanization and industrial activities pose significant threat to the quality of groundwater and soils through leakage, spills and disposal of chemicals such as fuels and chlorinated solvents.

National governments are exerting significant efforts for the development of adequate strategies to provide safe drinking water for their inhabitants. Despite these efforts, safe water, free of pathogens and other contaminants, is unavailable to much of the population in many developing countries. Water contamination is also a major concern for developed countries with good water supplies and advanced treatment systems (Minogue, 2008).

The contamination of groundwater resources by organic compounds is one of the most widespread and challenging environmental problems. Because of their physical and chemical properties, these contaminants are often found in the subsurface in the form of non-aqueous phase liquids (NAPL) which can partially dissolve into water at very slow rates. Organic liquids that are heavier than water are referred to as dense, non-aqueous phase liquids (DNAPLs). Because they are denser than water, DNAPLs have the potential to migrate to greater depths below the water table. Organic liquids that are lighter than water are referred to as light, non-aqueous phase liquids (LNAPLs).

When introduced at or near ground level, gravity causes the NAPLs to move downward through the vadose zone leaving behind residual NAPL trapped in the pore spaces. The trapped NAPL mass is referred to as ganglia or blobs. Provided that the spill mass is sufficiently large, LNAPLs continue to migrate downwards until they reach the water table. At the water table, LNAPLs tend to spread horizontally because of their relatively low densities. On the other hand, DNAPLs continue to travel downwards until

they reach some low permeability layer such as a clay layer. The low permeability layer acts as a barrier to further downward migration, causing the DNAPL to accumulate in the form of pools.

As groundwater flows through the porous medium it gets in contact with pooled or residual NAPL, promoting dissolution of the NAPL and the development of dissolved contaminant plumes. Because of the low solubility of many organic compounds and their persistence in the subsurface, the trapped NAPL can act as secondary sources of contamination, gradually dissolving into the groundwater for many decades. Residual saturation and trapping above and below the water table by capillary forces make NAPLs extremely difficult to control in the subsurface (Palomino and Grubb, 2004). The most challenging NAPL contamination problems are those involving mixtures of organic solvents and fuels, and occurring in complex highly heterogeneous geological systems which complicate the spread of the NAPL and any subsequent remedial effort.

The common presence of these compounds was discovered by accidents during the 1970's as a result of an interest in the trihalomethane compounds that can be formed when drinking water is chlorinated (Bedient et al., 1999). By the end of the 1980's dissolved NAPLs in groundwater became widely recognized. Many remediation efforts failed because of the misunderstandings in defining the persistent NAPL sources present in the field (Pankow and Cherry, 1996). Once released into the subsurface environment, these compounds can render large portions of groundwater resources unusable because of their drastic negative impact on human health and the environment.

The fate and transport of these organic contaminants in the subsurface are controlled by the physical and chemical properties such as solubility, viscosity, density and interfacial tension. The physical behaviour of multiple fluid phases is even more complex, arising from the interaction and interdependence of the interfacial chemistry governing the system with porous medium heterogeneity at both the pore and field scales (Bedient et al., 1999).

Many of the compounds that form NAPLs are of concern to human health and the environment. Some of these compounds such as benzene and vinyl chloride are known human carcinogens (Pankow and Cherry, 1996; Golfinopoulos, 2001). Others such as

trichloroethylene and tetrachloroethylene are possible or probable carcinogens. Even though all of these compounds have low aqueous solubilities, their solubilities are significantly higher than the maximum allowable limits. Many of these compounds are very persistent in the subsurface. Therefore, to limit the further spread of these contaminants in the soil and groundwater, it is essential that the NAPL source be identified and removed from the subsurface. For this purpose, efficient enhanced recovery techniques are required to control the movement of this source.

It is now widely recognized that conventional pump-and-treat approaches, in which groundwater is extracted from the subsurface and treated above ground to remove dissolved phase contaminants, may be effective in limiting the spread of dissolved plumes, but are ineffective for recovering appreciable fractions of contaminant mass from NAPL source zones (Mackay and Cherry, 1989). Over the past two decades numerous emerging technologies were developed and tested for the remediation of NAPL sources. These innovative strategies for source zone treatment include in-situ chemical oxidation, thermal treatment and cosolvent and/or surfactant flushing. All of these treatment strategies have advantages and disadvantages but can be used coordinately to maximize the benefits.

In-situ flushing, the focus of this thesis, is a process where chemical agents are used to overcome the limitations associated with pump-and-treat remediation of nonaqueous phase liquid (NAPL) source zones (Palmer and Fish, 1992). The technique aims for an accelerated recovery of the contaminants from the subsurface through enhanced solubilization and/or mobilization of the NAPL. Further treatment of the effluent would be needed after recovery, but as the uncertainties and unknown interaction parameters of the subsurface no longer exist, remediation alternatives can be applied more efficiently. Implementation of flushing based removal methods necessitates a step-wise sequential approach involving the initial assessment of applicability, laboratory studies, numerical simulations, pilot scale field evaluations and finally full-scale implementation.

Chemical agent flushing refers to the cycling of an injected chemical solution through zones of the subsurface contaminated by NAPL (National Research Council, 2004). The chemical solution is introduced to the system with wells or drainlines and upon contact with the NAPL, the total aqueous solubility of the contaminants increase, thereby

accelerating the rate of dissolution into groundwater. Physical mobilization of the NAPL can also be experienced with the flushing solution composition. Regardless of whether the primary removal mechanism is solubilization, mobilization, or a combination of the two, fluids must be recovered from the subsurface and either treated on site or shipped off site for disposal. Methods of on-site final treatment have included biological treatment, steam stripping, incineration and air stripping (Shah et al., 1995).

Predicting the possible removal pathways of the soil contaminants, experimentally and numerically derived data are important steps for the success of any remediation work in the field. Bench scale and column experiments are preferred in the initial screening as the set-up is relatively simple and easy to control. The bench scale experiment procedure utilized in this research is based on the preparation of ternary phase diagrams which can significantly aid in the selection of the appropriate flushing solution composition and system parameters. These diagrams are constructed and the interrelated parameters (density, viscosity solubility and interfacial tension) are evaluated together in order to predict the performance of different remediation alternatives. Phase diagrams are used for the formulation of different chemical agents in order to identify the most practical extraction zones for subsurface contaminants and can be drawn with either experimental data or numerical data. After the initial screening based on ternary phase diagrams, column experiments provide an important intermediate step for the identification of the governing mechanisms prior to any field scale application.

Another promising alternative for NAPL zone remediation is the use of thermal treatment. This technology involves the injection of steam, hot air, or hot water to render the contaminant more mobile, followed by groundwater and soil vapor extraction. Although these technologies are currently being tested for NAPL zone remediation, the application of in-situ flushing with thermal enhancements has not been systematically tested. Therefore, as part of this thesis, the effect of heat on the performance of flushing trials was examined.

1.2. Research Objectives

This thesis will first evaluate the use of experimentally and numerically derived ternary phase diagrams for the rapid screening of different chemical agents for NAPL remediation. The NAPLS considered for this task are toluene and 1,2-dichlorobenzene, two of the most widely encountered NAPLs in the environment. The former is an LNAPL, while the latter is a DNAPL. This is followed by bench scale flushing experiments that examine the effect of different parameters, namely: flushing solution composition, groundwater velocity, and thermal enhancements on NAPL mobility and removal. The target NAPL for this part of the work is toluene. The specific objectives of the study are:

1. screening diverse chemical agents for their use in the construction of the ternary phase diagrams
2. preparing a bench scale experimental procedure for serial evaluation of the efficiency of the flushing solution compositions
3. developing a computer code for the generation of ternary phase compositions numerically based on fundamental multiphase equilibrium and thermodynamics principles
4. performing flushing experiments for different chemical agent compositions and at different groundwater velocities
5. examining the effect of thermal enhancements on the performance of flushing experiments
6. evaluating the overall parameters influencing in-situ flushing of NAPLs.

Overall, the findings in this study will provide an important contribution towards the understanding of the behaviour of some NAPLs in the subsurface and the key parameters that should be taken into consideration during remediation-based pollution management activities.

1.3. Thesis Organization

The rest of this thesis is organized as follows. The second chapter of this study reviews the main concepts that influence subsurface clean-up activities. This chapter also includes a literature review of field and laboratory scale studies related to NAPL zone remediation using the in-situ flushing technology. In the third chapter, the concept of ternary phase diagrams is explained along with a literature review of their application to NAPL remediation. This chapter also includes a description of the experimental procedures and numerical codes developed in this study for the determination of ternary phase diagrams, and the results obtained for toluene and 1,2-dichlorobenzene in conjunction with various chemical agents. Chapter 4 presents the results of the one-dimensional flushing experiments performed to evaluate the parameters influencing toluene recovery from sand using ethanol. In Chapter 5, the one-dimensional flushing experiments are extended to assess the effect of heat enhancement on NAPL recovery. Chapter 6 ties together the presented research and elaborates on potential future research areas in the field of enhanced chemical flushing of NAPLs in porous media.

2. BACKGROUND AND LITERATURE REVIEW

2.1. Organic Contaminants and Non-aqueous Phase Liquid (NAPL) Problem

Soil and groundwater pollution by organic contaminants pose a persistent environmental problem that can affect large portions of groundwater resources for many years to come. Subsurface contaminants are grouped into various classes such as synthetic organic compounds, naturally occurring organic compounds, metals, cations, anions, microorganisms and radionuclides (Lowe et al., 1999). Synthetic organic compounds encountered at contaminated sites are typically sparingly soluble in water and thus, they exist in the subsurface as a separate liquid phase, often referred to as a **non-aqueous phase liquid (NAPL)**. The term “NAPL” was coined in 1981 during studies of a hazardous waste site in Niagara Falls, New York. At the S-Area Landfill site an extraordinary organic liquid was discovered and researchers realized that this liquid was immiscible with water. The term was selected to differentiate the liquid from other contaminated materials (Pankow and Cherry, 1996). NAPLs are contaminants that remain undiluted as the original bulk liquid in the subsurface. They do not mix with water but form a separate phase. The most well-known examples of NAPLs are chlorinated compounds and petroleum hydrocarbons (RTDF, 2005).

Organic liquids that are heavier than water are referred to as dense, non-aqueous phase liquids (DNAPLs). Because they are denser than water, DNAPLs have the potential to migrate to greater depths below the water table. Organic liquids that are lighter than water are referred to as light, non-aqueous phase liquids (LNAPLs).

NAPLs represent a long-term source of subsurface contamination and as a result attention has been directed to the utilization of aggressive remediation technologies such as cosolvent flushing, surfactant flushing, thermal enhancements, etc. These technologies were originally developed in the petroleum industry to facilitate improved hydrocarbon recovery and became popular in aquifer remediation (Pope and Wade, 1995; Pennell et al., 1993).

The first research efforts directed to defining the character of the NAPLs are attributable to Friedrich Schuille. In his work conducted in the late 1960's to early 1970's, Schuille developed conceptual models and conducted preliminary physical model studies on the behaviour of NAPLs. The basis of his research was to clarify the mechanisms controlling the movement of DNAPLs in model subsurface systems and he examined how and when chlorinated solvents, in particular, penetrate into the unsaturated and saturated sands and into the fractured media. Schuille also conducted a research about the behaviour of LNAPLs in the subsurface (Schuille, 1988).

NAPLs result from a variety of sources. The common usage of the solvents ranging from dry cleaning to metal degreasing, has resulted in their widespread release into the environment, through both accidental spills and improper disposal. The two main sources of NAPLs are fuels and chlorinated solvents. Fuels include gasoline, diesel and heating oil and other refined petroleum products and are complex mixtures of aliphatic and cyclic hydrocarbons, polycyclic aromatic hydrocarbons and metals such as vanadium. Crude oil, the raw material for the fuels, can also be classified as LNAPL. Chlorinated solvents, on the other hand, include solvents that are used in dry cleaning, processing of textiles and industrial metal cleaning (Bedient et al., 1999).

Much of the NAPLs enter the groundwater through accidental releases (pipeline bursts, leaks from underground storage tanks, sewer line leaks), landfills, surface waste ponds and injection wells. Improper disposal in the past also resulted in large amounts of NAPLs entering groundwater aquifers (Newell et al., 1995).

2.1.1. Dense Non-aqueous Phase Liquids (DNAPLs)

Chlorinated solvent usage peaked during World War II and with the economic developments there occurred a decline due to increased awareness of environmental and health hazards associated with them (Pankow and Cherry, 1996). DNAPLs represent significant environmental and public health problems when they exist in natural systems. As they should be avoided from natural systems, their primary routes of entry to the subsurface should be well identified. Both physical and chemical characteristics of these compounds must be known to predict their migration pathways and later in any

remediation effort. The most common DNAPL types, their uses and sources are given in Table 2.1.

Table 2.1. The most common DNAPL types, their uses and sources
(Cohen and Mercer,1993).

DNAPL types	Uses and Sources
Halogenated solvents	Chemical manufacturing Solvent manufacturing and reprocessing Degreasing operations Commercial dry cleaning operations Electronic equipment manufacturing Machine shops and metal works Military equipment manufacturing Textile processing, dyeing and finishing Dry plasma etching of semiconductor chips Pharmaceutical manufacturing Insecticide and herbicide production
Coal tar and creosote	Wood treating plants Coal tar distillation plants Steel industry coking operations Manufactured gas plant
PCBs	Transformer/capacitor oil production, reprocessing and disposal facilities
Mixed DNAPLs	Waste handling, reprocessing and disposal sites Chemical industry facilities

DNAPL movement through the subsurface is primarily governed by gravity and capillary forces which have opposing effects most of the times. DNAPLs are denser than water and thus will tend to mobilize downwards as opposed to spreading on the water table like hydrocarbons. As a result, a DNAPL released to the subsurface has the capacity to sink below the water table where it can provide a long-term source of contamination. On the other hand, capillary forces (P_c) depend on the interfacial tension at the interface

between the DNAPL and the water or air and vary with changes in the radius of curvature of the interface caused by variations in the soil pore size. Geological heterogeneities also have significant impact on the migration pathways taken by the DNAPLs (Dekker and Abriola, 2000; Ataie-Ashtiani et al., 2001; Fu and Imhoff, 2002). The conceptual model of a DNAPL release and migration is given in Figure 2.1.

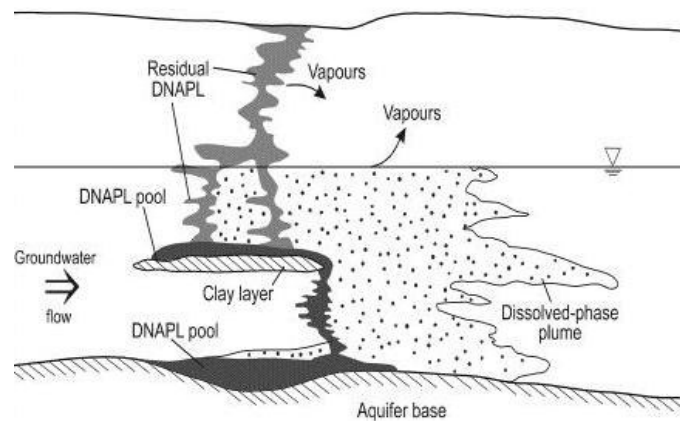


Figure 2.1. Simplified conceptual model of a DNAPL release and migration (Schmoll et al., 2006).

The properties of the most common DNAPLs are given in Table 2.2.

2.1.2. Light Non-aqueous Phase Liquids (LNAPLs)

Organic liquids that are lighter than water are referred to as light non-aqueous phase liquids (LNAPL). LNAPLs represent some of the most ubiquitous environmental contaminants, with oil-based products such as petroleum, diesel and kerosene being the most widespread LNAPLs in the environment (GeoDelft, 2003). The misuse, spillage and uncontrolled disposal of these contaminants such as petroleum fuels, solvents, coal tars and other mobile hydrocarbons poses serious groundwater, land and public health problems (Cassidy, 2007). As many LNAPLs are both sparingly soluble and highly mobile, assessing their time-varying concentrations and subsurface distribution can be extremely difficult. The most common LNAPLs and their properties are given in Table 2.3.

Table 2.2. The properties of the most common DNAPLs (Cohen and Mercer,1993).

Chemical	CAS Number	Empirical Formula	Molecular Weight (g)	Specific Density (g/mL)	Absolute Viscosity (cp)	Aqueous Solubility (mg/L)	Interfacial Tension (dyne/cm)	Surface Tension (dyne/cm)	Boiling Point (°C)	Melting Point (°C)
Trichloroethylene	79-01-6	C ₂ HCl ₃	131.39	1.464	0.57	1100	34.5	29.3	87	-73
Methylene Chloride	75-09-2	CH ₂ Cl ₂	84.93	1.327	0.43	20000	28.3	27.9	40	-95
Tetrachloroethene	127-18-4	C ₂ Cl ₄	165.83	1.623	0.89	150	44.4	31.3	121	-19
1,1,1,- Trichloroethane	71-55-6	C ₂ H ₃ Cl ₃	133.4	1.339	1.2	1360	45	25.4	74	-30
Chloroform	67-66-3	CHCl ₃	119.38	1.483	0.58	8000	32.8	27.2	62	-63
1,1-Dichloroethane	75-34-3	C ₂ H ₄ Cl ₂	98.96	1.176	0.44	5500	n/a	24.8	56	-97
1,2-Dichloroethene	156-60-5	C ₂ H ₂ Cl ₂	96.94	1.257	0.4	600	30	25	47	-50
1,1-Dichloroethene	75-35-4	C ₂ H ₂ Cl ₂	96.94	1.218	0.36	400	37	24	37	-122
1,2-Dichloroethane	107-062	C ₂ H ₄ Cl ₂	98.96	1.235	0.8	8690	30	32.2	83	-35
Chlorobenzene	1408-90-7	C ₆ H ₅ Cl	112.56	1.106	0.8	500	37.4	33.2	132	-46
1,2-Dichlorobenzene	95-50-1	C ₆ H ₄ Cl ₂	147	1.305	1.32	100	40	37	180	-17
Carbon Tetrachloride	56-23-5	CCl ₄	153.82	1.594	0.97	800	45	27	77	-23

Table 2.3. The properties of the most common LNAPLs.

Chemical	CAS No	Density (g/cm ³)	Absolute Viscosity (cp)	Molecular Weight (g/mole)	Aqueous Solubility (mg/L)	Vapor Pressure (mm Hg)	Henry's Law Constant (atm.m ³ /mol) ^a	Boiling Point (°C)	Interfacial Tension (dynes/cm at 20°C)	Surface Tension (dynes/cm at 20°C)
Methyl Ethyl Ketone	78-93-3	0.805	0.40	72.1	268000	71.2	2.74 E-05	79.6	24.6 ^a	25
4-Methyl-2-Pentanone	108-10-1	0.8017	0.5848	100.16 ^c	19000	16	1.55 E-04	116	10.1 ^d	23.6 ^c
Benzene	71-43-2	0.8765	0.6468	78.1 ^c	1780	76	5.43 E-03	80.1 ^d	35	28.9
Ethyl Benzene	100-41-4	0.867	0.678	106.2	152	7	7.9 E-03	136	35.38 ^e	30 ^f
Styrene	100-42-5	0.9060	0.751	104.15	300	5	2.28 E-03	145	n/a	34 ^f
Toluene	108-88-3	0.8669	0.58	92.14	515	22	6.61 E-03	110.6	36.1	28.4
Xylene	1330-20-7	0.8642	0.608	106.16	200	9	6.91 E-03	138.5	38.2	29 ^g

* The measurements are reported for 20°C unless other temperature is used.

^a EPA (1995)

^b http://www.chemiway.co.jp/en/data/03_m19.html

^c <http://ntp.niehs.nih.gov/>

^d Montgomery (1995)

^e http://esc.syrres.com/ABC/HSDB_pp.htm

^f www.petrochemistry.net/

^g <http://www.shellchemicals.com>

n/a: not available

Although LNAPL presence below the water table is not common, the seasonal water table fluctuations cause LNAPLs to be carried into the saturated zone. Seasonal water table rises lead to detection of LNAPLs below the water table (Helmig, 2003).

When LNAPLs are released into the subsurface, they tend to migrate downwards towards the water table or low-permeability zones. Simplified conceptual model of a LNAPL release and migration is given in Figure 2.2. Previous studies have shown that LNAPLs are distributed vertically in the vicinity of the fluctuating water table and become entrapped as a distinct phase both above and slightly below the water table. The different mechanisms of entrapment include infiltration of the LNAPLs (Schroth et al., 1995; Kechavarzi et al., 2000), fingering (Illangasekare et al., 1995a), entrapment of LNAPL in homogeneous media (Reddi et al., 1998), LNAPL entrapment in layered media (Illangasekare et al., 1995b) and entrapment in heterogeneous formations (Van Dijke and Van Der Zee, 1997).

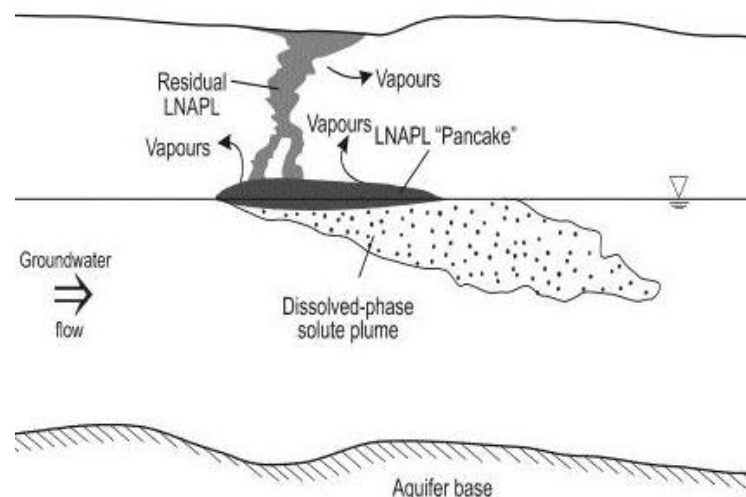


Figure 2.2. Simplified conceptual model of a LNAPL release and migration (Schmoll et al., 2006).

The transfer of mass from the LNAPL phase to the water phase is dependent upon the composition of the LNAPL and the chemical and physical character of the aqueous phase. The velocity of the groundwater and how the LNAPL is distributed vertically within the aquifer can significantly influence the mass transfer to the aqueous phase.

Most of the LNAPLs are biodegradable. This can be explained with the fact that LNAPL components have been present around the earth as natural substances for millions of years and bacteria have developed the necessary pathways to break them down to utilize as an energy source. At many sites, biodegradation is an active process and dissolved plumes become stable in time (Vayenas et al., 2002).

The degree of LNAPL saturation in the subsurface depends on the history, lithology, capillary parameters and fluid properties of the site and the volume of LNAPL released. LNAPLs occupy the pores and saturation decreases with depth until water fills all the pores. LNAPL recovery predictions are based on assumptions such as homogeneity and vertical equilibrium.

2.2. Subsurface Characteristics

Groundwater is an important resource and is relied upon by many communities throughout the world as a source of water. Upon contact with the groundwater, even a small amount of organic contamination source can pollute the whole groundwater reserve and this contamination can last for decades to centuries because of the resistant nature of these contaminants and their spreading ability in the subsurface. The complexity of interactions between the governing variables in the subsurface, together with the effects of scale, has led to observations of local entrapped NAPL saturations ranging from 1% up to 50% (Schwille, 1988; Lenhard et al., 1993).

It is important to clearly understand the mechanisms responsible for the fate and transport of organic contaminants in order to identify the various physical and technical barriers limiting contaminated soil treatment. Contaminants may move underground by one or a combination of several mechanisms, depending on their properties (National Research Council, 1999). The transport mechanisms of concern are summarized in Table 2.4.

The migration of contaminants in the subsurface is governed by properties of the present components, the resident fluid which would be soil gas and water in the vadose

zone and water only in the saturated zone and the solid medium. The resultant governing properties are density, viscosity, wettability, interfacial tension, capillary pressure, residual saturation, relative permeability and vapor pressure (Pankow and Cherry, 1996).

Table 2.4. Transport mechanisms in the subsurface (National Research Council, 1997).

Transport mechanism	Specifications
Vapor-phase transport	Vapors of volatile contaminants spread through the pores in the soil above the water table and dissolution takes place when contact with water is achieved.
Aqueous-phase transport	Contaminants dissolve in the flowing groundwater. The rate of dissolution depends on contaminant solubility and the extent of contact between the contaminant and water.
Non-aqueous-phase liquid (NAPL) transport	Contaminants enter the subsurface in the form of an immiscible liquid and low separately from groundwater.
Facilitated transport	Contaminants sorb to mobile colloidal particles or become a part of complexes of natural organic matter. When associated with colloidal particles and organic complexes, the contaminants can travel with the groundwater.

The difficulties encountered in cleanup efforts are directly related to physical heterogeneities, presence of non-aqueous-phase liquids, migration of contaminants to inaccessible regions and misunderstandings in characterizing the subsurface. The subsurface environment is composed of layers of materials with vastly different properties, such as sand and gravel over bedrock. The composition may vary over distances as small as a few centimeters (Freeze and Cherry, 1979). Fluids can move only through the pore spaces between the grains of sand and gravel or through fractures in solid rock (Theodoropoulos et al., 2001). The openings are often distributed non-uniformly and as a result, underground contaminant migration pathways are often extremely difficult to

predict. While moving through the subsurface, a portion of the liquid becomes trapped small immobile globules, which cannot be removed by pumping but can dissolve in and contaminate the passing groundwater through the zone of interest. Contaminants, on the other hand, may migrate to regions inaccessible to the flowing groundwater by molecular diffusion. These regions may either be microscopic (e.g., small pores within aggregated materials) or macroscopic (e.g., clay layers) (Fawcett et al., 2001). Within these regions, the contaminants can serve as long-term source of pollution as they slowly diffuse back into the cleaner groundwater (Bedient et al., 1999).

The pore structure of soils, sediment and rock is a central influence on groundwater movement. Porosity, permeability and hydraulic head are the main parameters that hydrologists focus on to quantify this influence (Delleur, 1998).

The hydraulic conductivity of the sediment is calculated using Equation 2.1 for constant head as follows (Helmig, 2003):

$$K = \frac{V.L}{A.t.h} \quad (2.1)$$

where:

K = hydraulic conductivity of the sediment sample [L]/[T]

V = volume of flow from the outflow tube [L]³

L = sample length [L]

A = cross sectional area of sample [L]²

t = time [T]

h = height of funnel overflow above outflow port [L]

When the pore space of the medium is occupied by two or more fluids, the permeability of the medium for one of the fluids is reduced due to the reduced number of pores and pore throats available for flow. The reduction in permeability can be defined as relative permeability (k_r).

$$k_r = \frac{k_{eff}}{k} \quad (2.2)$$

where k_r is the relative permeability of the fluid of interest and k_{eff} is the effective permeability of the fluid of interest. For multiphase systems, relative permeability curves are required to calculate the fluid flux.

The viscosity of the water changes with temperature. As temperature increases viscosity decreases and the permeability increases. The coefficient of permeability is standardized at 20°C and the permeability at any temperature T is related to K_{20} by the following ratio:

$$K_{20} = K_T \cdot \frac{\eta_T}{\eta_{20}} \quad (2.3)$$

where η_T and η_{20} are the viscosities at the measurement temperature and at 20°C, respectively.

The competition of the various fluids in the pore voids leads to the diminished mobility for each fluid. Relative permeability is the dimensionless ratio used for the quantification of the hindered mobility. The relations involving relative permeability appear in the definition of Darcy's law describing multiphase fluid flow and are generally represented as a function of saturation. The laboratory analysis of this parameter is also very difficult, as it is for $P_c(S_w)$. Several theoretical and empirical models are available in the literature that can be utilized to estimate these functions from $P_c(S_w)$ data (Cohen and Mercer, 1993).

In single-phase systems, Darcy's Law can be used to calculate the fluid flux. The flow rate through porous media is proportional to the head loss and inversely proportional to the length of the flow path (Bedient et al., 1999), as follows:

$$q_i = -\frac{k_{ij}}{\mu} \left[\frac{\partial P}{\partial x_j} + \rho g \frac{\partial z}{\partial x_i} \right] \quad i, j = x, y, z \quad (2.4)$$

where q_i is the flux in the i direction, k_{ij} is the permeability tensor and P is the fluid pressure.

For a system where more than one fluid phase is present, Equation 2.5 is written for each phase and is modified by incorporating the relative permeability function as follows:

$$q_{\alpha j} = -\frac{k_r^\alpha k_{ij}^\alpha}{\mu} \left[\frac{\partial P_\alpha}{\partial x_j} + \rho_\alpha g \frac{\partial z}{\partial x_j} \right] \quad \alpha = \text{air, water NAPL } i, j = x, y, z \quad (2.5)$$

where k_r^α is the relative permeability of the α phase.

In practice, the following form of Darcy's Law is often used to calculate the flux of groundwater in a steady-state, single-phase flow system:

$$q_i = -K_{ij} \cdot \nabla h \quad i, j = x, y, z \quad (2.6)$$

where q_i is the groundwater flux in the i direction, K_{ij} is the hydraulic conductivity tensor, ∇h is the average hydraulic gradient and h is the hydraulic head defined as:

$$h = \Psi + z \quad (2.7)$$

where Ψ is the pressure head and z is the elevation head.

Darcy's Law is valid for steady-state, laminar fluid flow, thus, when the fluid flow is transient, the partial differential equation describing fluid flow must be solved. Transient flow typically occurs during pumping or infiltration.

2.3. Mechanisms of Contaminant Fate and Transport in the Subsurface

The subsurface behaviour characteristics of NAPL types differ but the basic physics and mathematics describing the multiphase flow of DNAPLs and LNAPLs are the same (Pankow and Cherry, 1996). Non-aqueous phase liquids (NAPLs) migrate through the subsurface and ultimately become trapped in the soil matrix as residual and held in place by capillary forces. Because of their low solubility in water, residual NAPLs constitute a long-term source of groundwater contamination. The design of flushing based methods for accelerating the dissolution of these components requires knowledge of the dissolution rates. Dissolution of residual NAPL is a process that takes place at the pore scale, where wetting and capillary phenomena play an important role in deciding the distribution of the residual (Chevalier and Fonte, 2000).

It is widely acknowledged that the heterogeneity of geologic formations plays a critical role in the deliverability of the injected solutions towards the NAPLs. The heterogeneity of the soil may be characterized as physical or biochemical. Physical heterogeneity is primarily defined in terms of non-uniform permeability and porosity distributions. At field scale, the natural variability of the soil properties may prevent contact of NAPL and the fluids. Viscosity and density differences between the flooding fluid with the resident fluids may lead to hydrodynamically unstable displacement. Some techniques have been developed to improve deliverability and reduce the impact of soil heterogeneity (Lunn et. al., 1999; Grubb and Sitar, 1999; Chevalier and Peterson, 1999). Nonetheless, heterogeneity remains a major impediment in the application of numerous remediation techniques to field problems.

NAPLs can be present in the subsurface either as residual or as pools. Residual NAPL refers to the presence of small, disconnected blobs and ganglia of organic liquid that are trapped in the pore spaces of porous media or fractures by capillary forces. Residuals are formed at the end of a migrating NAPL body by snap-off and by-passing mechanisms. Below the water table, residual NAPLs dissolve into adjacent groundwater and this causes the formation of dissolved contaminant plumes. Pooled NAPL, on the other hand, refers to the presence of NAPL at saturations higher than residual. The continuous fluid distribution of pooled NAPLs leads to mobility in the subsurface. NAPL pools tend to form above

capillary barriers like fine-grained lenses. Pooling of LNAPLs occur in the vicinity of the water table whereas pooling of DNAPLs are expected to take place on the low permeability zones such as clay. Due to the heterogeneous nature of subsurface layers, the pools can form at all elevations and can also be located on areas other than the clay aquitards and bedrock surfaces. The main problem with NAPL pools is the vertical short circuiting experienced during drilling (Helmig, 2003). NAPL pools also can be mobilized in response to groundwater pumping, which can be an advantage if extraction wells are properly placed, but a disadvantage if mobilization occurs into previously uncontaminated regions of the subsurface.

NAPLs have tendency to partition among phases (NAPL-water-soil-air). The partitioning continues till the equilibrium distribution is reached. At equilibrium, the contaminant concentration in each phase of the system is defined. The partition coefficient describes the relative abundance of a chemical between two adjacent phases in equilibrium (Pankow and Cherry, 1996). The distribution of NAPLs in the subsurface is controlled by four phase partitioning processes:

- volatilization of dissolved chemicals from water into air (Henry's Law)
- dissolution of NAPLs into water (solubility)
- sorption of dissolved chemicals from water to solid surfaces (tailing effects in pump/treat systems)
- vaporization of the NAPL components into air (Raoult's Law)

Volatilization is the partitioning of components from the water phase to the air phase and the concentrations arising from volatilization is described by Henry's Constant. This constant is defined as the equilibrium concentration in the air phase divided by the equilibrium concentration in water. High affinity for the air phase causes the Henry's Constant to have a high value (Lyman et al., 1990).

Dissolution of immobile NAPLs to mobile aqueous phase has been investigated by many researchers at microscale level (Jia et al., 1999; Fontenot and Vigil, 2002; Sahloul et al., 2002) and at macroscale level (Powers et al., 1991; Geller and Hunt, 1993; Kim and Chrysikopoulos, 1999; Bradford et al., 2000). The macroscale experiments are performed under quasistatic conditions in homogeneous one-dimensional systems. Typically NAPL at

residual saturation in a liquid-saturated porous medium is prepared to observe the rate at which NAPL dissolution to a mobile aqueous phase occurs with the effect of various system properties. Because of the inherent limitations associated with macroscale NAPL dissolution experiments, efforts have been diverted to microscale NAPL dissolution experiments. The aim of these experiments is to determine and quantify the pore-scale flow and transport processes that result in the overall NAPL dissolution observed at the macroscale. Microscale experiments provide information on the morphology and topology of a three-dimensional pore structure, the distribution of fluids present as a function of space and time and the spatial-temporal velocity of the aqueous phase and NAPL (Pan et al., 2007).

Flushing operations necessitate the detailed knowledge of the behaviour of solutions in the subsurface. The solute transport for a continuous source in a uniform 1D column can be expressed as Equation 2.8 (Helmig, 2003).

$$\frac{C(x,t)}{C_0} = \frac{1}{2} \left[\operatorname{erfc} \left(\frac{x-v_x t}{2\sqrt{D_L t}} \right) + \exp \left(\frac{v_x t}{D_L} \right) \operatorname{erfc} \left(\frac{x+v_x t}{2\sqrt{D_L t}} \right) \right] \quad (2.8)$$

where C is the solute concentration, D_L is the longitudinal hydrodynamic dispersion coefficient, t is time, x is the spatial coordinate along the length of the column and v_x is the solute velocity (Delleur, 1998).

The partitioning of components from the water phase to solid matter such as sand grains and fracture walls is referred to as sorption. There are two mechanisms in sorption. The partitioning of components to the actual surface of solid matter is adsorption whereas, diffusion of components into the pore space within soil grains is defined as absorption. At sites where sorption occurs, the leading edge of the contaminant plume migrates at a slower rate than the groundwater. This process is commonly referred to as retardation and the ratio of groundwater velocity to contaminant velocity can be characterized by the retardation factor which is given in Equation 2.9 (Logan, 1999).

$$R = 1 + \frac{\rho_b}{\phi} K_d = \frac{v_{ave}}{v_c} \quad (2.9)$$

where R is the retardation factor, ρ_b is the dry bulk density of the medium, ϕ is the medium porosity, K_d is the distribution coefficient, v_{ave} is the average linear groundwater velocity and v_c is the contaminant velocity. Equation 2.10 assumes a linear equilibrium sorption isotherm. Modifications are required where the sorption process is rate limited. The distribution coefficient, K_d , is often approximated as:

$$K_d = K_{oc} \cdot f_{oc} \quad (2.10)$$

where K_{oc} is the organic carbon partition coefficient and f_{oc} is the fraction of organic carbon present on the solid matter.

The transfer of components from the NAPL phase to the air phase is referred to as vaporization. The contaminant vapors formed in the unsaturated media can disperse through the air pathways in unsaturated media. This causes the contamination to spread beyond the zone occupied by the NAPL. The rate of vaporization is proportional to a compound's vapor pressure which can be defined as the pressure exerted in the air phase above the pure compound in a closed container. Vapor pressure is a strong function of temperature and typically increases with higher temperatures. Raoult's Law can be used in calculating the effective vapor pressures of the components and is expressed as the product of the vapor pressure of the component and its mole fraction in the NAPL phase.

There are many numerical solution alternatives for the flow and transport patterns of NAPLs. The scale and system composition determines the equations to be used in characterizing the behaviour of NAPLs. Many properties related to the prediction of multiphase flow typically vary spatially in natural porous media over several scales. The scales are separated into four groups by Freeze and Cherry (1979):

- the molecular level - surface properties influence wettability,
- the microscale level – composed of individual pores at which topology influences entrapment behaviour,
- the macroscale level - the flow is modeled using continuum concepts,
- the field scale level - variability in properties with distances such as meters or even kilometers.

Multiphase-multicomponent flow and transport refers to the migration of fluid phases through the subsurface and the simultaneous migration of any number of components within any of the phases. The multiphase flow, transport and reaction processes in porous media are of critical importance to define the problems of groundwater supply and remediation. The modeling efforts through multiphase flow and transport is a well-known practice in the petroleum engineering (Liu et al., 2004) and due to similarities in the unknown behaviour of the components present, similar models have been developed for the characterization of the contaminant plume and the simulation-design of remediation systems (Rahbeh and Mohtar, 2007).

The microscale geometry and processes that control large-scale systems are in most cases hard to gather thus this limits the ability to fully simulate multiphase problems. At the microscopic scale, the pore-scale hydrodynamics and mass transfer can be evaluated but for the field scale problems, determining the properties at the microscale level are impractical. Thus, physical processes must be described at the macroscale scale (Culligan et al., 2006). Therefore, most laboratory experiments mimic the macroscopic scale (Khachikian and Harmon, 2000). Macroscale models are formulated in order to retain consistency with microscale physics and thermodynamics. There should be consistent relations between microscale (pore-scale) fluid distributions and transport phenomena and macroscale (porous media) systems. In theory, specific models can be derived at the microscale and upscaled to larger scales to provide this relation (Pan et al., 2007). A brief list of equations for micro and macroscale systems and for single and multiphase compositions is given in Table 2.5.

2.4. Pollution Control Techniques

Aquifer remediation is the implementation of remedial measures to improve water quality within the subsurface, or to prevent the problems in permeable materials which contain or are capable of containing groundwater (NATO/CCMS, 2003). The low solubilities of the NAPL components lead to difficulties in the traditional pump and treat remediation efforts (Mackay and Cherry, 1989; Haley et al., 1991). In most cases, the

separate phase cannot be removed and the dissolved mass removed with the water is extremely small compared to the separate phase.

Table 2.5. List of equations for micro and macroscale systems and for single and multiphase composition (Helmig, 2003).

	Microscale	Macroscale
Single Phase Systems		
Flow Equations	Navier Stokes Equation	Darcy's Law
Means of Transport	Advection/Diffusion	Advection/Diffusion/Dispersion
Reactions	Biofilm growth	Mixed reactions
	Chemical reactions	
Multiphase Systems		
Flow Equations	Navier Stokes Equation Supplemental Equations (capillary pressure)	Darcy's Law
		Supplemental Equations (capillary pressure, relative permeability)
		Residual Saturation
		Hysteresis
		Dispersion
Means of Transport	Advection/Diffusion of each component in each phase	Advection/Diffusion/Dispersion of each component in each phase
Reactions	Biofilm growth	Mixed reactions
	Chemical reactions	

Cleanup of contaminated groundwater is inherently complex and will require large expenditures and long time periods. Pump and treat based technologies have been applied to many contaminated sites in the past but the poor performance of these schemes led to the continued efforts to develop improved methods for the remediation of these areas. The new technologies for the zone restoration follow two trends (Pankow and Cherry, 1996):

- destroying the contamination in-situ (chemical oxidation, dehalogenation, thermal treatment, etc.)

- bringing the contaminant mass to the surface successfully and without spreading, for treatment (enhanced flushing technologies with chemical agents, thermal enhancements, etc.)

According to the EPA 2004 annual report on treatment technologies for site cleanup in USA (Lee et al., 2007), 863 treatment technologies were selected for source control over fiscal year 1982-2002 and of these, 42% were *in-situ* technologies and 58% were *ex-situ* technologies.

The main concepts and the status of the technologies in remediation activities are presented in Figure 2.3 as a pyramid (from Pankow and Cherry, 1996). The pyramid is drawn based on the status of the technology. The proven technologies have a considerable base of site experience and success. Furthermore, the commercial organizations offer the technology in the marketplace and the performance of the technology is more or less predictable. Emerging technologies also have many developments but still there are some uncertainties in performance and costs. Therefore, more research is required for these technologies. Experimental technologies, on the other hand, necessitate detailed laboratory and field trials before being commercially available in the marketplace.

2.4.1. Pump-and-treat

Pump and treat (PT) is a traditional technology used in aquifer remediation. The treatment system is composed of an extraction well or system of wells, a water pumping system, an above ground treatment system and injection wells. PT systems can be used for hydraulic containment of contaminant plumes and/or for the removal of dissolved contaminants from groundwater. The effectiveness of traditional PT systems in remediating NAPL and their associated groundwater plumes is limited due to the low solubility, higher viscosity and higher retardation coefficients typically associated with NAPLs (Mackay and Cherry, 1989). Experience with this technique showed that aqueous concentrations of contaminants decrease over time and the removal rates decrease even when the concentrations of the contaminants in the subsurface remain above cleanup goals (Mackay and Cherry, 1989; Travis and Doty, 1990).

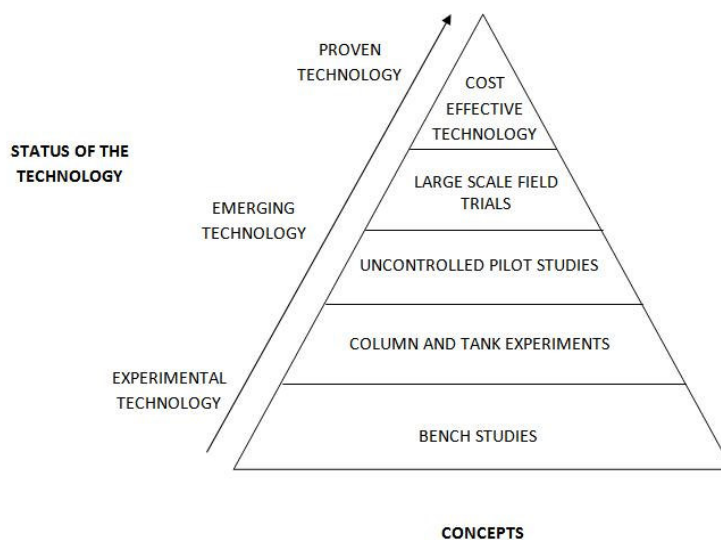


Figure 2.3. The main concepts and the status of the technologies in remediation activities.

PT technology has been proven to be ineffective in removing contaminants that are immiscible in water, that have diffused into micro pores or zones within the aquifer material not accessible to substantial water flow, that are sorbed to subsurface materials and that exist in heterogeneous subsurface environments. However, PT can still be an effective method to control the migration of the dissolved plume and is often used as a secondary safety precaution in many sites together with other remediation and plume treatment techniques (Palmer and Fish, 1992).

2.4.2. Chemical Agent Flushing

Enhanced flushing based remediation strategies include the use of chemical agents such as alcohols and surfactants to increase NAPL mobility and enhance contaminant recovery in pumping wells. Flushing with chemical agents is an aggressive method for the recovery of contaminants from the subsurface. The technology has the potential to remove large amounts of NAPL in a relatively short time. However, there are also some risks associated with the implementation of this technology. The most important risk is the extension of contamination through uncontrolled vertical NAPL mobilization. The elevated contaminated concentrations in groundwater may represent a risk and the long-term containment of unrecovered contaminants may be required. The theory of chemical agent flushing is very similar to PT. The flushing process begins with the drilling of injection and

extraction wells into the ground where the contamination has been found. The number, location and depth of the injection and extraction wells should be decided based on several geological factors and engineering considerations. The soil flooding equipment pumps the flushing solution into the injection wells (Sawyer and Kamakoti, 1998). The flushing solution passes through the soil and dissolves the contaminants as it moves towards the extraction wells. The extraction wells collect the flushing solution containing the contaminants. The solution-contaminant mixture is pumped out of the treatment zone through the extraction wells and the mixture is typically treated by a wastewater treatment system to remove the contaminants and reclaim the flushing solvents whenever possible.

In recent years, chemically enhanced remedial methods have been employed to remove NAPLs from contaminated soils and aquifers (Jawitz et al., 1998; Shiau et al., 2000). Soil flooding with chemical agents is a “source control” treatment technology, which is designed to treat the source of contamination such as soil, sediment, sludge and solid wastes. Meanwhile it is clear that treatment of the groundwater by soil flooding is not accomplished directly. Additional treatment methods are required to remove the contaminants from the effluent.

Cosolvent flushing, which is based on methods developed in petroleum engineering, involves the use of cosolvents to solubilize and mobilize the NAPL. Surfactant-enhanced NAPL removal is based on two key processes: (a) micellar solubilization of the entrapped NAPL to increase aqueous solubility and (b) mobilization of the NAPL through interfacial tension reductions (Butler and Hayes, 1998).

Surfactants and cosolvents have been tested at the bench scale in laboratories, at the pilot scale in controlled and contained environments and at full scale in actual field studies (Jin et al., 1995, McCray et al., 2000). Laboratory experiments (Pennell, et al., 1993; Abriola, et al., 1993; Mason and Kueper, 1996) and field experiments (Fountain, et al., 1996) have demonstrated that the micellar solubilization process can be rate-limited. The rate of NAPL solubilization was observed to be depending on groundwater velocity and the NAPL-water interfacial area. Mason and Kueper (1996) investigated the effect of groundwater velocity and they found out that slow groundwater velocities increase the efficiency in the remediation process, enabling higher contact times.

Besides enhancing removal efficiencies of low solubility subsurface contaminants, some of the considered chemical agents also introduce toxicity and refractory species into the system. Therefore, it is desirable that any agents used for the remediation be of low toxicity and biodegradable (West et al., 1992; Mulligan et al., 2001; Chu and Chan, 2003). To reduce the risk of toxicity, Shiau et al. (1995) suggested the utilization of food grade surfactants which have been approved by the Food and Drug Administration. Some plant-based surfactants were also found to be beneficial for the removal of benzene containing compounds (Roy et al., 1997). Because of these toxicity concerns, some researches have suggested the use of biosurfactants in subsurface as well as surface waters (Bai et al., 1997; Kanga et al., 1997; McCray et al., 2001).

Viscous fingering is one of the problems in chemical agent flushing as a less viscous fluid displaces a more viscous fluid. This causes a considerable part of the subsurface not being contacted by the flushed solution. Since some chemical agents are more viscous than water, viscous fingering takes place at the back end of the injected solution. Gravitational instability is another problematic formation and is quite similar to viscous fingering where a less dense fluid displaces a more dense fluid upwards and this causes by-passing of certain regions in the subsurface. The use of polymers and foams helps to prevent the formation of unstable displacements (Jeong and Corapcioglu, 2003).

Because of the complexity and interrelationship of the factors controlling the mobility and solubility of NAPLs, no single agent can optimally modify NAPL properties. Some researchers have proposed the multi-step manipulation of NAPL properties to control mobility of the NAPLs (Kostarelos et al., 1998; Lunn et al., 1999; Zhong et al., 2003). It is important that detailed research be conducted to demonstrate the enhanced recovery of DNAPLs taking into account the combined influence of all the injected agents.

Field-scale flushing studies require intensive site characterization and careful design. In particular, hydrologic control, surfactant/cosolvent selection and the risk for uncontrolled NAPL remobilization need to be thoroughly assessed prior to remediation activity through laboratory bench-scale experiments and numerical modeling. Additionally, potential regulatory concerns related to the injection of surfactants/cosolvents may need to be addressed.

The cost of implementing a chemical agent flush may vary from site to site depending on the ability to reuse injected chemicals, methods of waste disposal and the amount of chemical that needs to be purchased per unit of mass removed (Lehr, 2004).

2.4.3. In-situ Chemical Treatment

In situ chemical treatment technologies include destroying organic chemicals in-situ either with oxidation or reduction. In situ oxidation involves the injection of reagents to stimulate degradative chemical reactions with the contaminants in the groundwater. Strong oxidizing agents such as hydrogen peroxide and iron (Fenton's reaction), potassium permanganate and ozone are used to chemically transform the contaminants into carbon dioxide, water and other byproducts. Chemical oxidation can be used to treat a wide range of organic contaminants (Conrad et al., 2002). The operations are largely unaffected by contaminant concentrations and is relatively inexpensive. Effective delivery of the oxidizing agent to contaminants is an important consideration in remediation design.

The two potential problems associated with in-situ chemical treatment are precipitation of ferric iron and manganese and formation of CO₂. The by-products affect the hydraulic properties of the porous media and cause plugging. Oxidation of immobile metals such as chromium III (Cr³⁺) to more mobile and toxic forms (i.e., chromium VI (Cr⁶⁺)) can in some cases take place (Schroth et al., 2001).

Chemical reduction may also be used to remediate groundwater contamination. The theory is based on reduction of chromium (VI), which is a toxic and mutagenic form of chromium, to chromium (III), which poses a lesser health concern. Iron (II) and iron (0) are traditionally used as reductants and recently calcium polysulfide was proven to be more effective (Sabatini, 1997; Christ and Abriola, 2006).

In situ chemical treatment is a promising method but additional tests are required under realistic conditions. Furthermore, health and safety risks exist for workers handling these hazardous oxidizing chemicals. Thus, safety precautions should fully be taken while using this method.

2.4.4. Soil Vapor Extraction

Soil vapor extraction (SVE) is another method applied especially in the remediation of volatile NAPL components in the vadose zone and near and above the water table. In this method the subsurface airflow is induced through the contaminated zone and aims to volatilize the constituents which have sufficiently high vapor pressures. Advective vapor phase flow is induced within the subsurface to enhance the volatilization of NAPLs entrapped in the subsurface. The major physical mechanisms observed in SVE operations are mass transfer and mass transport. The method effectively removes the contaminated pore water in the unsaturated zone and the sorbed contaminants (Anwar et al., 2003).

In SVE, the properties of the contaminants and the soil must be suitable for the system requirements. Partitioning based mass transfer causes the volatile and semi-volatile compounds to enter the vapor phase by evaporating from the pure phase liquids or volatilizing from the soil moisture. Subsurface temperature, soil humidity and contaminant properties (solubility, vapor pressure and density) affect the removal rates. On the other hand, mass transport controls the movement of vapor in the subsurface which takes place primarily by advection. Advection is related to the existence of pressure gradients that are developed during the operation of vapor extraction wells. Subsurface parameters such as soil permeability and humidity affect the mechanisms. The transport of the vapors depends on the magnitude of vacuum pressure imposed by the SVE system (Nobre and Nobre, 2004).

Developments have been made in SVE remediation technologies for the determination of the closure times through theoretical and laboratory studies. Sawyer and Kamakoti (1998) conducted a research on the optimal flow rates and well locations for soil vapor extraction design and reported that optimization procedures should be coordinately used with SVE models to enhance the SVE design decision-making process.

Poppendieck et al. (1999) conducted column studies to obtain field SVOC (soil vapour organic carbon) removal rate constants in order to estimate the treatment time prior to field scale implementation of a thermally enhanced SVE operation and reported that field removal constants can successfully be used to estimate the time required for a field-

scale thermally enhanced SVE system to reduce the concentration of individual compounds to a specified level.

2.4.5. Thermal Remediation

Thermal treatment is another technology for the remediation of soils contaminated with NAPLS. In the past, thermal treatment has been applied to the excavated soils. The excavated soils are incinerated to release and/or destroy the contaminants (Lighty et al., 1968). However, excavation of the contaminated soils is not always practical and can be extremely costly when the contamination occurs at great depths or covers a large area. Excavation also increases the risk of exposure to and further dispersion of the contaminants during material handling steps (Dev et al., 1989). Heat-based in-situ remediation methods can be used in many places where excavation is not possible.

Heat is employed in the source zone to volatilize or mobilize NAPLS. Upon heating, the density of the organic chemicals and their adsorption onto solid phases or absorption into soil organic matter decrease, whereas their vapor pressure and molecular diffusion in the aqueous and gaseous phase increase (Atkins, 1998). The viscosity of a liquid decreases as the temperature increases, but the viscosity of gases increases with temperature. The expansion of liquids with temperature causes a reduction in the interaction between molecules and thus a reduction in its viscosity.

Various approaches have been used in thermal treatment, such as electrical resistive heating, hot air injection, hot water injection, steam injection, radio frequency (RF)-heating, thermal conductive heating and vitrification (Lee et al., 2007).

In electrical resistance heating, arrays of electrodes are installed around a central neutral electrode and a concentrated flow of currents toward the central point is formed. The resistance to flow in the soils leads to the production of steam at elevated temperatures. The mobile contaminants are extracted via vacuum application and are processed at the surface.

Thermal treatment often involves the injection of hot ingredients. The typical forms are hot water, hot air and steam. Through the injection of hot water, the viscosity of the contaminants decrease and remediation through enhanced recovery in the subsurface is accelerated. Injection of hot air can also volatilize organic contaminants in a similar way (Burden et al., 2002). In surface soils, hot air is usually applied in combination with soil mixing or tilling, either in situ or ex situ. Steam injection allows heating the soil and groundwater and enhances the release of contaminants from the soil matrix by decreasing viscosity and accelerating volatilization. As steam is injected through a series of wells within and around a source area, the steam zone grows radially around each injection well.

Radio frequency heating is an in-situ process that uses electromagnetic energy to heat soil and enhance soil vapor extraction. Soil is heated through rows of vertical electrodes embedded in soil or other media. When energy is applied to the electrode arrays, heating begins at the top center and proceeds vertically downward and laterally outward through the soil volume (Poppendieck et al., 1999).

Thermal conduction supplies heat to the soil through steel wells or with a blanket that covers the ground surface. Temperature increase leads to destruction of the contaminants and a carrier gas or vacuum system is utilized to transport the volatilized water and organics to a treatment system.

Vitrification also uses electric currents but the temperatures reached in the zone of interest are higher and this causes melting of the contaminated soil at elevated temperatures. Upon cooling, the melted soil becomes a chemically stable, leach-resistant, glass and crystalline material similar to obsidian or basalt rock. The high temperatures help destruction of the organic materials and radionuclides and heavy metals are retained within the vitrified product (Jones et al., 2002).

The one significant advantage of heat-based remediation techniques over other in-situ remediation techniques is that heat-based remediation techniques do not require the injection of chemicals that can be toxic at some concentrations. Heat-based remediation techniques, on the other hand, face some operational limitations due to heterogeneities in

the subsurface and this may necessitate some amending remediation methods to be used coordinately.

A successful application of a thermal remediation technology may require significant design effort including an assessment of subsurface response to heating, contaminant behaviour, vacuum extraction design and groundwater control and dewatering.

2.4.6. Permeable Reactive Barriers

The technology is based on the installment of a permeable wall of reactive material in the groundwater flow path, which treats contaminated groundwater as it passes through. Permeable reactive barrier (PRB) materials consist of permanent, semi permanent or replaceable reactive media. As the contaminant moves through the material, reaction that occurs transform the contaminants into less harmful (non-toxic) or immobile species. The PRB is not a barrier to the groundwater, but it is a barrier to the contaminants. In order to maximize groundwater capture funnel-and-gate design is often used (Beitinger, 1998). A variety of contaminant remediation techniques have been incorporated into reactive barriers, including transformation via zero-valent iron or other media (Roberts et al., 1996; Wüst et al., 1998), sorption via replaceable granular activated carbon (GAC) (Beitinger, 1998; Huttenlock et al., 2001; Kelly, 2002), enhanced biodegradation via nutrient addition and volatilization via air sparging curtains (Rijnaarts, 1998; Ritter et al., 2002, ITRC, 2005).

PRB zones may be most economically used as a pathway control procedure but clean-up of the source will be a slow process. The pathway control is essential but it should not be designed to achieve more than slow source clean-up as this minimizes the rate at which any treatment chemicals, energy or other process inputs are required (Beitinger, 1998).

Hydrogeological site characterization is necessary for successful reactive barrier design and bench-scale experiments together with modeling. Assessment of the contaminant degradation rates, reactive material life and the capacity for clogging and bypass flow are important for the performance of the method used (ITRC, 2005).

2.4.7. Natural Attenuation and Enhanced Bioremediation

Natural attenuation of contaminants is a combination of naturally induced nondestructive (dilution, sorption, volatilization) and destructive (biodegradation, oxidation, hydrolysis) processes (Carey et al., 2002). Biodegradation is a significant mechanism for dissolved contaminant destruction since naturally occurring biodegradation activity can be enhanced by the addition of electron acceptors and/or donors and manipulation of subsurface conditions. The biodegradation of NAPL phase is generally considered negligible, but natural attenuation processes may be sufficient to control plume migration and eliminate the need for NAPL removal at some sites (Vayenas et al., 2002).

Most petroleum fuels are readily metabolized by naturally-occurring microorganisms under aerobic conditions where oxygen is the electron acceptor. On the other hand, chlorinated solvents cannot be degraded in aerobic conditions but reducing conditions may promote degradation through reductive dechlorination. Reductive dechlorination occurs when indigenous anaerobic microbes (such as acetogens) metabolize organic carbon (USEPA, 2000). As a result of the reactions taking place, hydrogen is produced. Reductive dechlorination can be enhanced by the supply of additional carbon sources, such as molasses, vegetable oil, landfill leachate, or coalescing hydrocarbon fuel plumes (Adamson et al., 2003).

Natural attenuation as a site remediation strategy typically requires the collection of additional groundwater quality data (dissolved oxygen, redox potential, etc) and long-term monitoring.

2.5. Chemical Agents Used in Enhanced Flushing

In this section we discuss the chemical agents that have been considered for NAPL removal through enhanced flushing, the focus of this thesis.

The chemical agents that are considered for use in enhanced flushing include alcohols, surfactants, modified sugars, polymers and humic materials. These chemical agents are defined as compounds that change the bulk phase behaviour of the phases (Winsor, 1968).

Ternary phase diagrams for various chemical agent-NAPL systems are presented by a variety of authors (Brandes, 1992; Falta et al., 1996; Lunn and Kueper, 1999). The work of Lunn and Kueper (1999) shows that ternary phase diagrams provide suitable data in predicting the performance in two-dimensional laboratory experiments involving single-component DNAPLs whereas Peters and Luthy (1993) demonstrated that ternary phase diagrams can be used to predict performance in multicomponent systems (creosote and coal tar). The most common chemical agents are discussed in detail in the following sections.

2.5.1. Alcohols

Alcohols have one or more OH group in their structure and miscible with water. As they are biodegradable and have the potential for mobility, alcohols are used in NAPL remediation on their own to enhance the NAPL dissolution or physical NAPL mobilization or can be used to enhance the performance of other chemical agents (Bedient et al., 1999). The main alcohols being considered for environmental applications are water-miscible alcohols. When alcohols are injected at high concentrations, the term alcohol flushing is usually used rather than the term cosolvent flushing. Cosolvent flushing generally refers to the injection of low alcohol concentrations. The properties of the most common alcohols are given in Table 2.6. Because of the tendency of some alcohols to partition significantly into the NAPL phase, the density of the NAPL can be manipulated in-situ through appropriate alcohol selection (Hofstee et al., 2003). Ramsburg and Pennell (2002) conducted experiments with two DNAPLs, chlorobenzene and trichloroethene, to investigate whether it is possible to accomplish DNAPL density conversion through the

introduction of a partitioning (swelling) alcohol, n-butanol (BuOH), in a pre-displacement flush using conventional horizontal flushing schemes. Subsequent displacement and recovery of the resulting LNAPL was achieved by flushing with a low interfacial tension surfactant solution.

Table 2.6. The properties of the most common alcohols (Verschuieren, 1983).

Chemical	Molecular Weight (g/mole)	Density (g/mL)	Solubility (mole/L)	Viscosity (cP)	Surface Tension (dyne/cm, 20°C)
methanol	32	0.7914	Miscible	0.6	22.6
ethanol	46	0.7893	Miscible	1.08	22.3
1-propanol	60	0.8035	Miscible	1.722	23.7
n-butanol	74	0.8098	0.851	3	24.6
sec-butanol	74	0.8079	2.45	3.7	23
tert-butanol	74	0.7887	Miscible	3.32	20.7
1-pentanol	88.15	0.8144	0.25	3.31	31.55
1-octanol	130.23	0.8270	0.00447	8.925	27.53

For short-chain polar alcohols and hydrophobic NAPLs, the alcohol does not partition into the organic phase to any significant extent. NAPLs can be recovered using these alcohols by the increased solubility of the organic in the aqueous phase. However, it is very difficult to mobilize or displace the NAPLs without partitioning. For longer-chain, more nonpolar alcohols, the alcohol partitions into the organic phase. This causes swelling of the residual NAPL phase in addition to the interfacial tension reduction (Lunn and Kueper, 1996). As the residual NAPL swells and combines to form a continuous fluid phase, it can be mobilized and pumped out of the aquifer. Salts can also be used to increase the partitioning into the NAPL phase (Pennell et al., 1996; Dwarakanath et al., 1999; Zhong et al., 2003).

When large amounts of alcohol are added to a NAPL-water system, the alcohol partitions into both phases and this leads to changes in NAPL viscosity, density and solubility (Lunn and Kueper, 1999). If the amount of alcohol in contact with the NAPL-

water system is increased, one phase system is reached where the NAPL is completely solubilized in the alcohol-water mixture.

The cosolvent effect of alcohols to aqueous solution results in the desorption of organic contaminants from aquifer solids. Sorption of alcohol to aquifer solids is generally not of concern in remediation applications (Butler and Hayes, 1998).

Alcohols, when present in the subsurface at low concentrations in the order of 1%, are reported to be readily biodegradable (Brusseau, et al., 1994). In environmental applications where high concentration alcohol solutions are injected to facilitate NAPL removal, this property is a benefit in operations. Flushing solutions with high concentration solutions of alcohol can be flammable and explosive, therefore, precautions during transportation, handling and injection should be taken.

2.5.2. Surfactants

The surfactant molecule is typically composed of a strongly hydrophilic group, or moiety and a strongly hydrophobic moiety. The entire surfactant monomer is often referred to as amphiphilic because of its dual nature. The hydrophobic portion of the surfactant monomer is typically a long hydrocarbon chain, referred to as the "tail" of the molecule. The hydrophilic "head" group often includes anions or cations such as sodium, chloride, or bromide. The molecular weight of surfactants under consideration for environmental applications typically ranges from 200 g/mol to 2000 g/mol (West and Harwell, 1992).

The hydrophilic group of the surfactant monomer provides most surfactants with a high solubility in water. The hydrophobic group of the monomer, however, prefers to reside in a hydrophobic phase such as LNAPL or DNAPL. These competing effects result in the accumulation or congregation of surfactant monomers at NAPL-water interfaces, with the hydrophobic tail group embedded in the NAPL phase and the hydrophilic head group oriented toward the water phase (Rosen, 1978).

The use of surfactants in the remediation of organic contaminants in the subsurface is not an old application but the application dates back to 1960's when the use of these

compounds were patented for widespread use in enhanced oil recovery efforts (Pope and Wade, 1995).

In a solubilizing surfactant flush, surfactants are injected into the subsurface as an aqueous solution and flushed through the zones containing NAPL. Upon contact with the NAPL, the surfactants bring about an increase in the total aqueous solubility of the chemical components comprising the NAPL through a process referred to as micellar solubilization, thereby accelerating the dissolution process (Butler and Hayes, 1997; Martel et al., 1998). In a mobilizing surfactant flush, surfactants are again injected as part of an aqueous solution, but the objective is to lower NAPL-water interfacial tension to the point that physical mobilization of the NAPL takes place. This may be undesirable at some DNAPL sites where vertical mobilization may lead to a worsening of the extent of contamination. The degree of solubilization versus mobilization occurring in a surfactant flush can be controlled through appropriate surfactant selection.

Surfactants form aggregates. When their concentration is increased to a certain level, the critical micelle concentration (CMC) is reached. This aggregate is spherical, the hydrophobic part of the surfactant which is mainly the carbon chain turns toward the inside and the hydrophilic part is turned toward outside. Therefore, the organic contaminant can easily go inside the micelle. A suitable surfactant effects the NAPL-water partitioning when present at levels above its CMC (Kile and Chiou, 1989; Khachikian and Harmon, 2000).

The distribution of chemical agents and fluid phases in a NAPL-surfactant-water system can be characterized by Winsor Phase Diagrams. The type of the Winsor phase system depends on the surfactant used and the aqueous phase chemistry. The typical Winsor type phase diagrams for NAPL-surfactant-water systems are given in Figure 2.4.

In Winsor Type I (or named as type II- in some references) systems, a separate NAPL phase and an aqueous phase rich in surfactant micelles containing dissolved NAPL are present. The micelles are surfactant monomers with their hydrophobic tails pointed inward. The tie lines slope down toward the NAPL apex, indicating that the surfactant partitions preferentially into the aqueous phase. The majority of surfactant resides in the aqueous

phase and contaminant recovery is promoted by partitioning of contaminant into surfactant micelles. Winsor Type I systems are also expressed as “single-phase microemulsions”. Microemulsions are thermodynamically stable solution of micelles and structured aggregates of micelles (Zarur et al., 2000).

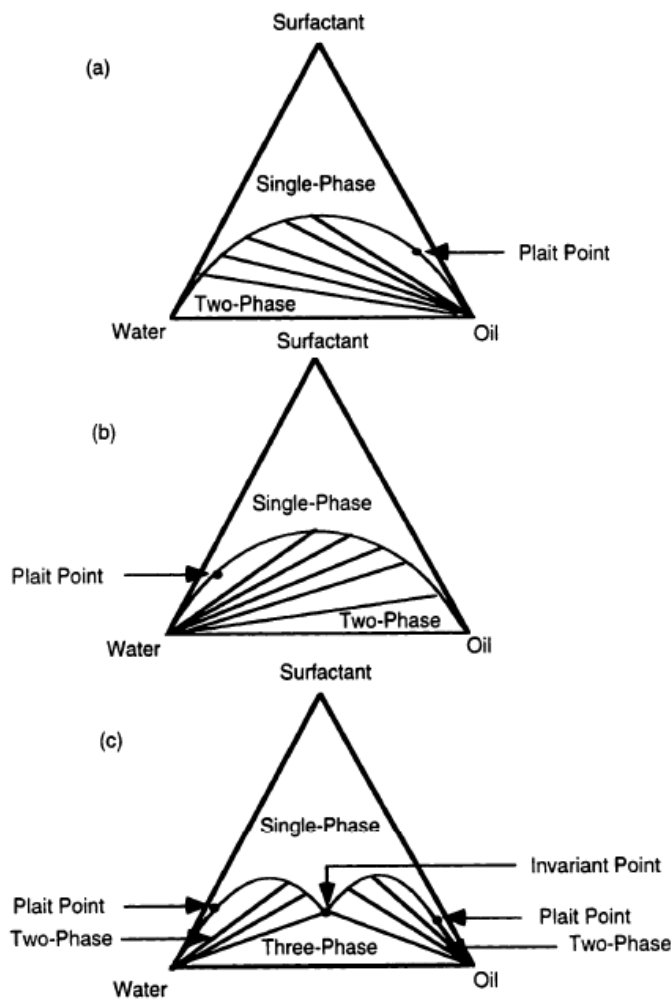


Figure 2.4. Phase diagram for oil-water-surfactant systems (West and Harwell, 1998)

(a) Winsor Type I (II-), (b) Winsor Type II (II+), (c) Winsor Type III.

By reducing the concentration of the surfactant a separate middle phase microemulsion can be formed (Kostarelos et al., 1998). This third phase creates an ultra-low interfacial tension and mobilization of NAPLs becomes the primary recovery mechanism due to this new property. These systems are referred to as a Winsor Type III

systems and they are suitable for NAPL mobilization flushes. Reduction of the concentration of surfactant to very low levels causes a separate water phase, in equilibrium with the NAPL phase rich in surfactant micelles containing water, to form. The surfactant molecules forming the micelles are however oriented with their hydrophobic tail groups pointing outward toward the NAPL phase. Such systems are typically referred to as Winsor Type II, or type II (+) systems. In this type of Winsor system, the tie lines slope down toward the water apex, indicating that the surfactant partitions preferentially into the NAPL phase.

The NAPL-rich phase is referred to as a micro-emulsion as it contains the majority of surfactant in the form of micelles. These systems are often undesirable as the partitioning of surfactant into the NAPL phase represents a significant surfactant loss. Microemulsion systems with respect to the salinity or temperature changes are presented in Figure 2.5.

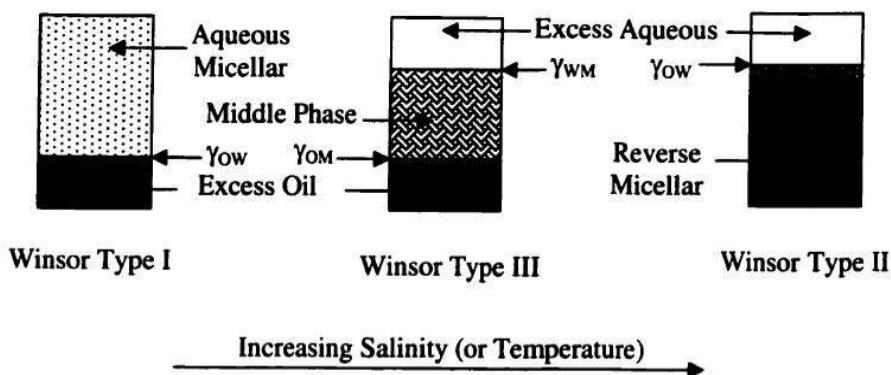


Figure 2.5. Microemulsion systems with respect to the salinity or temperature changes (Palmer and Fish, 1992).

Surfactants can be generally classified according to the nature of their hydrophilic head group. Some of the common commercial surfactants are listed in Table 2.7. Anionic surfactants give rise to a negatively charged surfactant ion and a positively charged counterion upon dissolution in water. They tend to be good solubilizers and are relatively nontoxic. They have been used in petroleum oil recovery operations as well as in contaminant hydrogeology remediation applications (Pope, 2003).

Table 2.7. Properties of some common commercial surfactants (Zhou and Rhue, 2000).

Chemical class	Trade name	Chemical name
Anionics		
alkyl sulfates sulfates of ethoxylated alcohol alpha-olefin sulfonates	sodium dodecyl sulfate	sodium dodecyl sulfate
	Witcolate S-1285C	laureth sulfate
	Witconate AOS	alkyl(C14-C16) olefin
dialkyl sulfosuccinates	Aerosol AY 65	diamyl sulfosuccinate
	Aerosol MA 80-1	dihexyl sulfosuccinate
	Aerosol AOT	dioctyl sulfosuccinate
Nonionics		
ethoxylated alcohols	Brij 35	POE(23) lauryl
	Brij 97	POE(10) oleyl
	Brij 98	POE(20) oleyl
	Genepol 26-L-45	POE(6.3)C12-C16
	Trycol 5953	POE(6) decyl
	Macol LA 790	POE(7) lauryl
	Ritoleth 10	Oleth 10
ethoxylated fatty acids	Myrj 52	POE(40) stearate
	Nopalcol 2-L	PEG(2000) monolaurate
ethoxylated alkylphenols	Igepal CO-630	nonylphenol ethoxylate
propoxylated/ethoxylated alcohols	Antarox LA-EP 15	modified oxyethylated
	Rexonic P-5	ethoxylated/propoxylated linear alcohol
block polymers	Pluronic L43	block copolymers of
polyglycerol esters	Aldisperse ML-23	POE(23) glyceryl monolaurate
polysorbates	Tween 20	POE(20) sorbitan monolaurate
	Tween 40	POE(20) sorbitan monopalmitate
	Tween 80	POE(20) sorbitan monooleate
sucrose fatty acid esters	DeSulf GOS-P-70	alkylpolyglycoside
thio and mercapto derivatives	Alcodet SK	polyoxyethylene thioether
Amphoterics		
betaine derivatives	Detaine PB	cetyl betaine

Cationic surfactants, on the other hand, yield a positively charged surfactant ion and a negatively charged counterion upon dissolution in water. Polyamines and their salts, quaternary ammonium salts and amine oxides are the common cationics. Cationic surfactants tend to be toxic and are therefore not widely used in environmental applications. Furthermore, they tend to sorb to anionic surfaces and so can be severely retarded in groundwater systems. Nonionic surfactants are characterized by hydrophilic head groups that do not ionize appreciably in water. They are usually easily blended with

other types of surfactants (i.e., used as cosurfactants) and therefore have found widespread use in petroleum and environmental applications (Butler and Hayes, 1998; Zimmerman et al., 1999; Zhou and Rhue, 2000; Cowell et al., 2000; Zhao et al., 2006). The performance of nonionic surfactants, unlike anionic surfactants, is relatively insensitive to the presence of salts in solution.

For in situ flushing, it is desirable to select surfactants that will not adsorb to the soil particles, because surfactant adsorption leads to reduce the micellization and solubilization capacity of the surfactant and it can result in the contaminant partitioning to the adsorbed surfactant molecules (Edwards et al., 1994; Ko et al., 1998). Thus, high surfactant adsorption will result in poor flushing solution performance.

2.5.3. Cyclodextrins

The most common modified sugars used in remediation activities are cyclodextrins. Cyclodextrins (CDs) are produced at commercial scale from the enzymatic transformation of starch by bacteria. The agent is a glucose-based toroidal-shaped molecule and has a hydrophobic cavity within which the organic compounds of appropriate shape and size can form inclusion complexes. This property was first used in the pharmaceutical research for the drug delivery (Boving and Brusseau, 2000). Over the last few years they have found a wide range of applications in food, pharmaceutical and chemical industries as well as agriculture and environmental engineering. The selected physical properties of cyclodextrin derivatives are given in Table 2.8. The chemical structures of the three main types of cyclodextrins are given in Figure 2.6.

Table 2.8. Selected physical properties of cyclodextrin derivatives (Szehtli, 1998).

Cyclodextrin	Substitution	MW (g/L)	Cavity Volume (nm ³)
HP- α -CD	0.6	1180	0.174
HP- β -CD	0.6	1380	0.262
HP- γ -CD	0.6	1576	0.427
M- β -CD	1.8	1312	0.262

Typical cyclodextrins contain a number of glucose monomers ranging from six to eight units in a ring and are named with respect to this ring size as below:

- α -cyclodextrin: six membered ring molecule
- β -cyclodextrin: seven membered ring molecule
- γ -cyclodextrin: eight membered ring molecule

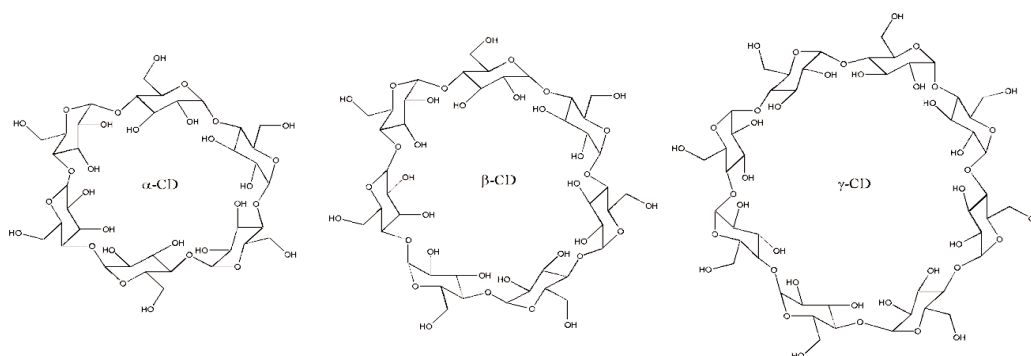


Figure 2.6. Chemical structure of the three main types of cyclodextrins (<http://en.wikipedia.org/wiki/Cyclodextrin>).

Cyclodextrins, constituted only by 6-8 glucopyranoside units, can be topologically represented as toroids with the larger and the smaller openings of the toroid exposing to the solvent secondary and primary hydroxyl groups respectively. Because of this arrangement, the interior of the toroids is considerably less hydrophilic than the aqueous environment and thus able to host other hydrophobic molecules. On the contrary, the exterior is hydrophilic and impart the water solubility of cyclodextrins (Tuck et al., 2003).

Nowadays, cyclodextrins are evaluated for their performance in complexing nonpolar organic pollutants such as chlorinated solvents. The nonpolar organic compounds are trapped in the central hydrophobic cavity of the cyclodextrin. Individual cyclodextrin molecules complex molecules of contaminants, so this enables cyclodextrins to enhance solubility at all concentrations. One other advantage of using cyclodextrins is that their performance is not affected by the changes in pH, ionic strength and temperature. The beneficial properties of cyclodextrins in remediation include:

- low sorption to the aquifer solids (Brusseau et al., 1994)
- do not partition much to the organic phase (McCray, 1998) – regulatory concerns
- behave practically as conservative tracers

- generally nontoxic and nonreducing
- have a high solubility enhancing ability due to the polar exterior
- stable under typical environmental conditions
- do not appear to harm resident microbial populations during remediation (Wang et al., 1998)

2.5.4. Humic Substances

Humic substances are natural polydisperse organic materials exhibiting solubility enhancement behaviour for oils and other relatively water insoluble compounds. Humic and fulvic components of the natural organic matter are entitled under humic substances but in most references humic acids are used to represent these fractions (Johnson and John, 1999).

Humic acids are found in nature as a result of the decay of leaves and other natural organic matter. Since the humic acid is a component of the soil organic matter, it contains structural units such as carboxylic, hydroxylic, phenolic and aliphatic groups. The presence of these groups in the humic molecule can vary which makes the humic acids unique. As the behaviour and structure of humic acids vary, they are less well known as potential remediation agents.

The ability of humic substances to solubilize the hydrophobic organic compounds enables them to enhance hydrophobic organic solubility through partitioning (Chiou et al., 1987). Humic acids have hydrophobic exteriors and hydrophilic interiors (Abdul et al., 1990) and they are generally conceptualized as separate phases that can retain hydrophobic organic contaminants. They have a surface activity similar to that of surfactants (Boving and Brusseau, 2000) and can facilitate the transport of organic contaminants.

The effects of humic substances on the solubility and mobility of organic contaminants have been the subject of numerous studies. Experimental studies suggest that a linear relationship exists between NAPL solubility and dissolved humic substance concentration (Webster et al., 1986; Johnson-Logan et al., 1992).

The organic contaminants are primarily bound to the organic carbon part of the soil and aquifer materials and the dissolved humic acids increase the water solubility of the organic contaminants, as a result, the organic contaminant migration through aquifers can be accelerated or retarded depending on the partition coefficient of the organic contaminants to that of the humic acid (Abdul et al., 1990).

Chiou et al. (1987) described the increase in solubility in an aqueous system containing dissolved humic acid as:

$$S_w^* = S_w(1 + C_{hs}K_{ha}) \quad (3.4)$$

where, S_w^* and S_w are the solubilities of the organic contaminants in the humic acid solution and in pure water respectively. C_{hs} is the concentration of the humic acid (g/mL of water) and K_{ha} is the partition coefficient of the organic contaminant between the humic acid and water.

Aggregation concentration is used to define the concentration above which humic acid molecules aggregate, which is analogous to surfactant CMC (Hayase and Tsubota, 1983).

2.5.5. Polymers

Polymers are substances with repeating structural units - monomers. They are connected by covalent chemical bonds. The experiences gained in the petroleum industry showed that polymer solutions can be injected during surfactant flushing to improve mobility control and to increase the overall sweep efficiency (Robert et al., 2006). Subsurface heterogeneities lead to stratification of various permeability materials which adversely affect the flushing performance. Preferential flow channels can form which leaves the zones in low permeability layers uncontacted. Instability is also observed due to low sweep efficiency which causes the formation of fingers of the flushing solution into the resident fluid. For aquifer remediation with in situ soil washing techniques, the same processes are observed. Viscous fingering occurs generally when the displacing fluid is

less viscous than the displaced fluid, as is the case when water is used to displace a more viscous washing solution (Lake, 1989).

Polymers can be added to flushing solutions to improve sweep efficiency by increasing the viscosity of the injection water, which increases the displacing phase viscosity. This will decrease viscous fingering and thereby increase sweep efficiency (Martel et al., 2004). A reduction in hydraulic conductivity of the areas with higher permeability areas will promote flow into areas with lower permeability, thereby decreasing the influence of heterogeneity.

A variety of polymer types have been evaluated for use to increase viscosity in the petroleum industry such as xanthan gum, hydrolyzed polyacrylamide, hydroxethylcellulose, carboxymethylhydroxyethylcellulose and glucan. Among these, polyacrylamide and xanthan gum are the most widely used polymers for altering the mobility ratio. Polyacrylamide is the only polymer that will increase solution viscosity and cause a significant reduction in effective water permeability. The other most common polymer, xanthan gums (biopolymers and polysaccharides), are produced by a mutant of *Xanthomonas campestris* (Lunn and Kueper, 1999).

2.6. Legal Aspects of NAPL Management in the Subsurface

The awareness and concern developed for the hazards threatening the groundwater sources is increasing as the water sources are becoming scarce day by day. NAPL contamination is perceived as a significant environmental threat by the general public and the regulatory communities and as a result, NAPL remediation standards are extremely conservative. In Turkey, there is a growing recognition of soil and groundwater pollution problems after the enforcement of the regulations of the Control of Solid Wastes (Official Gazette, 1991) and the Control of Hazardous Wastes (Official Gazette, 1995). The main purpose of these regulations is to provide a legal framework for the management of municipal solid wastes and hazardous wastes throughout the nation. The collection, transportation and disposal of wastes that can be harmful to human health and the environment are the focus of these regulations which provide technical and administrative

standards for construction and operation of disposal sites and related legal and punitive responsibilities (Pankow and Cherry, 1996).

Turkey presently relies heavily on surface water resources to satisfy the main daily water supply demands. Groundwater constitutes a relatively small component of total available resources (17%) but it represents a significant portion (27%) of total water withdrawal. However, due to growing water demand parallel to rapid population and industrial growth, an increasing demand for food production, urban expansion and accelerated degradation of surface water quality, protection of clean groundwater resources as well as remediation of contaminated soil and groundwater sites are becoming environmental issues of high priority. Although legislation on groundwater exists, their protection appears to be neglected in many areas. With the spread of uncontrolled irrigation practices, the pollution threat to groundwater is also increasing. The control of soil and groundwater contamination is essential to Turkey's reliance on groundwater resources for potable water (NATO/CCMS, 2003).

3. TERNARY PHASE DIAGRAMS

3.1. Phase Behaviour and Equilibrium

The phase behaviour concept is a useful tool for describing the solubilization potential of the components within the various phases present in the system. Within a water-NAPL-chemical agent system, the NAPL phase behaviour. Understanding the compositional changes that a water-NAPL-agent system undergoes is a rapid means for predicting the performance of any remedial action involving in-situ flooding. It particularly quantifies the degree of solubilization (increase solubility of the organic phase in the aqueous phase) or partitioning (increase solubility of the aqueous phase in the organic phase).

In order to visualize these relations, ternary phase diagrams are widely used (Falta, 1998; Martel et al., 1998; Roeder, 1998; Reitsma et al., 1998; Ramsburg et al., 2002; Parker, 2003; St-Pierre et al., 2004). These diagrams are composed of miscibility curves and tie-lines and are particularly useful in that they show all three components of a reaction system on one plot. The curve separating the regions where all liquids are fully miscible from the region where the liquids are not fully immiscible is called the miscibility curve. The tie lines, on the other hand, are defined as the line of constant interfacial tension which join the aqueous and organic segments of the miscibility curve. These lines indicate the equilibrium compositions of the two phases and transect the two-phase region. The points connected by the tie lines define the composition of the aqueous phase and the organic phase (Falta, 1998).

For the determination of the miscibility envelope experimentally, visual titration is used, whereas for the tie-lines chemical analysis of the components present in each phase is required. The details of the construction of the miscibility curves and tie lines with experimental and numerical data are given in the following sections.

3.2. Theory of Ternary Phase Diagrams

. The ternary phase diagrams can be experimentally determined by the analysis of a binary mixture of miscible liquids titrated with a third liquid that is miscible with only one of the components. Using the three axis, the overall system mass fractions of the three components can be determined for any point inside the miscibility envelope (Falta, 1998). A typical ternary phase diagram and its components are given in Figure 3.1. The curve separating the the regions where all liquids are fully miscible from the region wherethe liquids are not fully immiscible is called the miscibility curve.

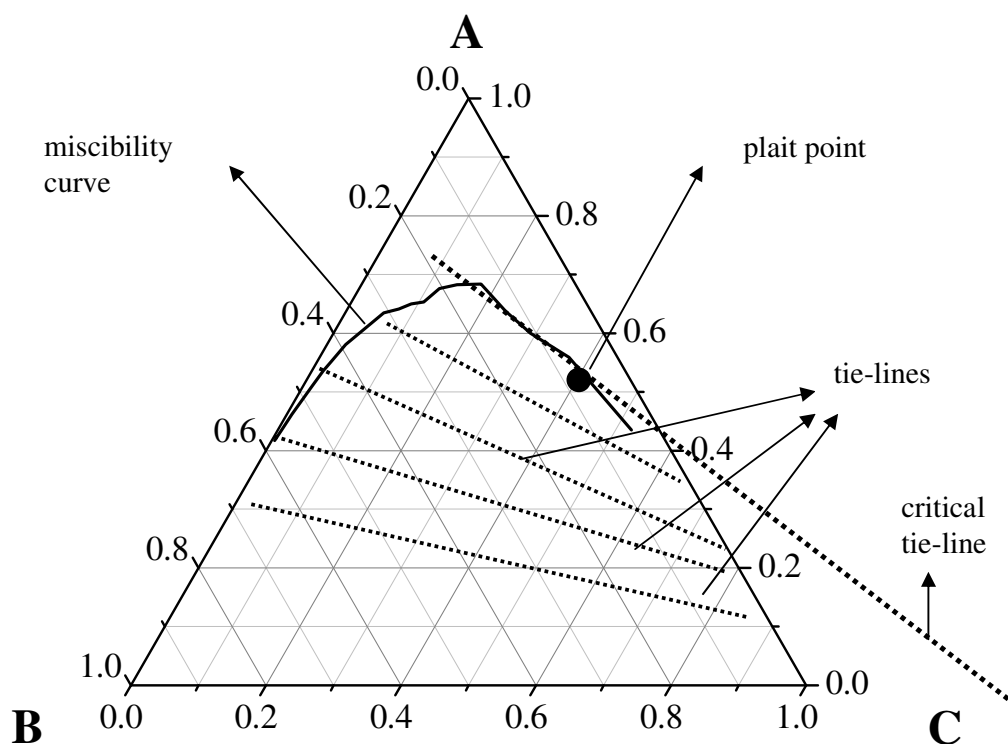


Figure 3.1. Ternary phase diagram.

The presence of single or multiple phases is detected by the transparent or cloudy appearance of liquids. The presence of the cloud point indicates the boundary between the single-phase zone and the multiple-phase zone (Martel et. al., 1998; St-Pierre et. al., 2004). The area below the miscibility curve indicates the range of the component fractions where the three components exist as two separate phases while the upper part of the curve the

composition range is indicated where these components exist as a single phase. The data points required to draw a miscibility curve in a phase diagram can easily be obtained by the titration of the components against each other or by numerical simulation based on the principles of thermodynamics and multiphase equilibrium (Lee and Peters, 2004).

The composition conditions in which the three coexisting phases of partially soluble components of a three-phase liquid system approach each other in composition gives the plait point (Parker, 2003). The plait point can also be located by the zero interfacial tension.

Ternary phase diagrams can give a rough estimate of the preference of the chemical agent in a NAPL-water system. When the tie lines slope down toward the NAPL endpoint, it indicates that the chemical agent in the system is preferentially soluble in water. In such a case, when the chemical agent concentration is below the miscibility curve, the primary removal mechanism will be NAPL dissolution. Imhoff et al. (1995) reported that the dissolution process in such systems can be rate-limited. Addition of the chemical agent reaching levels close to the miscibility curve can also reduce the interfacial tension which may cause NAPL mobilization. If chemical agent content in the system exceeds miscibility levels, the interfacial tension will be reduced to zero where complete miscibility and mobilization of the NAPL is experienced.

Ternary phase diagrams with tie lines sloping down toward the water axis can be defined such that the chemical agent is preferentially soluble in the NAPL phase. If chemical agent concentrations are kept below the miscibility curve, the primary removal mechanism will be NAPL mobilization in response to a reduction of interfacial tension and swelling of the NAPL phase (Falta, 1998).

Three composition variables, x_A , x_B and x_C are needed to specify the composition of an arbitrary mixture of three components where A represents the chemical agent(s); B, water and C, the contaminant. Alternatively, the diagram could be shown such that each axis shows the mass ratio of each component. For one mole of such a mixture, the following equation of constraint should be taken into account and only two composition variables are independent.

$$x_A + x_B + x_C = 1 \quad (3.1)$$

All points on the ternary phase diagrams satisfy Equation 3.1. Compositional phase diagrams for three-component systems are constructed on the basis of this triangle. The apex at the bottom left corresponds to 100% of component A. The opposing apex, on the other hand correspond to 0% of component A, but the line maps out components B-C mixtures from 0% component B at the bottom-right apex to 100% component B at bottom-left apex. The gridlines in between correspond to increasing amounts of component B while moving from the bottom-right apex to the bottom-left apex.

For three component systems the phase rule can be expressed as follows:

$$\text{number of phases} + \text{degrees of freedom} = \text{number of components} + 2 = 5 \quad (3.2)$$

or

$$\text{degrees of freedom} = 5 - \text{number of phases} \quad (3.3)$$

If the mixture consists of a single phase then the degree of freedom equals 4. If the values of pressure and temperature are specified then the two remaining degrees of freedom, i.e. the composition can be changed without altering the number of phases, which is a single phase system in this case. On the other hand, if two phases are present then only one composition variable exists at fixed temperature and pressure. If the mole fraction of one component is specified, then no degrees of freedom remains and the proportions of all three components are fixed in each phase (Atkins, 1998).

3.3. Numerical Methods for the Construction of TPDs

In addition to the experimental procedures ternary phase diagrams can be determined numerically. The main advantage of developing a numerical method for constructing ternary phase diagrams is that they can be used to quickly and inexpensively evaluate the performance of different flushing agents, or to assess the sensitivity of the multiphase system to the operational parameters such as temperature. For optimal reliability, it is

important however that the numerically derived results are validated with the experimentally determined ones.

Mathematically, the multiphase equilibrium can be represented by a series of algebraic equations that relates the mole fraction of each component within the different phases. For a multiphase system consisting of two phases, an aqueous phase (w) and a NAPL phase (n), and three components (water, w; NAPL, n; and Agent a): The governing system of algebraic equations is

$$\begin{aligned} \gamma_{w,w}x_{w,w} &= \gamma_{w,n}x_{w,n} \\ \gamma_{n,w}x_{n,w} &= \gamma_{n,n}x_{n,n} \\ \gamma_{a,w}x_{a,w} &= \gamma_{a,n}x_{a,n} \end{aligned} \tag{3.4}$$

where x is the mole fraction, $\gamma_{i,j}$ is the activity coefficient, the first subscript denotes the component (w, n, or a) and the second subscript denotes the phase (w or n). Because the activity coefficient data are function of the mole fractions, the resultant system of equations is nonlinear. Therefore, an iterative procedure must be used to compute the mole fractions at equilibrium.

Fluid phase equilibrium and mixing properties are of primary interest for various applications such as equipment optimization, mathematical models, parameter estimation, etc). The knowledge of multicomponent phase equilibrium data is important for liquid-liquid systems (Reitsma and Kueper, 1998). To extend the scarce knowledge of mixing thermodynamic, liquid-liquid equilibrium systems can be identified using activity coefficient data. One of the most popular methods for estimation of activity coefficient data is the group contribution method UNIFAC (UNIQuac Functional-group Activity Coefficient). This method has been integrated into many commercial simulators. Due to the importance of theoretical data on industrial design, functional group contribution methods were applied. The functional group contribution methods are a reliable path for, at least, a qualitative prediction of liquid-phase activity coefficients.

The UNIFAC method was also integrated into a FORTRAN computer program that was developed to determine the miscibility curve up to the plait point, and the tie line. The general algorithm used for the calculation of the equilibrium mole fractions was to develop first a database of activity coefficients for the compounds of interest and for various mole fractions using UNIFAC. This database was then used in the iterative procedure to compute the mole fractions representing multiphase equilibrium conditions.

In the following sections, the principles behind the UNIFAC methodology are first described. This is followed by a description of the computer code that was written for the determination of the TPD. This program was primarily used to compute the non-linear system of equations describing multiphase equilibrium.

3.3.1. UNIFAC Model and Activity Coefficients

UNIFAC is a group contribution method that is used to predict equilibria in systems of binary and multiphase systems. The method is based on the UNIQUAC (UNiversal QUAasiChemical) equation, but is completely predictive in the sense that it does not require interaction parameters. Instead, these are computed from group contributions of all the molecules in the mixture (Fredenslund et al., 1975). UNIFAC is preferred based on its predictive capability for a large number of strongly polar chemical components. In the group contribution concept of the method, each compound is considered as basic functional groups. The mixture of compounds is defined as a mixture of these functional groups and properties of the mixture is computed with the functional groups and interactions in between (Lee and Peters, 2004). In the model it is also assumed that any pair of the functional groups interacts in the same manner regardless of the presence of any other groups. The logarithm of the activity coefficient is predicted as the sum of the two contributions, residual and combinatorial.

$$\ln \gamma_i = \underbrace{\ln \gamma_i^C}_{\text{combinatorial}} + \underbrace{\ln \gamma_i^R}_{\text{residual}} \quad (3.5)$$

The combinatorial contribution comes from differences in size and shape of the compounds in the mixture and is expressed as:

$$\ln \gamma_i = \ln \frac{\phi_i}{x_i} + \frac{z}{2} q_i \ln \frac{\theta_i}{\phi_i} + \ell_i - \frac{\phi_i}{x_i} \sum_{j=1}^N x_j \ell_j \quad (3.6)$$

where θ_i is the molecular surface area fraction for component i and is defined as:

$$\theta_i = \frac{q_i x_i}{\sum_{j=1}^N x_j q_j} \quad (3.7)$$

and ϕ_i is the molecular volume fraction for component i which is computed as follows:

$$\phi_i = \frac{r_i x_i}{\sum_{j=1}^N r_j x_j} \quad (3.8)$$

The van der Waals surface area and volume for molecule i are calculated from:

$$r_i = \sum_{k=1}^{n_e} v_k^i R_k \quad \text{and} \quad q_i = \sum_{k=1}^{n_e} v_k^i Q_k \quad (3.9)$$

where v_k^i is the number of group k in the molecule i . R_k and Q_k are the surface area and volume for group.

The parameter ℓ_i in the combinatorial term is computed as:

$$\ell_i = \frac{z}{2} (r_i - q_i) - (r_i - 1) \quad ; \quad z = 10 \quad (3.10)$$

where z is the coordination number and is usually taken as 1.

The residual contribution, on the other hand, results from energy interactions and is computed as:

$$\ln \gamma_i^R = \sum_{k=1}^{n_e} v_k^i (\ln \Gamma_k - \ln \Gamma_k^i) \quad (3.11)$$

The residual activity coefficient of group k is estimated from:

$$\ln \Gamma_k = Q_k \left[1 - \ln \left(\sum_{m=1}^{N_e} \theta_m \psi_{mk} \right) - \sum_{m=1}^{N_e} \frac{\theta_m \psi_{mk}}{\sum_{n=1}^{N_e} \theta_n \psi_{nm}} \right] \quad (3.12)$$

where θ_m is the surface area function group of group m and is calculated from:

$$\theta_m = \frac{x_m Q_m}{\sum_{n=1}^{N_e} x_n Q_n} \quad (3.13)$$

x_m is defined as the mole fraction of group m in mixture and can be formulated as:

$$x_m = \frac{\sum_{j=1}^N v_m^j x_j}{\sum_{j=1}^N \sum_{n=1}^{n_e} v_n^j x_j} \quad (3.14)$$

Finally, the parameter ψ_{mk} is expressed as:

$$\psi_{mk} = \exp \left(-\frac{a_{nm}}{T} \right) \quad (3.15)$$

where a_{nm} is the interaction energy between groups m and n.

Main Groups in used UNIFAC calculations are given in Table 3.1, whereas the sub groups are listed in Table 3.2.

Table 3.1. Main Groups for UNIFAC calculations (Magnussen et al., 1981).

1	CH2	10	CHO	19	CCN	28	CS2	37	CICC	46	CON
2	C=C	11	COOC	20	COOH	29	CH3SH	38	ACF	47	OCCOH
3	ACH	12	HCOO	21	CCl	30	Furfur.	39	DMF	48	CH2S
4	ACCH2	13	CH2O	22	CCl2	31	DOH	40	CF2	49	Morpholine
5	OH	14	CNH2	23	CCl3	32	I	41	COO	50	Thiophene
6	MeOH	15	CNH	24	CCl4	33	Br	42	SiH2	51	NMC
7	H2O	16	C3N	25	ACCl	34	C#C	43	SiO	52	N(C)CO
8	ACOH	17	ACNH2	26	CNO2	35	DMSO	44	NMP	53	SO2
9	CH2CO	18	Pyridine	27	ACNO2	36	ACRY	45	CCIF	54	BF3

Table 3.2. Subgroups for UNIFAC calculations (Magnussen et al., 1981).

1	CH3-	24	HCOO-	47	>CCl-	70	-Cl	93	CCl2F2
2	-CH2-	25	CH3O-	48	CH2Cl2	71	ACF	94	-CONH2
3	-CH<	26	-CH2O-	49	-CHCl2	72	DMF-1	95	-CONHCH3
4	>C<	27	>CHO-	50	>CCl2	73	DMF-2	96	-CONHCH2-
5	CH2=CH-	28	>FCH2O-	51	CHCl3	74	-CF3	97	-CON(CH3)2
6	-CH=CH-	29	CH3NH2	52	-CCl3	75	-CF2-	98	-CONMeCH2-
7	CH2=C<	30	-CH2NH2	53	CCl4	76	>CF-	99	-CON(CH2-)-2
8	-CH=C<	31	>CHNH2	54	ACCl	77	-COO-	100	C2H5O2
9	>C=C<	32	CH3NH-	55	CH3NO2	78	-SiH3	101	C2H4O2-
10	ACH	33	-CH2NH-	56	-CH2NO2	79	>SiH2	102	CH3S-
11	AC-	34	>CHNH-	57	>CHNO2	80	>SiH-	103	-CH2S-
12	AC-CH3	35	CH3N<	58	ACNO2	81	>Si<	104	>CHS-
13	AC-CH2-	36	-CH2N<	59	CS2	82	-SiH2O-	105	Morpholine
14	AC-CH<	37	ACNH2	60	CH3SH	83	>SiHO-	106	C4H4S
15	-OH	38	C5H5N	61	-CH2SH	84	->SiO-	107	C4H3S
16	CH3OH	39	C5H4N-	62	Furfural	85	NMP	108	C4H2S
17	H2O	40	C5H3N<	63	(CH2OH)2	86	CCl3F	109	NMC
18	AC-OH	41	CH3CN	64	I-	87	CCl2F-	110	-N(CH3)CO
19	CH3-CO-	42	-CH2CN	65	Br-	88	HCCl2F	111	-N(CH2-)CO-
20	-CH2-CO-	43	-COOH	66	HC#C-	89	HCClF-	112	-N(CH<)CO-
21	-CHO	44	HCOOH	67	-C#C-	90	CClF2-	113	-N(C<-)CO-
22	CH3COO-	45	-CH2Cl	68	DMSO	91	HCClF2	114	SO2
23	-CH2COO-	46	>CHCl	69	ACRY	92	CClF3	115	BF3

3.3.2. Simulation of Activity Data

The UNIFACAL software developed by Choy and Reible (1996) was used in this thesis for the calculation of the activity coefficients using UNIFAC method. The program's interface is shown in Figure 3.2.

The software enables calculation of multicomponent-multiphase activity coefficients at different temperatures provided that the components are already defined in the database or the subgroups are specified for that component. Once the components are defined (Figure 3.3) and the temperature is selected, the activity coefficients are calculated for different molar compositions and recorded in an excel chart. In some instances, the basic supported program sometimes gave erroneous results outside the expected range, in such cases interpolation is applied with the data close to that region. The UNIFAC interaction parameters used in the computer program are obtained from Hansen et al. (1991).

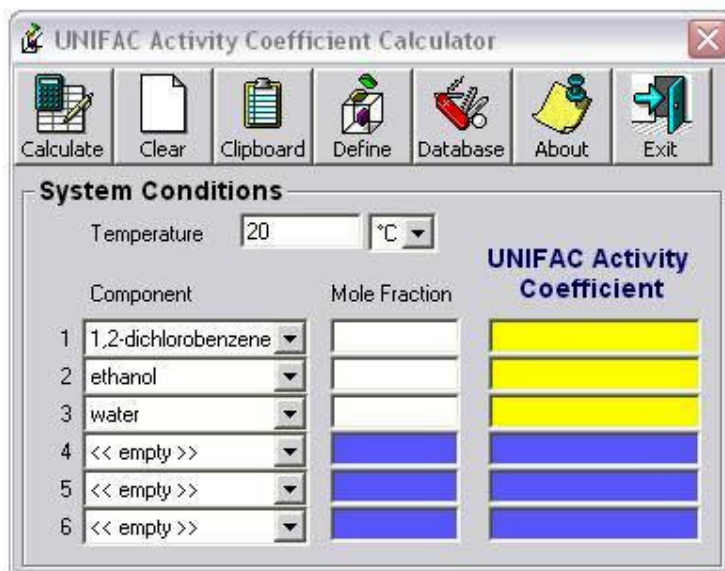


Figure 3.2. The UNIFACAL Interface.

A sample activity coefficient database file is shown in Figure 3.4. The values in the first row and in the first column are the mole fractions for NAPL and chemical agent, respectively. The values in the middle of the spreadsheet are the activity coefficients computed from UNIFAC. This file is used as an input file to the FORTRAN code that is used to calculate the equilibrium mole fraction. The FORTRAN code is described in the following section.

Sub #	Group	Main #	R	Q	Number
1	CH3	1	.9011	.848	1
2	CH2	1	.6744	.54	1
15	OH	5	1	1.2	1

Figure 3.3. A sample definition of components in UNIFACAL Software.

input - Not Deferi											
Dosya	Düzen	Bijim	Görünüm	Yardım							
0.	0.	0.1	0.2	0.3	0.4	0.5	0.6	0.7	0.8	0.9	1.
0.	193330.	12499.0	2112.50	599.05	231.74	109.3900	58.9550	34.7520	21.7410	14.1090	9.3206
0.001	173300.	11679.0	2015.30	578.42	225.49	107.0000	57.8810	34.2120	21.4470	13.9380	9.3206
0.002	155640.	10923.0	1923.50	558.67	219.46	104.6800	56.8330	33.6830	21.1570	13.7700	9.3206
0.005	113970.	8978.80	1677.00	504.25	202.54	98.0870	53.8350	32.1590	20.3190	13.2830	9.3206
0.01	70099.0	6578.60	1346.20	427.46	177.87	88.2540	49.2850	29.8180	19.0190	12.5210	9.3206
0.02	29581.0	3720.00	894.090	313.18	139.02	72.1360	41.6040	25.7760	16.7350	11.1640	9.3206
0.05	4004.10	927.750	318.610	140.24	72.7050	42.1190	26.3290	17.3210	11.7640	8.1158	9.3206
0.1	458.230	183.370	89.7850	50.3800	31.0540	20.4290	14.0460	9.9301	7.1193	5.1139	-9.0000
0.2	41.8130	26.6640	9.6503	13.0340	9.7794	7.2998	5.5845	5.2726	3.2605	-9.0000	-9.0000
0.3	11.5340	8.8453	6.9532	5.5556	4.4787	3.6180	3.3249	2.3151	-9.0000	-9.0000	-9.0000
0.4	5.2058	4.3518	3.6624	3.0876	2.5947	2.1627	1.7821	-9.0000	-9.0000	-9.0000	-9.0000
0.5	3.0480	2.6616	2.3188	2.0079	1.7217	1.4609	-9.0000	-9.0000	-9.0000	-9.0000	-9.0000
0.6	2.0804	1.8583	1.6476	1.5119	1.2597	-9.0000	-9.0000	-9.0000	-9.0000	-9.0000	-9.0000
0.7	1.5667	1.4164	1.3128	1.1324	-9.0000	-9.0000	-9.0000	-9.0000	-9.0000	-9.0000	-9.0000
0.8	1.2642	1.1535	1.0547	-9.0000	-9.0000	-9.0000	-9.0000	-9.0000	-9.0000	-9.0000	-9.0000
0.9	1.0806	1.0130	-9.0000	-9.0000	-9.0000	-9.0000	-9.0000	-9.0000	-9.0000	-9.0000	-9.0000
1.	1.0000	-9.0000	-9.0000	-9.0000	-9.0000	-9.0000	-9.0000	-9.0000	-9.0000	-9.0000	-9.0000
0.	7.6988	3.4345	2.1509	1.6147	1.3473	1.1999	1.1138	1.0616	1.0291	1.0087	1.0000
0.001	7.4366	3.3671	2.1244	1.6015	1.3399	1.1953	1.1109	1.0597	1.0279	1.0082	1.0000
0.002	7.1882	3.3021	2.0985	1.5886	1.3325	1.1908	1.1080	1.0579	1.0268	1.0076	1.0000
0.005	6.5170	3.1200	2.0248	1.5515	1.3113	1.1778	1.0997	1.0527	1.0237	1.0061	1.0000
0.01	5.6007	2.8543	1.9135	1.4943	1.2782	1.1573	1.0867	1.0445	1.0189	1.0040	1.0000
0.02	4.2960	2.4334	1.7271	1.3955	1.2201	1.1211	1.0637	1.0301	1.0108	1.0009	1.0000
0.05	2.4035	1.6899	1.3594	1.1878	1.0936	1.0415	1.0139	1.0010	0.9971	1.0012	1.0000
0.1	1.3789	1.1734	1.0655	1.0091	0.9826	0.9742	0.9773	0.9876	1.0039	1.0310	-9.0000
0.2	0.8919	0.8845	0.9401	0.9127	0.9736	0.9733	1.0112	1.0909	1.1153	-9.0000	-9.0000
0.3	0.8300	0.8686	0.9136	0.9640	1.0196	1.0809	1.1947	1.2493	-9.0000	-9.0000	-9.0000
0.4	0.8958	0.9594	1.0291	1.1056	1.1911	1.2928	1.4374	-9.0000	-9.0000	-9.0000	-9.0000
0.5	1.0407	1.1297	1.2287	1.3421	1.4817	1.6903	-9.0000	-9.0000	-9.0000	-9.0000	-9.0000
0.6	1.2651	1.3906	1.5382	1.8430	2.0250	-9.0000	-9.0000	-9.0000	-9.0000	-9.0000	-9.0000
0.7	1.5958	1.7870	2.2108	2.4665	-9.0000	-9.0000	-9.0000	-9.0000	-9.0000	-9.0000	-9.0000
0.8	2.0988	2.4405	3.0513	-9.0000	-9.0000	-9.0000	-9.0000	-9.0000	-9.0000	-9.0000	-9.0000
0.9	2.9487	3.8322	-9.0000	-9.0000	-9.0000	-9.0000	-9.0000	-9.0000	-9.0000	-9.0000	-9.0000
1.	4.8866	-9.0000	-9.0000	-9.0000	-9.0000	-9.0000	-9.0000	-9.0000	-9.0000	-9.0000	-9.0000
0.	1.0000	1.0397	1.1269	1.2381	1.3634	1.4978	1.6395	1.7914	1.9665	2.2051	2.6405
0.001	1.0001	1.0421	1.1304	1.2425	1.3685	1.5036	1.6460	1.7988	1.9751	2.2162	2.6405
0.002	1.0002	1.0444	1.1340	1.2469	1.3737	1.5094	1.6525	1.8061	1.9838	2.2274	2.6405
0.005	1.0013	1.0519	1.1449	1.2603	1.3892	1.5269	1.6722	1.8285	2.0102	2.2614	2.6405
0.01	1.0050	1.0652	1.1638	1.2833	1.4157	1.5568	1.7057	1.8666	2.0552	2.3200	2.6405
0.02	1.0182	1.0950	1.2039	1.3313	1.4707	1.6187	1.7753	1.9459	2.1497	2.4447	2.6405
0.05	1.0927	1.2068	1.3425	1.4926	1.6534	1.8236	2.0059	2.2114	2.4730	2.8913	2.6405
0.1	1.2968	1.4569	1.6327	1.8212	2.0219	2.2375	2.4778	2.7705	3.1946	4.0158	-9.0000
0.2	1.9468	2.1955	3.0749	2.7533	2.9209	3.4497	3.9322	5.6697	6.2092	-9.0000	-9.0000
0.3	2.9681	3.3428	3.7594	4.3279	4.8211	5.6122	8.7421	9.7670	-9.0000	-9.0000	-9.0000
0.4	4.5356	5.1348	5.8482	6.7563	8.0511	10.2860	15.6570	-9.0000	-9.0000	-9.0000	-9.0000
0.5	7.0095	8.0768	9.4929	11.6100	15.4800	25.6420	-9.0000	-9.0000	-9.0000	-9.0000	-9.0000
0.6	11.1640	13.3750	16.8370	36.4640	43.0440	-9.0000	-9.0000	-9.0000	-9.0000	-9.0000	-9.0000
0.7	18.9050	24.5700	62.1680	74.3650	-9.0000	-9.0000	-9.0000	-9.0000	-9.0000	-9.0000	-9.0000
0.8	36.1030	56.5570	132.900	-9.0000	-9.0000	-9.0000	-9.0000	-9.0000	-9.0000	-9.0000	-9.0000
0.9	89.4970	247.320	-9.0000	-9.0000	-9.0000	-9.0000	-9.0000	-9.0000	-9.0000	-9.0000	-9.0000
1.	483.410	-9.0000	-9.0000	-9.0000	-9.0000	-9.0000	-9.0000	-9.0000	-9.0000	-9.0000	-9.0000

Figure 3.4. A sample input file.

3.3.3. FORTRAN Programme for Phase Equilibrium Calculations

A FORTRAN computer program was developed to calculate phase equilibrium in a ternary two-phase system by simultaneously solving the equilibrium equations for all three components. The computer program was designed to construct an entire ternary phase diagram by initially determining, in the absence of any cosolvent, the equilibrium mole fractions of the NAPL component in the aqueous phase and the water component in the NAPL phase. The program incrementally increases the cosolvent mole fraction in the aqueous phase and calculates new equilibrium mole fractions for all components in both aqueous and NAPL phases. The calculations start with an initial guess for all parameters

and these parameters are given with boundary information. A sample guess file is given in Figure 3.5.

Parameter	Initial Guess	Upper Bound	Lower Bound	Comment
7				! number of points on miscibility curve
0.00	0.999	0.00	0.01	! xaw and initial guesses for xww, xan, xwn
	0.999999	0.00	0.05	! upper bounds for xww, xan, xwn
	0.99	0.00	0.00	! lower bounds for xww, xan, xwn
0.10	0.88	0.05	0.01	! xaw and initial guesses for xww, xan, xwn
	0.9	0.1	0.05	! upper bounds for xww, xan, xwn
	0.85	0.0	0.00	! lower bounds for xww, xan, xwn
0.20	0.75	0.10	0.05	! xaw and initial guesses for xww, xan, xwn
	0.799999	0.2	0.1	! upper bounds for xww, xan, xwn
	0.70	0.0	0.00	! lower bounds for xww, xan, xwn
0.30	0.65	0.1	0.05	! xaw and initial guesses for xww, xan, xwn
	0.699999	0.2	0.1	! upper bounds for xww, xan, xwn
	0.60	0.0	0.00	! lower bounds for xww, xan, xwn
0.40	0.50	0.2	0.05	! xaw and initial guesses for xww, xan, xwn
	0.599999	0.4	0.1	! upper bounds for xww, xan, xwn
	0.40	0.0	0.00	! lower bounds for xww, xan, xwn
0.50	0.40	0.25	0.05	! xaw and initial guesses for xww, xan, xwn
	0.499999	0.30	0.1	! upper bounds for xww, xan, xwn
	0.20	0.0	0.00	! lower bounds for xww, xan, xwn
0.52	0.30	0.3	0.1	! xaw and initial guesses for xww, xan, xwn
	0.399999	0.6	0.2	! upper bounds for xww, xan, xwn
	0.20	0.0	0.00	! lower bounds for xww, xan, xwn

Figure 3.5. A sample guess file.

The number of points to be used in the iterations- initial guesses for the chemical agent content of the water phase (x_{aw}), the water content in the aqueous phase (x_{ww}), the chemical agent content of the NAPL phase (x_{an}) and the water content in the NAPL phase (x_{wn})- are given as guess values with upper and lower bounds. These bound values tend to reduce the number of iterations needed to compute the equilibrium mole fractions.

Starting with the initial values of the mole fractions for each component in the aqueous and NAPL phases, the mole fractions corresponding to multiphase equilibrium are computed iteratively. The goal of the iterative procedure is to reduce the function F which is defined as:

$$F = \sum_{i=1}^3 \text{ABS}(x_i^N \gamma_i^N - x_i^W \gamma_i^W) \quad (3.16)$$

At equilibrium, the F function should be exactly or very close to zero. The algorithm used for the minimization of the F objective function given in Equation 3.16 is BC POL subroutine from the IMSL library (Version 1, 1987). At the beginning of each iteration, the program retrieves from the activity coefficient database the activity coefficient values corresponding to the current mole fractions. The current mole fractions are the guess

values for the first iteration or the values obtained at the end of the previous iteration for iterations two and above.

Because the current mole fractions may not match exactly the stored mole fractions in the activity coefficient database, an interpolation scheme is used. The Fortran code includes two different interpolation options, a linear interpolation scheme and a logarithmic interpolation scheme. The latter scheme takes the natural log of all the activity coefficients prior to interpolation. Once the interpolation with the log transforms of the data is performed, the exponential of the interpolated values are computed and used in the minimization of the F objective function. Results showed that both interpolation schemes produced close results, provided the mole fraction intervals in the activity coefficient database were small. Furthermore, it was found that using smaller intervals wherever the activity coefficient exhibited large variations produced more accurate results.

The calculation is repeated until the two phases converge to the plait point. The interface of the Fortran code used for the determination of tie-line data and plait point is given in Figure 3.6. A listing of the full Fortran code is given in Appendix A.

```

Microsoft Developer Studio - code - [code nonequal intervals.for]
File Edit View Insert Build Tools Window Help
input
code - Win32 Debug
code files
  code.for
  MATHD.LIB
  MATHS.LIB
c constructs ternary phase diagrams from UNIFAC output
c Feb 26, 2007
c with option for LiNEAR logarithm interpolation
c implicit double precision (a-h, o-z)
parameter (N=3,na0=11,nn0=17,ninta=101,nintn=101)
common fff,xaw,gn(na0,nn0),ga(na0,nn0),gw(na0,nn0)
common xa0(na0),xn0(nn0),ilog

c interpolated activity coefficient (NOT used in the minimization of F)
Dimension xa(ninta),xn(nintn),
& gamman(ninta,nintn),gammaa(ninta,nintn),gammav(ninta,nintn)

c variables used in the BCPOL subroutine
REAL FVALUE, X(N), XGUESS(N), XLB(N), XUB(N)
EXTERNAL BCPOL, FCN
EXTERNAL DBCPOL, FCN

c variables used in the BCONF subroutine
c DIMENSION XSCALE(N), IPARAM(N), RPARAM(N)
c *****

ilog=0
c List of parameters
c ilog=0 linear interpolation
c ilog=1 interpolation using the log of the activity coefficients
c na0: no of agent mole fractions in the input file (from UNIFAC)
c nn0: no of NAPL mole fractions in the input file (from UNIFAC)
c ninta: no of interpolated data- agent
c nintn: no of interpolated data- napl
c gn,ga,gw: activity coef. data from UNIFAC- input
c gamman,gammaa,gammav: interpolated activity coef. data
c xa,xn: interpolated agent and napl mole fractions
c three unknowns are: x(1)=xww, x(2)=xan, x(3)=xwn

c DATA XSCALE/1.0,1.0,1.0/
c *****

```

-----Configuration: code - Win32 Debug-----
code.exe - 0 error(s), 0 warning(s)

Build Debug Find in Files Profile

Figure 3.6. Fortran Code used in simulations

3.3.4. Analysis of the Fortran Derived Data

The typical output file of the simulations is given in Figure 3.7. Corresponding phase compositions are written on the same line together with the F-function which shows how close the output data is to the theoretical data with the given guess and input data. The results in the last line in the output file below is an example of the “plait point” where the concentrations of the NAPL phase and aqueous phase are same. The very low value of the F-function is also supporting the fact that the plait point is reached.

xnw,	xaw,	xww,	xnn,	xan,	xwn	f
.000001	.000000	.999999	.997895	.000000	.002105	.792240
.000000	.100000	.900000	.912600	.084249	.003151	.914941
.000001	.200000	.799999	.910550	.087432	.002018	.851029
.001283	.300000	.698717	.897800	.100005	.002196	.023051
.003459	.400000	.596541	.922561	.076421	.001018	.000072
.007115	.500000	.492885	.924709	.074514	.000778	.000034
.279997	.520000	.200003	.280004	.519996	.200000	.000038

Figure 3.7. A sample output file.

3.4. Experimental Methods for the Construction of TPDs

3.4.1. Chemicals

1,2-Dichlorobenzene and toluene were selected as the model contaminants in the TPD experiments. Both contaminants are listed under “EPA-List of Priority Pollutants” as groundwater contaminants (Bedient et al., 1999). 1,2-Dichlorobenzene was employed in the study as a DNAPL model substance representative of aromatic chlorinated solvents. Toluene was selected as the LNAPL model because BTEX (benzene-toluene-ethylbenzene-xylene) are the most common LNAPL contaminants in soil and groundwater and toluene is representative of nonchlorinated solvents. The 3D molecular structures of 1,2 dichlorobenzene and toluene are given in Figures 3.8 and 3.9, respectively. The properties of the model contaminants are summarized in Table 3.3. For visualization

purposes, an organic soluble dye, Oil-Red-O (Figure 3.10) was added at a concentration of $4 \cdot 10^{-4}$ M to color the organic contaminants.

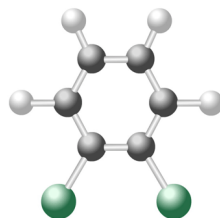


Figure 3.8. Molecular structure of 1,2-dichlorobenzene (www.karlyoder.com).

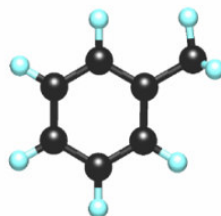


Figure 3.9. Molecular structure of toluene (www.tennoji-h.oku.ed.jp).

Table 3.3. Fluid properties at room temperature .

Property	1,2-Dichlorobenzene	Toluene
Aqueous Solubility (mg/L)	100	515
Density (mg/L)	1.305	0.8669
Dynamic Viscosity (cp)	1.32	0.58
Vapor Pressure (mmHg)	1.2	22

1,2-Dichlorobenzene, toluene, ethanol (absolute), methanol, chloroform, SDS, Hyamine and potassium 2-p-toluidynaphthalene-6-sulfonate (TNS) were purchased from Merck and used as received. Hydroxypropyl- β -cyclodextrin (HPCD) was purchased from Acros Chemicals Inc. Distilled water was used for all tests.

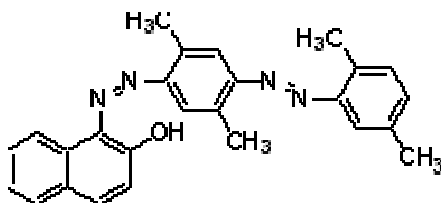


Figure 3.10. Molecular structure of Oil-Red-O (Tuck et al., 2003).

3.4.2. Analysis Procedures for the determination of TPDs

3.4.2.1. Cloud point titration. The titrations conducted for the determination of the turnover points between one-phase and two-phase regions were accomplished in mini-titration vials. The experimental set-up that was used in titrations is given in Figure 3.11. All equilibrium phase behaviour experiments were conducted at room temperature around 24°C.



Figure 3.11. The titration set-up used for the determination of miscibility points.

Known amount of a chemical solution (containing alcohol, surfactant, organic contaminant, etc.) was placed in a glass vial capped with a Teflon minivalve to minimise contaminant losses due to evaporation. The components of the ternary phase diagram (contaminant, water and chemical agents) were added gradually to the solution using gastight macrosyringes as shown in Figure 3.12. The turning point was observed directly from the change in transparency. After the determination of the first point, chemical solution was further added to move the mixture out of the cloudy zone to reach the one

phase zone again. The second point of the miscibility curve was obtained by adding water to reach again a cloudy zone. The miscibility curve was drawn with 5-9 of the determined values. Phase diagrams were established on mass basis. The basic steps of constructing a ternary phase diagrams is sketched shown in Figure 3.13.



Figure 3.12. Gastight macrosyringes.

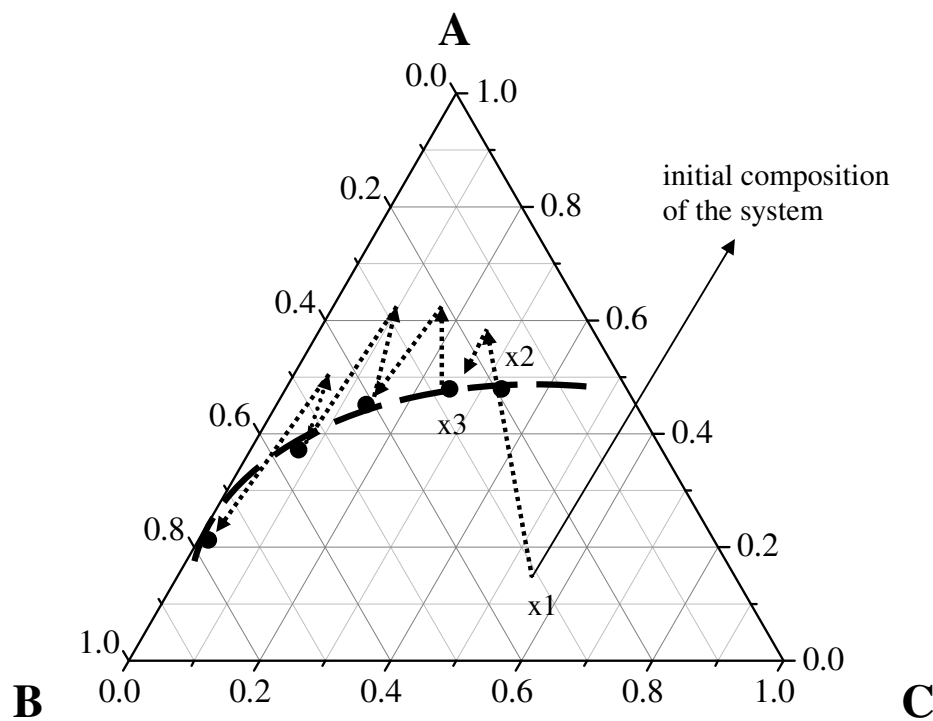


Figure 3.13. The basic steps of constructing ternary phase diagrams.

In order to construct a ternary phase diagram a sample system is prepared in Figure 3.13. Before starting the titration procedure a reference point is selected and recorded. This reference consists of 20% A, 30% B and 50% C at point x1. These percentages are all based on weights and the mixture at point x1 is cloudy, which means that two phases are present. Then, component A is added gradually to this mixture till the stirred mixture reaches a transparent appearance. This composition is recorded as the first point (x2) on the miscibility curve. Component A is added in excess to move further towards point and after an excess of approximately 10% (x3), component B is added to move the overall composition to present a two phase system. As the transparent appearance turns cloudy, this composition is recorded again as another point on the miscibility curve. The cloudy mixture is then titrated with component A again to move the system towards the one phase system and this procedure is continued till the points are very close to point B.

3.4.2.2. Gas chromatography analysis. Chemical analysis of the organic contaminants were conducted using an Agilent 6890N gas chromatograph (GC) equipped with an autosampler and a mass spectroscopy detector (MS). The GC was operated with 5973 Network and fitted with a DB-WAX column (0.25mm*30m*0.24 μ m). The MS detector was preferred both in the identification and quantification of the organic contaminants as the mass spectroscopy detector generated the best results. Samples of 0.2 μ L were directly injected after required dilutions. Total run time of the analysis of 1,2-dichlorobenzene containing samples was set as 15.40 minutes and the system stayed at 40⁰C for 6 minutes followed by the elevation of the temperature at 25⁰C/minute till 200⁰C and hold at 200⁰C for 3 minutes. The total run time of the analysis of toluene, on the other hand, was set as 10.40 minutes and the system stayed at 40⁰C for 4 minutes followed by the elevation of the temperature at 25⁰C/minute till 200⁰C. The components were verified by Wiley database at percentages over 96.

Throughout the titrations and chemical analyses, all the glassware, such as vials and sample bottles, were chosen to be clean and free of any contamination. The calibration standards for NAPL analyses by (GC/MS) were prepared in two different concentration ranges and each series contained at least four standard solutions that covered an order of magnitude in concentration or more. The linearity of the calibration graph was always checked to make sure that the regression coefficient (R^2) was close to one and sample

blanks, without contamination, were injected regularly to ensure that the system remained uncontaminated. Duplicate standard samples were commonly injected to certify a uniform response and to ensure that the calibration graph and the baseline remained stable. The syringe was rinsed with pure ethanol several times between sample injections to reduce contamination carryover.

3.4.2.3. Determination of the water content. The water content of the samples were determined volumetrically via Methrohm 795 Karl Fisher (KF) Titrino (Figure 3.14) whenever required. The titration is based on Equation 3.17 which takes place in the presence of a base and a solvent. The typical solvent used in water determinations is methanol and the base is imidazole.



Once the iodine in the KF reagent is determined, the unknown concentration of water in the sample can be determined. As the reaction occurs the amount of I (iodine) used during the titration must be equal to the unknown amount of water present in the sample.



Figure 3.14. Karl Fisher Titrator.

The volumetric KF method is used for ppm levels up to 100% water i.e. (high level moisture) whereas the coulometric method is used for moisture levels in the range of 10 micrograms to 10 mg of water in a sample (low level moisture). Volumetric KF determinations are preferentially carried out between pH 4 and 7. The titration is carried

basically in 3 steps. First, the KF reagent is dispensed into the reaction cell. The end point of the reaction between the KF reagent and water is detected automatically and the moisture content in the sample is calculated (www.metrohm.co.uk).

3.4.2.4. Determination of the anionic surfactants. Two phase titration method is used in the analysis of anionic surfactant (SLS). Anionic active matter is determined by titration with a standard cationic-active solution. The indicator consists of the mixture of Dimidium Bromide (cationic dye) and Disulphine Blue VN (anionic dye). The titration is carried out in a two phase aqueous-chloroform system. The anionic surfactant forms a salt with the cationic surfactant (Hyamine) which dissolves in the chloroform layer, causing a pink color to form. As the end point is reached Hyamine cation displaces the Dimidium cation from the chloroform soluble salt. Excess Hyamine causes color change and the end point is detected with the change in color to greyish blue.

The molecular structures of SLS and Hyamine surfactants used in the experiments are given in Figure 3.15 and 3.16, respectively.

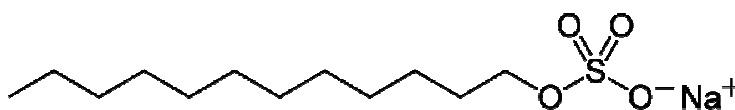


Figure 3.15. Molecular structure of SLS.

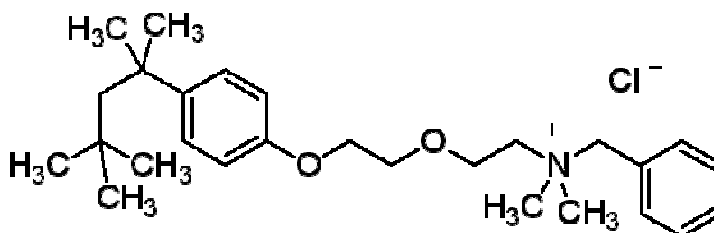


Figure 3.16. Molecular structure of Hyamine.

The procedure included titrating the 20 mL sample solution with Hyamine in the presence of 10 mL of distilled water and 15 mL of chloroform. The same procedure was also applied in the determination of nonionic surfactants with the titration solution of SDS instead of Hyamine (Reid et al., 1967). The surfactant concentration was calculated as given below.

$$\text{Active matter (\% by weight)} = [(1.25) (T) (f) (M) / (W)] \quad (3.18)$$

where;

T: mL of titrant used for a 20 mL sample

f: molarity of titrant

M: molecular weight of active-matter

W: g of sample taken

3.4.2.5. Determination of the HPCD. Analysis of HPCD was achieved by measuring the fluorescence of HPCD complexed with TNS (Brusseau et al., 1994) at the excitation wavelength of 300 nm and emission wavelength of 440 nm. 30 mg of TNS was dissolved with 100 mL of distilled water in a 100 mL volumetric flask (300 mg/L). HPCD stock solution was prepared by dissolving 100 mg of HPCD with 100 mL distilled water in a 100-mL volumetric flask. The concentration of this HPCD solution was 1000 mg/L. Two standard curves were prepared, one for the low HPCD concentrations ranging from 0 to 25 mg/L. 50, 100, 150, 200 and 250 ml aliquots of the HPCD stock solution was transferred to five 10-mL volumetric flasks, respectively 1 mL of TNS stock solution was added to each and diluted to 10 mL with water. The blank was prepared by adding 1 mL of TNS stock solution in 10-mL flask and diluting to 10 mL with water. The concentrations of these standard solutions were 0, 5, 10, 15, 20 and 25 mg/L, respectively. The second standard curve was prepared for higher HPCD concentrations ranging from 0 200 mg/L by transferring 0.5, 1.0, 1.5 and 2.0 mL aliquots of the HPCD stock solution to four 10-mL volumetric flasks; respectively; then adding 1 mL of TNS stock solution and diluting the mixture to 10 mL with water. The blank was prepared with the same procedure as above. The concentrations of the standard solutions were 0, 50, 100, 150 and 200 mg/L, respectively. The fluorescent response of HPCD standard solutions was measured by a Perkin Elmer Fluorescence Spectrophotometer with excitation wavelength 310 nm and emission wavelength 440 nm.

It was observed that the HPCD concentrations of the unknown solutions should be well below 200 mg/L. Otherwise, the sample solutions should be diluted to a suitable level as the relationship of fluorescent response versus HPCD concentrations is linear only at lower HPCD concentrations (<http://hillafb.hgl.com/sop/hpcd.htm>).

For analysis of unknown aqueous samples, 9 mL aliquots were added into 20-mL test tubes, followed by 1 mL of TNS stock solution. The mixtures were shaken thoroughly and the fluorescent response of the mixtures was measured with the same wavelength as above. If the concentration of sample solutions was below 25 mg/l, the first standard curve was used to obtain the concentration of HPCD. The HPCD concentration (HPCD_o) of the original unknown sample was calculated according to following equation:

$$\text{HPCD}_o = \text{HPCD}_s \times 10/9 \quad (3.19)$$

where HPCD_s is the concentration of the mixture of sample solution with TNS solution.

3.4.3. Determination of Other Critical Physical Parameters

3.4.3.1. Interfacial tension (IFT). Interfacial tensions were measured with the tensiometer (Figure 3.17) using Du Nouy Ring method. The platinum ring was immersed into the liquid and measured the tension while the ring was pulled up. The sensitivity of the equipment was very important in determining the effect of changes in the phase behaviour.

The basic steps of the IFT measurement can be summarized as (Figure 3.18):

1. The ring was placed above the surface and the force was set to zero from the equipment.
2. The ring hit the surface. The positive force was noticed as a result of the adhesive force between the ring and the surface.
3. The ring was pushed through the surface and this caused a small negative force.
4. The ring broke through the surface and a small positive force was measured due to the supporting wires of the ring.
5. When lifted through the surface the measured force started to increase.
6. The force kept increasing.

7. The maximum force is reached
8. After the maximum value was reached there was a small decrease of in the force until the lamella breaks (www.kruss.de).



Figure 3.17. KSV 703 Digital Tensiometer.

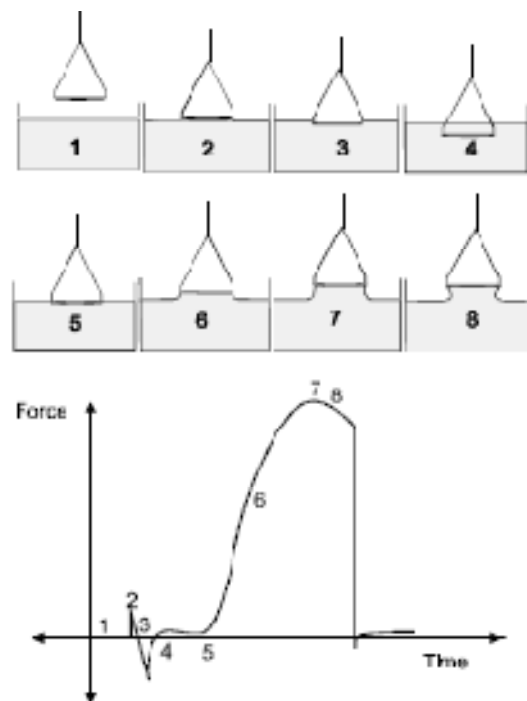


Figure 3.18. The steps of the measurement of interfacial tension with Du-Nouy Ring.

3.4.3.2. Density. Density is a measure of mass per unit of volume. The change in phase density is critical especially when the phase changes from LNAPL to DNAPL or DNAPL to LNAPL (Roeder et al., 2001). These critical changes play an important role in the behaviour pattern of the phases and effect the remedial challenges.

Density of an immiscible hydrocarbon fluid is the parameter which delineates LNAPLs from DNAPLs. The property varies not only with molecular weight but also molecular interaction and structure. In general, the density varies with temperature and pressure (Bear, 1972). Equivalent methods of expressing density are specific weight and specific gravity. The specific weight is defined as the weight of fluid per unit volume, i.e. kg/m^3 . The specific gravity (SG) or the relative density of a fluid is defined as the ratio of the weight of a given volume of substance at a specified temperature to the weight of the same volume of water at a given temperature (Lyman et al., 1990). Density is an important design parameter when considering the use of surfactants and cosolvents in removing the NAPLs from the subsurface.

Liquid densities were determined using 5 ml glass pycnometers in the experiments whenever needed. These pycnometers were calibrated gravimetrically prior to each use.

3.4.3.3. Viscosity. The viscosity of a fluid is an important property in the analysis of liquid behaviour and fluid motion near solid boundaries. The fluid resistance to shear or flow is typically called viscosity and it is a measure of the adhesive/cohesive or frictional fluid property. The resistance is caused by intermolecular friction exerted when layers of fluids attempts to slide by another (Thibodeaux, 1995). The knowledge of viscosity is needed for proper design of required temperatures for storage, pumping or injection of fluids. The most common units for viscosity are centipoise (cp) and centistokes (cSt). The relation between these two units is given below.

$$\text{centipoises (cp)} = \text{centistokes (cSt)} \times \text{density} \quad (3.20)$$

There are two related measures of fluid viscosity - known as dynamic (or absolute) and kinematic viscosity. Dynamic (absolute) viscosity is the tangential force per unit area required to move one horizontal plane with respect to the other at unit velocity when

maintained a unit distance apart by the fluid. On the other hand, kinematic viscosity is expressed as the ratio of absolute or dynamic viscosity to density - a quantity in which no force is involved.

Faster rates of recovery can be expected for low-viscosity NAPLs compared to high-viscosity NAPLs. The ratio of NAPL to flushing solution viscosity will affect the unstable and uneven displacement fronts where NAPL can be bypassed and penetrated by fingers of the flushing solution (Jeong and Corapcioglu, 2003).

The viscosity of a fluid is highly temperature dependent and for either dynamic or kinematic viscosity to be meaningful, the reference temperature must be quoted. For a liquid the kinematic viscosity will decrease with higher temperature whereas for a gas the kinematic viscosity will increase with higher temperature.

Viscosities of influent solutions and effluent samples are determined with Gilmont falling ball viscometers. 7 mL was the required volume for analysis of viscosity and stainless steel ball is used.

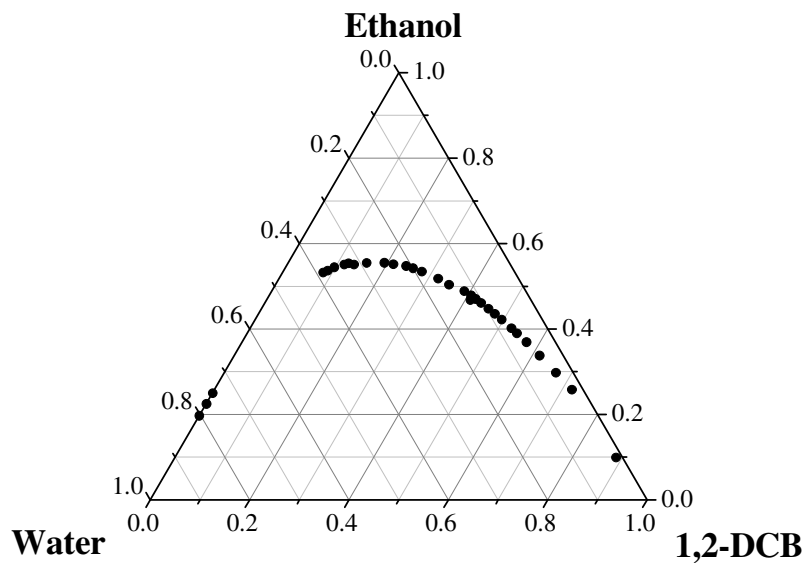
3.5. Results and Discussion

The miscibility curves were drawn for the chemical agents as described in section 3.4.2.1. The chemical agents were used alone in the titrations where possible, while the ones that could not be readily delivered into the reaction vessel were combined with appropriate solvents (ethanol or water) and used in the titrations.

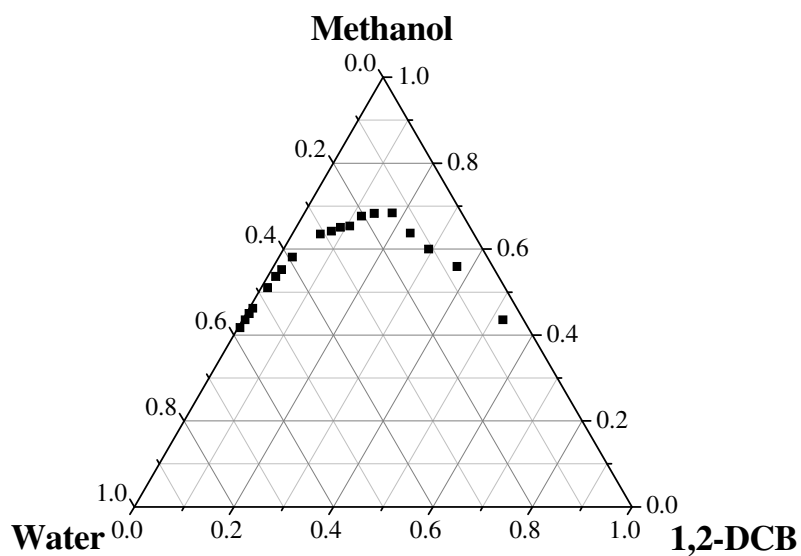
3.5.1. Titration Results for 1,2-Dichlorobenzene Containing Samples

In the first stage of chemical agent screening, the effectiveness of two alcohols, ethanol and methanol, in solubilizing 1,2-dichlorobenzene was evaluated. The miscibility curves generated from the titration data for ethanol and methanol containing systems are given in Figures 3.19(a) and (b), respectively. The height of the miscibility curve is an important initial factor for the prediction of the removal efficiency of the flushing solution

used. As it is seen from Figure 3.19 less ethanol was needed to solubilize 1,2-dichlorobenzene compared to methanol.



(a)



(b)

Figure 3.19. Miscibility curves for (a) 1,2-dichlorobenzene-ethanol-water system and (b) 1,2-dichlorobenzene- methanol-water system at 20°C.

In the second stage of the chemical agent screening process, surfactants and HPCD were evaluated for their efficiency in solubilizing 1,2-dichlorobenzene in ternary mixtures. Sodium lauryl sulphate (SLS), Tween 80 and Triton X100 were the surfactants used in the titrations. SLS is an anionic surfactant whereas Tween 80 and Triton X100 are nonionic. SLS was sold commercially in powder form and this caused difficulties in the prediction of cloud points upon addition in the titration vial.

When in contact with water, SLS also formed very stable foams. The foam occupied a considerable volume of the vial and this further complicated the titration-based determination of the cloud point. Also, the presence of SLS over 25% of the mixture promoted the formation of paste-like mixtures which reduced the efficiency of mixing. Further addition of 1,2-dichlorobenzene and SLS did not provide additional points for the definition of the miscibility curve. Figure 3.20 shows the resulting miscibility curve along with photographs of the encountered foaming and paste-formation problems.

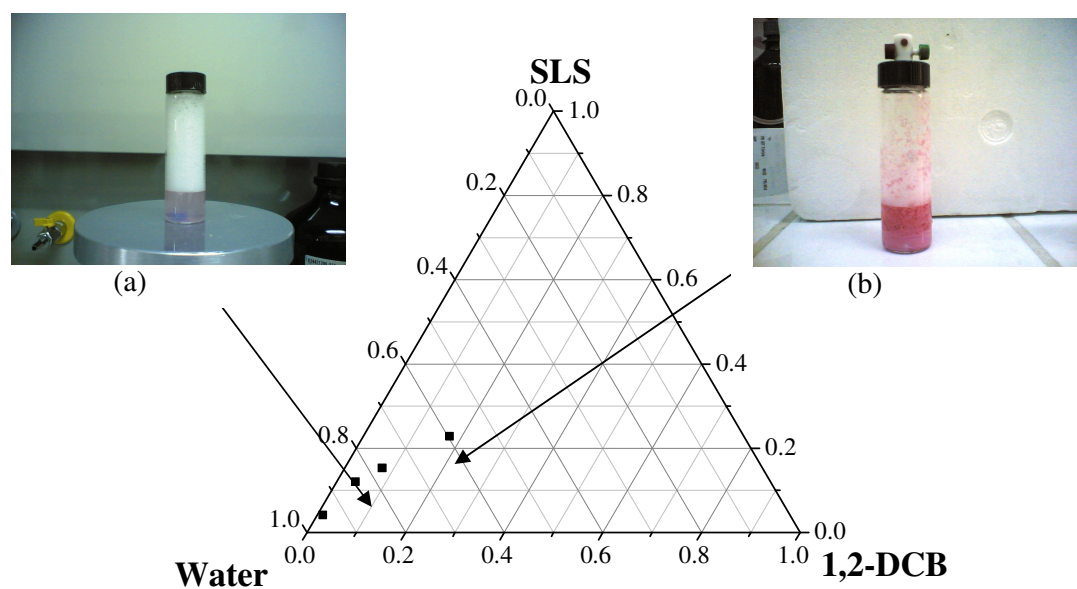


Figure 3.20. Miscibility curve for the 1,2-dichlorobenzene-SLS-water system showing the formation of (a) foam and (b) paste-like mixture at 20°C.

In the evaluation the effectiveness of Tween 80 in solubilizing 1,2-dichlorobenzene, some difficulties were encountered in the addition of Tween 80 to the system due to its

high viscosity and the formation of stable gels. To overcome these problems, Tween 80 was injected into the vials as a mixture with ethanol (at different mass ratios). Figure 3.21 shows the resultant miscibility curve for the case with Tween/ethanol ratio of 1:1. However, in comparison to miscibility curve based on pure ethanol which is less expensive and food-grade, no appreciable benefit is observed.

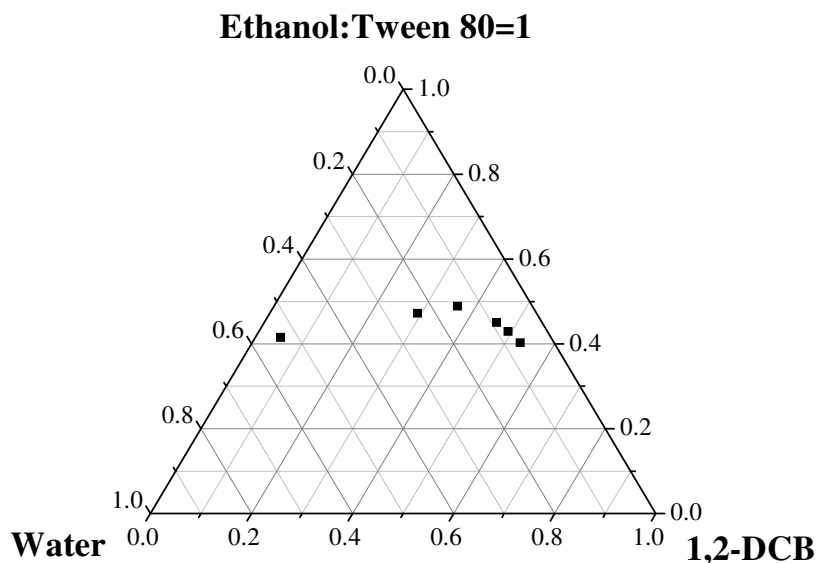
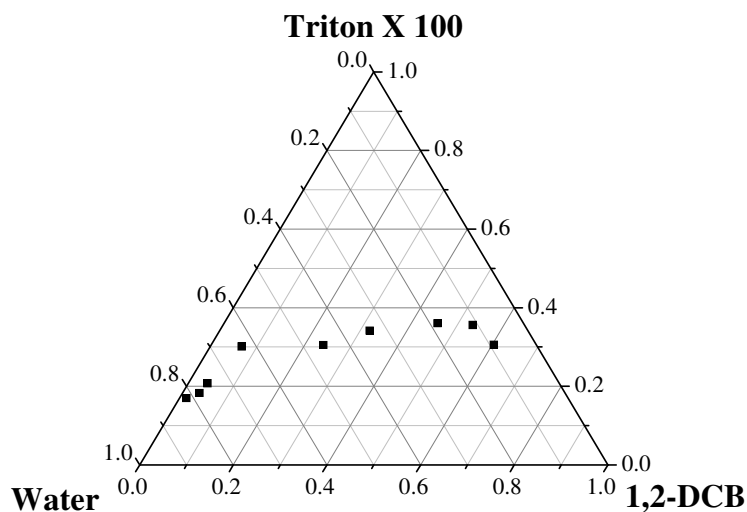
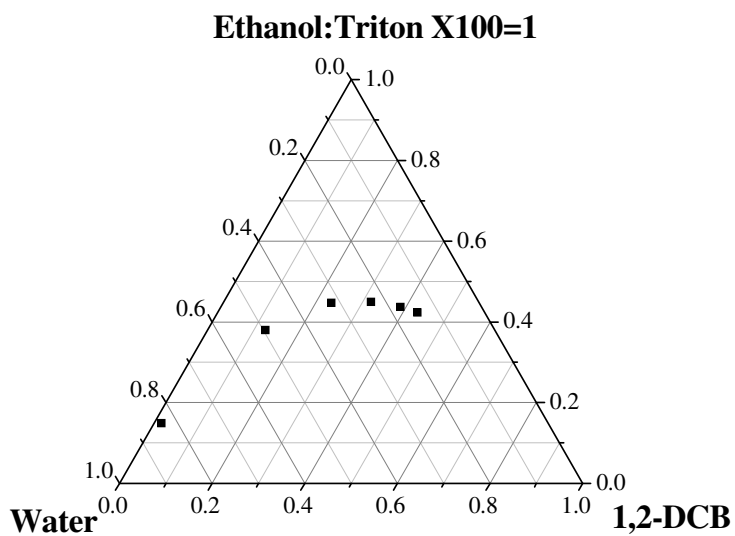


Figure 3.21. Miscibility curve for the 1,2-dichlorobenzene-(ethanol:Tween 80=1)-water system at 20°C.

The miscibility curve of pure Triton X100 and for ethanol/Triton ratio of 1:1 by mass is given in Figures 3.22 (a) and (b), respectively. Like Tween 80, some difficulties were encountered when Triton X100 was added at high concentrations to the NAPL-water system due to gel formation. Because of Triton X100's high viscosity, it was not possible to use gas tight syringes which tend to minimize loss of components in the mixture. In comparison to Figure 3.21, Triton X100 had a slightly lower miscibility curve than that of Tween/ethanol. Although SLS had an even lower miscibility curve (Figure 3.20), operational problems due to the powder nature of SLS made Triton X100 a more favorable alternative for use in ternary mixtures involving 1,2-dichlorobenzene.



(a)

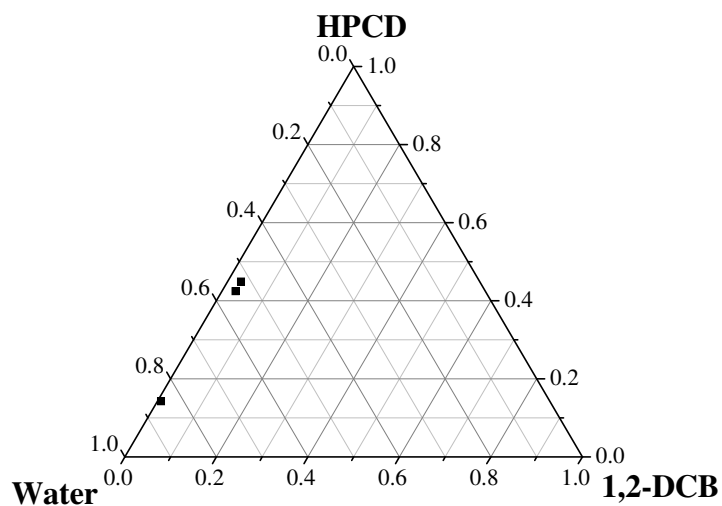


(b)

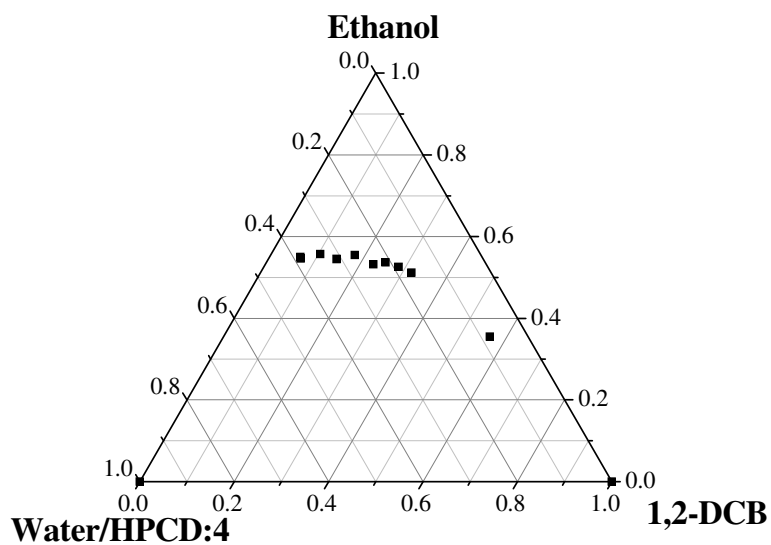
Figure 3.22. Miscibility curve for (a) 1,2-dichlorobenzene-Triton X100-water system and (b) 1,2-dichlorobenzene-(ethanol:Triton X100=1)-water system at 20°C

Recent field studies have shown that HPCD can be effective in the remediation of chlorinated solvents (Tuck et al., 2003). Therefore, it was selected as another potential agent for the enhanced removal of 1,2-dichlorobenzene. However, due to its low solubility in the 1,2-dichlorobenzene-water system, again a reasonable miscibility curve with pure

HPCD could not be generated. Therefore an aqueous solution of HPCD along with ethanol as the third component were tested. The resultant miscibility curves are shown in Figure 3.23 (a) and (b). The results indicate that HPCD does not have a significant impact on the solubilization of 1,2-dichlorobenzene.



(a)



(b)

Figure 3.23. Miscibility curve for (a) 1,2-dichlorobenzene-HPCD-water system, (b) 1,2-dichlorobenzene-ethanol-(water/HPCD:4) system at 20°C.

3.5.2. Titration Results for Toluene Containing Samples

Ethanol was chosen as the primary solvent in the titration of toluene-water system. The titration curve was constructed in two steps, starting from the water axis and toluene axis and titrations were done with the remaining two components. This enabled the system behaviour to be more clearly observed during titrations. The points on the miscibility curve were less visible in this mixture, this may be due to the solubilization properties of toluene, thus the exact turnover points were recorded but titration end points were extended to specify the turnover points. Ethanol partitioning and the effects of ethanol on solubility are illustrated on a ternary-phase diagram in Figure 3.24.

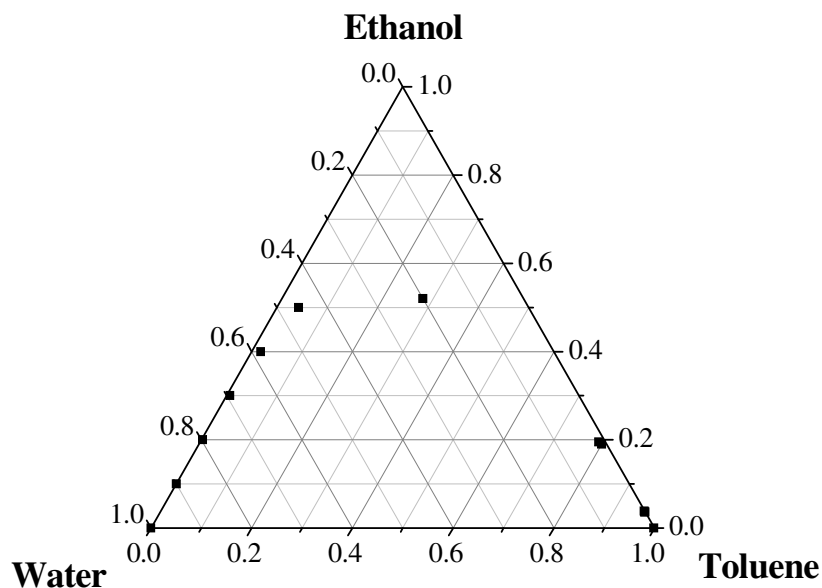


Figure 3.24. Miscibility curve for toluene-ethanol-water system at 20°C.

Surfactants were also evaluated for their efficiency in solubilizing toluene in ternary mixtures. Tween 80 and Triton X100 were the surfactants selected in this step of the study. During titrations it was observed that the same gel and foam formation problems occurred. Therefore, a proper miscibility curve could not be drawn with Tween 80 and only a miscibility curve up to 50% ethanol could be drawn. The miscibility curve generated for the ternary system of toluene-Triton X100-water is presented in Figure 3.25. When the location of the miscibility curves for ethanol and Triton X100 are compared, it is realized

that the miscibility curve generated with Triton X100 departs from the water-ethanol axis slightly more than the ethanol case. Since there were many difficulties associated with the addition of Triton X100 and no significant benefit was achieved with this chemical agent, it was concluded that ethanol would be a better alternative for toluene-water ternary system.

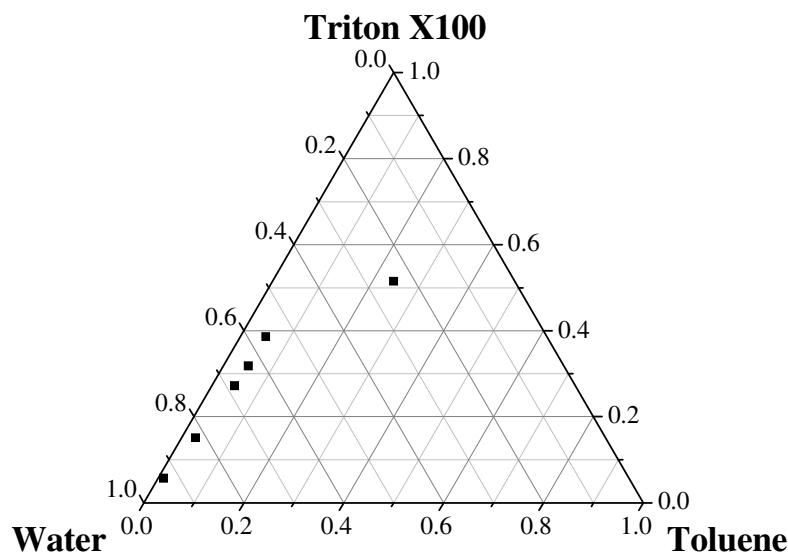


Figure 3.25. Miscibility curve for toluene-Triton X100-water system at 20°C.

3.5.3. Density Profiles of Toluene-Ethanol-Water Mixtures

The ternary phase behaviour was evaluated together with the density measurements. Different initial starting compositions of toluene and water were prepared and varying ethanol masses were added to reach different locations under the miscibility curve.

Known masses of toluene and water were mixed with varying masses of ethanol in beakers and mixed by shaking at room temperature for 1 hour and let to equilibrate. Since the phase separation of toluene and water is very fast, the phases became visible after only 10 minutes. Samples from each phase were taken and the densities were measured. The density profiles of the aqueous and the NAPL phases for equal initial amounts of toluene and water are presented in Figure 3.26. The same procedure was applied for different

initial ratios of toluene and water with varying ethanol contents and the results are given in Table 3.4.

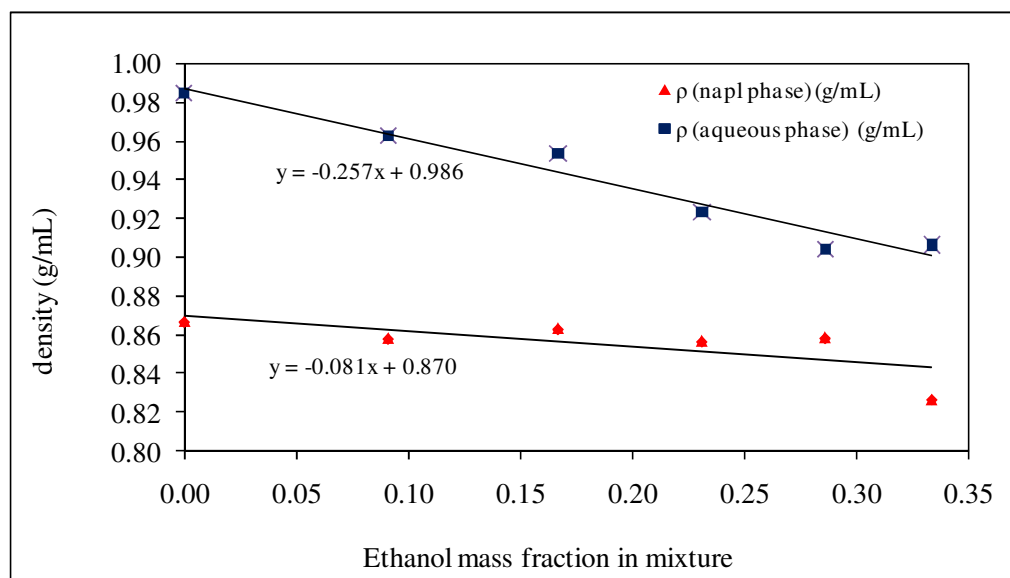


Figure 3.26. The density profiles of the aqueous and the NAPL phases in toluene (50%)-water (50%) with varying ethanol additions at 20⁰C.

The measured densities are presented on the ternary phase diagram in Figure 3.27 as a function of the mass ratios of the prepared solutions. The results showed that ethanol preferentially took place in the aqueous phase, as the volume of the aqueous phase directly increased with the addition of ethanol to the beakers. However, at high ethanol contents, ethanol also became a part of the NAPL phase, which was observed through volume comparison. It was also observed that the NAPL phase density was always slightly lower than the aqueous phase, thus it floated on the water rich phase.

Table 3.4. Density measurements for different initial ratios of toluene and water with varying ethanol contents.

SAMPLE	X_{toluene} (%)	X_{water} (%)	X_{ethanol} (%)	ρ (NAPL phase) (g/mL)	ρ (aqueous phase) (g/mL)
A	0.81	0.09	0.10	0.8572	0.9272
B	0.72	0.08	0.20	0.8497	0.8679
F	0.58	0.25	0.17	0.8503	0.8864
G	0.51	0.22	0.27	0.8308	0.8438
H	0.47	0.20	0.33	0.8202	0.8228
I	0.42	0.18	0.40	0.8102	0.8180
J	0.35	0.15	0.50	0.8025	0.8097
K	0.28	0.65	0.07	0.8602	0.9803
L	0.26	0.60	0.14	0.8563	0.9337
M	0.21	0.50	0.29	0.8429	0.8572
U	0.45	0.45	0.09	0.8582	0.9627
W	0.42	0.42	0.17	0.8532	0.9032
X	0.38	0.38	0.23	0.8468	0.8931
Y	0.36	0.36	0.29	0.8401	0.8541
Z	0.33	0.33	0.33	0.8190	0.8253

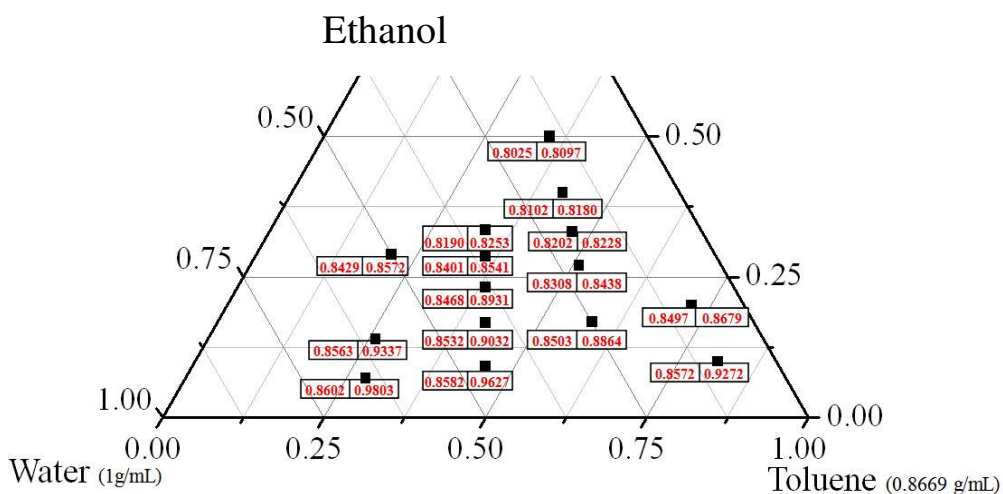


Figure 3.27. The measured densities with respect to the mass ratios of the prepared solutions at 20°C.

The ease of locating the phase interface was not similar for different initial compositions. For the toluene(9)-water(1) case, ethanol additions beyond 20% did not produce a distinct interface therefore density and interfacial tension measurements could not be performed. The same behaviour was observed in ethanol mass ratios above 50% as beyond this value, the system was entering the one phase region. The phase formations are presented for toluene(9)-water(1) with varying ethanol additions and toluene(7)-water(3) with varying ethanol additions in Figures 3.28 and 3.29, respectively.

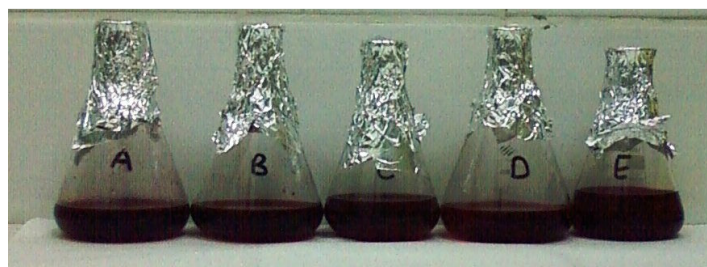


Figure 3.28. The phase separations of toluene(9)-water(1) with varying ethanol additions at 20°C.



Figure 3.29. The phase separations of toluene(7)-water(3) with varying ethanol additions at 20°C.

3.5.4. Interfacial Tension Profiles of Toluene-Ethanol-Water Mixtures

Direct measurement for interfacial tension show that the IFTs drops with increasing ethanol content in the aqueous phase. The change of interfacial tension with increasing ethanol contents are presented in Figure 3.30 for equal initial amounts of toluene and

water. The interfacial tension measurements performed are presented in Figure 3.31 and given in Table 3.5.

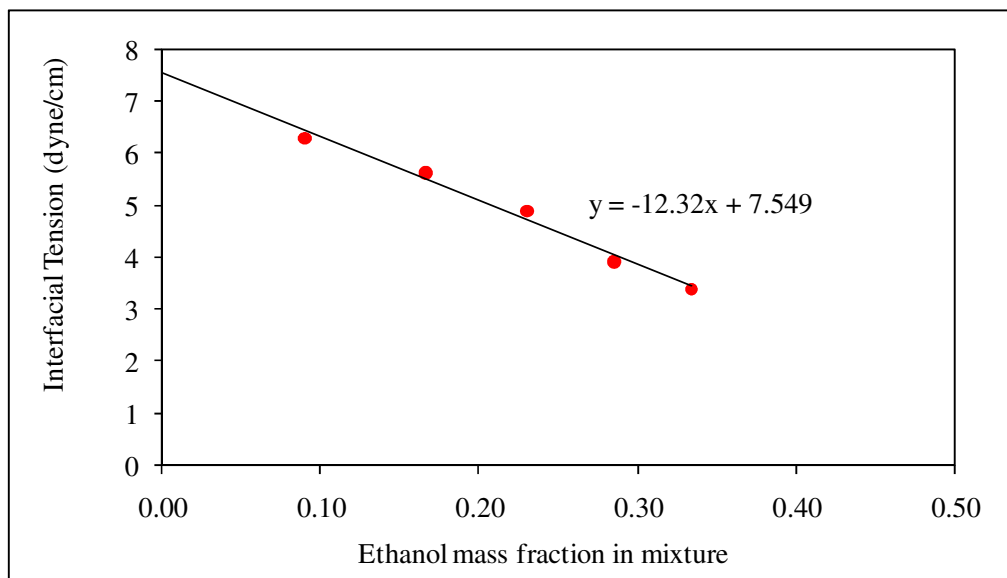


Figure 3.30. The interfacial tension profiles of the aqueous and the NAPL phases in toluene(1)-water(1) with varying ethanol additions at 20°C.

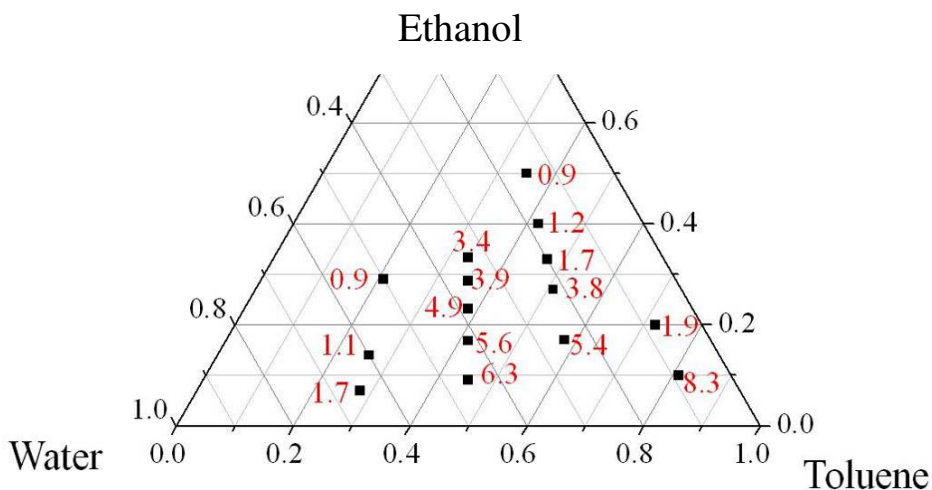


Figure 3.31. The measured interfacial tensions (dyne/cm) between the aqueous and NAPL phases as a function of mole fraction at 20°C.

Table 3.5. Interfacial tension measurements for different initial ratios of toluene and water with varying ethanol contents.

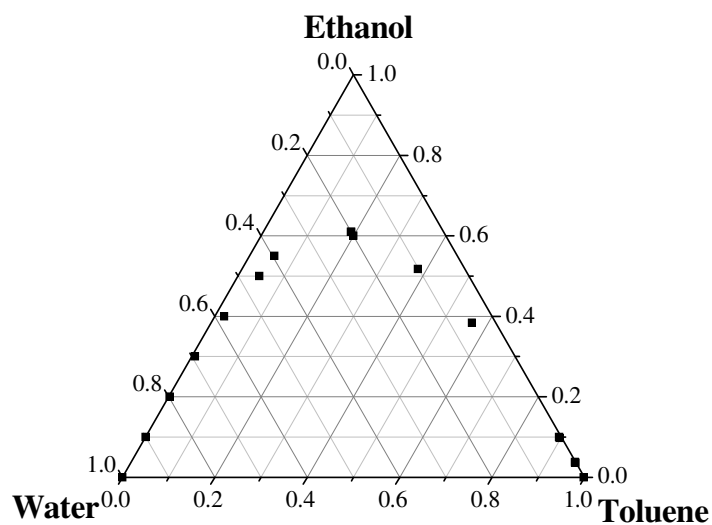
SAMPLE	x_{toluene} (%)	x_{water} (%)	x_{ethanol} (%)	Interfacial Tension (dyne/cm)
A	0.81	0.09	0.10	8.3
B	0.72	0.08	0.20	1.9
F	0.58	0.25	0.17	5.4
G	0.51	0.22	0.27	3.8
H	0.47	0.20	0.33	1.7
I	0.42	0.18	0.40	1.2
J	0.35	0.15	0.50	0.9
K	0.28	0.65	0.07	1.7
L	0.26	0.60	0.14	1.1
M	0.21	0.50	0.29	0.9
U	0.45	0.45	0.09	6.3
W	0.42	0.42	0.17	5.6
X	0.38	0.38	0.23	4.9
Y	0.36	0.36	0.29	3.9
Z	0.33	0.33	0.33	3.4

The interfacial tension measurements showed above indicate that the highest values were measured on the right side of the ternary phase diagram around 100% toluene. As the composition of the two phase mixture moved towards the water-ethanol axis, the interfacial tensions decreased. The dominance of toluene in the mixture caused higher interfacial tensions. It was also observed that the interfacial tension decreased more near the ethanol-toluene axis while moving upwards towards the 100% ethanol point. This may be explained with the location of the plait point, as the tie lines coincide towards the plait point and the decreases are more at the region where the plait point is located.

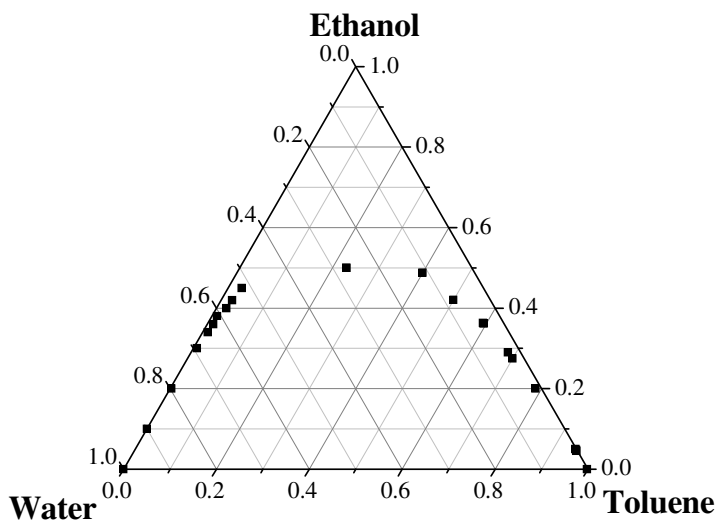
3.5.5. Numerical ternary phase diagram for the toluene-ethanol water system

The activity coefficients for the components were generated with UNIFACAL software and the file is used as the input for the Fortran simulation. The ternary phase diagrams for toluene-ethanol-water system at 20 and 40⁰C are presented in Figure 3.32. It

was observed that the peak point of the miscibility curve decreased from 62 to 50% ethanol in the overall mixture, which means that less ethanol will be needed to reach one phase mixture if the temperature of the mixture is increased to 40°C. This region is represented as the area where the system performance can be increased.



(a)



(b)

Figure 3.32. Numerical ternary phase diagrams of toluene-ethanol-water system at (a) 20°C and (b) 40°C.

3.6. Conclusions

Ternary phase diagrams through sequential titration represents a relatively simple and inexpensive laboratory procedure for the rapid evaluation of different remedial solutions. The evaluation process is based on ternary phase diagrams that assume multiphase equilibrium among the water, NAPL and flushing solution components. The results of these experiments can serve as initial tool for the screening and selection of the various remedial solutions.

The screening procedure was applied to a hypothetical NAPL contamination where the NAPL targets were 1,2-dichlorobenzene and toluene. The remedial agents considered were alcohols (ethanol and methanol), surfactants (SLS, Tween 80 and Triton X100) and HPCD.

Results indicated that the alcohols, in particular ethanol, were effective in solubilizing model NAPLs. However, the effectiveness of alcohols was enhanced when used together with surfactants, provided that the surfactants can be added to the system efficiently. Among the three surfactants considered, Triton X100 was the most favorable surfactant in the titrations and caused the least problems in the introduction to the vials.

Phase interface formations were not similar for mixtures having different initial compositions. For some cases a distinct interface could not be formed therefore density and interfacial tension measurements could not be performed. The results showed that ethanol preferentially took place in the aqueous phase, as the volume of the aqueous phase directly increased with the addition of ethanol to the beakers. At high ethanol contents, ethanol also became a part of the NAPL phase, which was observed through volume comparison. It was also observed that the NAPL phase density was always slightly lower than the aqueous phase, thus it floated on the water rich phase.

The results for the interfacial tension measurements showed that the highest interfacial tension values were measured on the right side of the ternary phase diagram around 100% toluene. As the composition of the two phase mixture moved towards the water-ethanol axis, the interfacial tensions decreased. The dominance of toluene in the

mixture caused higher interfacial tensions. It was also observed that the interfacial tension decreased more near the ethanol-toluene axis while moving upwards towards the 100% ethanol point. This may be explained with the location of the plait point, as the tie lines coincide towards the plait point and the decreases are more at the region where the plait point is located.

A numerical code was also developed for the computation of the mole fractions for the ternary systems at multiphase equilibrium. One of the advantages of the code is that it can be readily applied to different system temperatures. The numerical results obtained for a toluene-water-ethanol system at 20⁰C were in good agreement with the experimental results obtained with the titration method. The application of the code to a temperature of 40⁰C, showed that the ethanol content for a single phase to occur decreased from about 60% to 50%.

In summary, it is important to note that chemically enhanced remediation activities are contaminant-specific. The results generated provide important preliminary data for the effectiveness of different chemical agents in the enhanced mobilization of the model contaminants in the subsurface. With the relatively simple titration and numerical technique used in the study, different contaminants can be evaluated in a similar way.

4. ENHANCED CHEMICAL AGENT FLUSHING

This chapter describes the column experiments used to evaluate the effectiveness of ethanol in solubilizing and mobilizing toluene from porous media. The experiments consider different pore water velocities and ethanol contents in the flushing solution. Section 4.1 gives some background information on the use of NAPL flushing using cosolvents. Section 4.2 discusses the key operational parameters for the extraction process. Section 4.3 describes the experimental set up and laboratory analysis procedure used in this part of the study. Results and discussion of the column experiments are presented in Section 4.4.

4.1.Theory and Background Information

In-situ subsurface flooding is the extraction of contaminants from the soil and groundwater with water or other suitable chemical agent solutions. Traditional soil washing involves excavating the contaminated soil and treating it at the surface. Soil and groundwater chemical flooding is based on the same theory but involves an injection/recirculation process in-situ. Extraction is the process used for the separation of components in a mixture. The separation is mainly based on chemical differences and involves contacting a solution with a solvent that is immiscible with the original mixture. The solvent, on the other hand, must be soluble with a specific component present in the solution. Two phases may form upon addition of the solvent. The solute in the solution should have more affinity toward the added solvent in order to have the mass transfer of the solute from the solution to the solvent (Miller et al., 1990).

The selection of the candidate chemical agents can be accomplished based on information on solution chemistry, ability to solubilize the NAPL compounds, human health and environmental protection and compatibility with the enhanced in situ flushing remediation technique.

The majority of the studies that have considered in-situ flooding techniques were based on extremely simplified laboratory experiments consisting of one-dimensional flow in small-scale columns. Some researchers extended their experimental efforts to two dimensional media. However, most of these controlled laboratory experiments do not incorporate the effect of heterogeneity in the flow properties of the porous media that in reality would have a major impact on the effectiveness of the remedial scheme. Indeed numerous field studies have shown that heterogeneity of the natural geologic formations is the main factor limiting the efficiency of groundwater remediation activities (Walker et al., 1998; Grubb et al., 1999; Chevalier and Peterson, 1999). Consequently, it is important that future research work address the effect of heterogeneity of the porous media on the groundwater remediation.

Residuals left in the subsurface after in-situ soil flooding play an important role in the overall performance controls. Even though extensive flushing with water is commonly performed after flushing with chemical agents is completed, there is still a probability that there will be some residual or adsorbed chemical agent left in the soil after the remediation process is finished. Therefore, the optimal chemical agents must be effective and non-toxic and should not pose a threat to human health or the environment. Moreover, the chemical agents must be readily available, economically priced and preferably recyclable. Biodegradability of the chemical agents is also important and the solution should match well with the flushing technique and the subsurface environment, so advection and biodegradation are controlled (Fountain et al., 1995).

Typically, the main cosolvents that are employed for in situ flushing are miscible alcohols (Lowe et al., 1999), such as ethanol (Grubb and Sitar, 1999), methanol and isopropyl alcohol, since they are considerably less hazardous for the environment. Palomino and Grubb (2004) conducted a two-step chemical agent flushing scenario where 500 mL (each) of dodecane, toluene and octane were injected into separate sandpacks to simulate a relatively large spill of LNAPL. The ethanol flushing experiments were performed by delivering a combined pure ethanol and 50/50 (vol. %) ethanol–water blend to a soil system. The performed flushing strategy successfully mobilized and recovered the simulated large-volume LNAPL spills and the toluene and octane recoveries were approximately 84.9 and 88.1%, respectively.

Surfactants were also used to enhance the aqueous solubilization (Pennell et al., 1997; Harwell et al., 1999; Prak and Pritchard, 2002; Jawitz et al., 2003). Saba et al. (2001) conducted enhanced dissolution experiments in a two-dimensional test cell to measure rates of mass depletion from entrapped NAPLs to a flowing aqueous phase containing a surfactant. A single component lighter-than-water NAPL, p-xylene, was used as the test fluid. Tween 80 was used in the LNAPL-enhanced dissolution experiments. Inside the rectangular zones with entrapped LNAPL, dissolution fronts were observed to propagate from upstream and downstream of the rectangular contaminated source zones towards the center of these sources. This shape of the propagating dissolution front under 2-D flow conditions is different from the dissolution fronts that occur in 1-D laboratory columns.

The risk of downward migration of the contaminants and the flushing solution necessitates serious precautions such as the density modified displacement (DMD) method (Ramsburg and Pennell, 2002).

4.2. Operational Parameters for the Extraction Process

The key operational parameters for an extraction process are temperature, pressure, residence time, feed flow rate and composition. As in many separation processes, the pressure and temperature play a large role in the efficiency of the separation. Selectivity, mutual solubility, precipitation of solid and vapor pressure are the other parameters considered in the operations (www.cheresources.com).

The solvent selected to be used in the extraction must be partially soluble with the carrier. On the other hand, the feed components must be immiscible with the solvent. The solute, on the other hand, must be soluble in the carrier and at the same time completely or partially soluble in the solvent. The selected solvent should preferably have different density than the feed components for high efficiencies (Perry and Green, 1984).

Separation occurs for compositions in the region between the feed composition and that pure phase location of the carrier. The ratio of the concentration of solute to feed solvent in the extract phase to that in raffinate phase is called the selectivity or separation

factor. Selectivity is a measure of the effectiveness of the extraction solvent for separating the constituents of feed and the selectivity for the solute should be high to dissolve the maximum amount of solute and the minimum amount of the carrier. For all extraction operations selectivity should be greater than 1. If it is equal to 1, then separation by extraction is not possible (Seader and Henley, 1999).

Interfacial tension and viscosity are key parameters influencing the performance of in-situ flushing. High interfacial tension and viscosity leads to more power being supplied to maintain rapid mass transfer throughout the extraction process. Low interfacial tension and viscosity, on the other hand, lead to the formation of an emulsion.

Temperature must be high in order to benefit from the increase in solubility, but should not exceed the critical solution temperature. Moderate temperatures can facilitate the selection of a suitable solvent. Elevated temperatures are preferred in some cases to keep the viscosity very low in order to minimize the mass-transfer resistances.

Pressure must be maintained below the vapor pressure of the solutions to prevent vapor phase formation. Volatilization must be prohibited, otherwise, the process will be adversely affected if one or more of the components are allowed to vaporize.

Chapter 4 focuses on the influence of chemical agent composition in NAPL recovery from the porous media. Flushing experiments are repeated with varying ethanol contents and at different flow rates to investigate the effect of contact between the NAPL and the flushing solution. The influence of temperature on NAPL recovery is examined in Chapter 5.

4.3. Experimental Set-up

4.3.1. Model Aquifer Construction

The column experiments were conducted with 60-70 AFS Siltas sand which was pre-sieved to obtain an average of 0.2 mm particle size. The uniformity was reported as 84% and hydraulic conductivity values were similar to subsurface values. Prior to use, Siltas sand was washed with deionized water and oven dried to remove all the moisture. The sand was reported to contain 98.6% SiO₂ with no clay, silt sized particles and organic content. The properties of the sand used are given in Table 4.1. The grain size diameter varies from 0.1 to 0.3 mm and the mean grain diameter (d_{50}) is 0.2 mm. The specific surface area is 115.97 cm²/g. The complete analysis report of the Siltas 60/70 AFS sand used in the study is represented in Appendix B.

Table 4.1. 60/70 AFS sand properties.

Parameter	Value	Unit
Particle size	65.42	AFS
	203.95	μm
Theoretical surface area	115.97	cm ² /g
Distribution ratio	1.41	S ₀ =Q ₁ /Q ₃
	0.24	Q ₁ (mm)
	0.17	Q ₃ (mm)
Average particle size	0.20	Mk
	50	M50
	84	Degree of homogeneity
Composition	98.6	SiO ₂ (%)
	0.23	Fe ₂ O ₃ (%)
	0.02	CaO+MgO (%)
	0.07	Na ₂ O+KO (%)
	0.54	Al ₂ O ₃ (%)
Sinterization temperature	>1500	°C

Flushing experiments were performed in a Kontes glass column (diameter: 5cm, length: 30cm). The columns were capped at both ends using a perforated Teflon® cap. A Viton® O-Ring provided a seal between the glass cylinder and the Teflon® cap. A stainless steel screen placed inside the caps prevented the loss of fines. Inside each cap, a small reservoir was built to allow the uniform distribution of injected liquids. The columns were incrementally filled with sand in steps of approximately 2 cm sand layers. Each layer was compacted uniformly by hitting the column to the bench 5 times. The weight of the column and dry soil were recorded to determine the pore volume after the saturation of the media.

4.3.2. Saturation of the Column

After the compaction of the sand in the column, distilled water was injected from the bottom of the column at very slow flowrates (1 mL/min) to remove the air trapped in the column. When all the soil is wetted, the flowrate is increased to reach an effluent of roughly 4 mL/min. This flowrate was kept steady for approximately 2 days before the initiation of the flushing experiments. Meanwhile, the soil matrix in the column was examined for the air entrapment. When air pockets were observed, the column flushing was kept for longer periods to remove all the air to reach maximum saturation levels. The saturated column was weighed to find the amount of water remaining in the media. The difference was recorded as the pore volume (PV) and this value was taken as the basis for the amount of water flushed.

4.3.3. Tracer Controls

Calcium chloride was used as non-reactive tracer to assess the hydrodynamic characteristics of the packed columns. The tracer electrolytic conductivity was set to 1170 mS and the average flow rate was recorded as 3.14 mL/min during the tracer experiments. The columns were packed and saturated by pumping water upwards at a very low flowrate. After the system reached saturation, a pulse of non-reactive tracer (Cl⁻) solution was introduced into the system and the experiment was continued till the effluent concentration of the tracer reached the inlet concentration. After this step, the column was flushed with background water to remove the tracer from the system. Samples were collected from the

effluent periodically and during each experiment the tracer concentrations of the samples were monitored with a conductivity meter. The parameters used in the tracer experiment are presented in Table 4.2.

STANMOD software was utilized to fit the measured column data to the analytical solutions of the advective-dispersive equation for estimating transport parameters. STANMOD (STudio of ANalytical MODels) is a suite of solute transport models created by the U.S. Salinity Laboratory. Specifically, STANMOD 2.0 includes CHAIN, CFITM, CFITIM, CXTFIT, 3DADE and N3DADE. These models are based on analytical solutions of the convection-dispersion equation and consider a variety of complex solute transport processes, including sequential first-order decay and chemical/physical non-equilibrium (rate-limited) processes.

Table 4.2. Parameters of the tracer control experiments.

Parameter	Value	Unit
Initial concentration	3.5	$\mu\text{S/cm}$
Tracer concentration	1170	$\mu\text{S/cm}$
Injection time	223	min
Flowrate	3.14	mL/min
Pore volume (PV)	193.39	mL
Column volume	588.75	mL
Weight of the dry soil per unit volume	1.432	G
Total weight of the dry soil and the column	1474	G
Weight of the column	631	G
Weight of the water saturated soil and the column	1667.39	G
Darcy velocity	9.60	cm/h
Real velocity	29.23	cm/h
Time for one flushing	61.59	min

For complex field-scale solute transport problems, stochastic methods may be needed to estimate the flow models. However, for small scale laboratory experiments with relative homogeneous soil properties, such efforts are not warranted. Because they are based on analytical solutions, STANMOD codes assume homogeneous medium properties and steady boundary conditions. Consequently, accuracy of the models is related to the degree

to which actual conditions deviate from these and other model assumptions. While there are no modifications of the previously-released versions of the underlying transport models, STANMOD greatly increases utility of these models by providing straightforward pre-processor and useful post-processor/plotting options (Simunek et al., 1999).

The breakthrough curve of the non-reactive tracer (chloride) is shown in Figure 4.1. The best-fit analytic break through curve for the rising portion of the curve is also shown on the same figure. The near symmetrical increases and decreases of the concentration changes represent close to ideal transport behaviour in the column. The best-fit dispersion coefficient was calculated and found to be approximately $0.1 \text{ cm}^2/\text{min}$. For a velocity of about $0.5 \text{ cm}/\text{min}$, this corresponds to a dispersivity of 0.2 cm ($\alpha=D/V$). This is a realistic value for a 30-cm column with uniform sand.

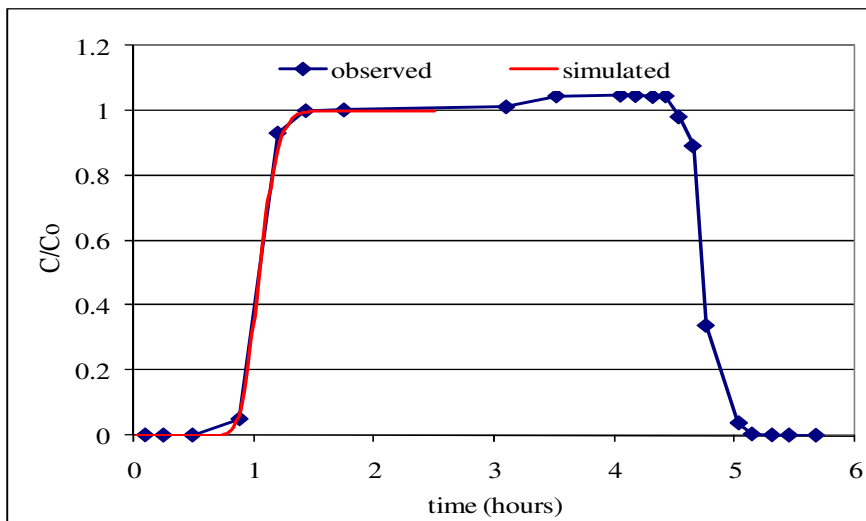


Figure 4.1. The breakthrough curve of the non-reactive tracer (chloride).

4.3.4. Determination of the Hydraulic Conductivity

Hydraulic conductivity refers to the ease with which water can flow through a soil media (Bedient et al., 1999). There are two general types of permeability test methods that are routinely applied in the laboratory. Hydraulic Conductivity was measured with the procedure given in the standardized ASTM D2434 (2000) “Standard Test Method for Permeability of Granular Solid (Constant Head)” reference document.

The constant head method is used for sandy sediments with moderate to high K values such as the sand used in this study. To determine the hydraulic conductivity, the sediment was first inspected and the grain size recorded. The length of the sample (L) and the height of the overflow tube above the outflow port (h) were measured. Deionized water at room-temperature was used in the experiments. Water was poured into the funnel from the top and adequate time was allowed for the flow pattern to stabilize before recording the volume versus time. The time to fill a volume of 750-1000 mL was measured using a graduated cylinder together with the temperature of the water. This process was repeated several times and the average time, average volume and average temperature were computed.

4.3.5. Contamination of the Sandpack

Contamination of soil was achieved by introducing the predetermined mass of contaminant into the sandpack through a gastight syringe connected to a vial equipped with a Mininert valve to minimize losses by evaporation.

4.3.6. Chemicals Used

The NAPL selected for the column flushing experiments was toluene. Ethanol was chosen as the chemical agent in this part of the research because it had a higher LD₅₀ than the other alcohols. This decision was critical as some studies showed that high cosolvent concentrations may be necessary for contaminant removal (Staples and Gieselmann, 1988) and high ethanol concentrations exhibited success at solubilizing NAPLs (Jafvert, 1996; National Research Council, 1997). Toluene was dyed with Oil red O (100 mg/L) to enable visual inspections in the flushing experiments (Seagren et al., 2002).

4.3.7. Sampling

The effluent was collected at predecided pore volumes and diluted to keep the assumed concentrations in the range that GC analysis could be acceptable. The color of the samples was taken as the reference for the level of dilutions. Trial GC analysis were conducted with different toluene concentrations which had varying colors to develop visual

guidelines for the require level of dilution. The samples were transferred to vials where dilution was performed. The samples were kept at 4⁰C till analysis. No samples were stored for more than a week to minimize losses.

4.3.8. Analysis Procedures

The analysis was conducted in a gas chromatography coupled with a mass spectrometry (MS) detector. The details of the method used were given in Section 3.4.2.2. The chromatographic capillary column was DB-WAX (0.25mm*30m*0.24um) and the system was operated under constant flow. The injection volume was predetermined as 0.2 uL and the carrier gas was helium. After the injection of the sample, the MS detector was closed for the first 4 minutes to minimize damages that the water content of the samples may cause in the MS detector structure. The ethanol peak was also observed between 2 and 4 minutes, so the ethanol concentrations could not be determined via GC-MS. The oven temperature increased by 25°C/min till 200°C and the total analysis runtime added up to 10:40 minutes for toluene. The components were verified by Wiley database at percentages over 96. The absorbance data gathered from GC analysis were all converted to concentration values using the calibration results.

4.4. Results and Discussion

Toluene was injected into the saturated sandpack upwards to better distribute through the column. Experiments were conducted with flushing scenarios containing 20, 40, 60 and 100% ethanol by mass. The effects of ethanol content in the flushing solution and flushing flow rate on the recovery performances were investigated. For all experiments, the flow rate was kept uniform at about 3.5 mL/min which corresponds to a groundwater velocity of about 2.56 m/day.

20% ethanol solution was the first run selected to see the effect of very low levels of ethanol on the dissolution of toluene injected into the column from bottom end. In the second and third runs, 40% and 60% ethanol solutions respectively were flushed through contaminated soil column, the latter close to the miscibility curve (the ternary phase

diagram of water-toluene-ethanol is shown in Figure 3.24). Finally, pure ethanol was flushed through the contaminated sandpack to investigate the extent of solubilization. In the second part of this section, the flow rate was increased from 3.5 mL/min to 7 mL/min, keeping all other parameters exactly same, to see the effect of the flow rate on the flushing efficiency. In the last experiment the effect of contact time between the flushing solution and the contaminant was investigated through intermittent flow rate application.

4.4.1. Dissolution Performance of Ethanol Solutions at Low Flow Rate (20⁰C)

Moderately low flow rates were applied in this part of the flushing activities. The average initial flow rate was in the range of 3-4 mL/min. After the injection of toluene, the effluent flow rate decreased for some time till the resistance was overcome through solubilization upon contact with ethanol. This was observed in all the experiments and the flow rate was not changed throughout the experiment.

4.4.1.1. Dissolution performance of 20% ethanol solution at low flow rate (20⁰C). 10 g of toluene was injected into the column from the bottom end and after all toluene entered the column, 20% ethanol solution was flushed upwards at the same flowrate. A slight decrease in the effluent flowrate was observed which can either be a result of the delay between the shift in flushing (toluene to ethanol solution) or the resistance to flow because of the toluene trapped in the lower parts of the column. The toluene immediately migrated upwards and formed channels in the outer side of the column and no movement was observed during flushing of the ethanol solution.

Figure 4.2 presents a photograph showing the distribution of toluene in the soil column just prior to the 20% ethanol flush. The cumulative toluene removal is given in Figure 4.3 with respect to pore volumes passed through the system and the effluent concentration of the toluene is presented in Figure 4.4.

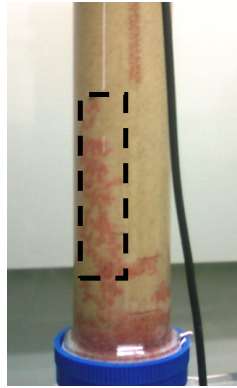


Figure 4.2. The formation of channels during flushing with 20% ethanol solution at 20⁰C.

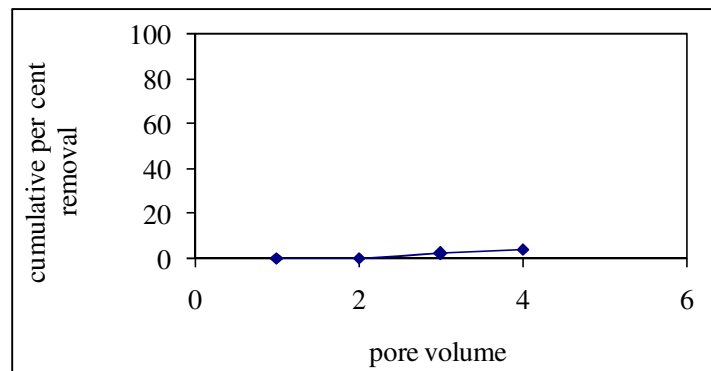


Figure 4.3. The cumulative toluene removal with 20% ethanol flushing at low flow rate (20⁰C).

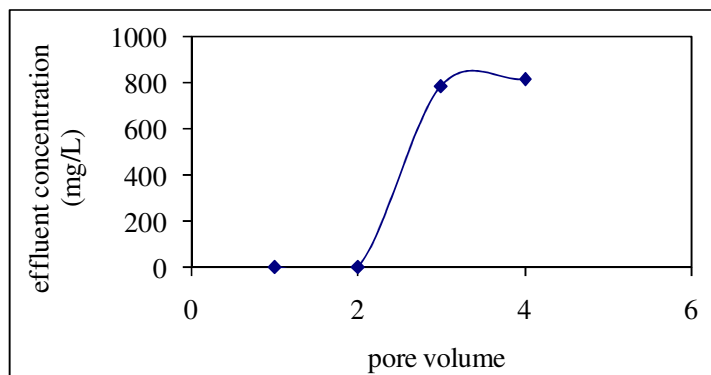


Figure 4.4. The effluent toluene concentration profiles with 20% ethanol flushing at low flow rate (20⁰C).

The color and transparency of the effluent did not reach a level that can be detected by the naked eye; this was also verified by the GC analysis results. The total amount of toluene removed was 4.05% of the total toluene injected and the slight toluene removal started after two pore volumes were passed through the system. The dissolution was delayed due to the very low ethanol content of the flushing solution and this was expected before the initiation of the experiment. In the early stages (first and second pore volumes) ethanol had difficulty migrating in the toluene spill. When sufficient local concentrations of ethanol were created in the lower parts of the column, ethanol was able to dissolve toluene which caused a slight toluene removal from the column after the third pore volume. The removal rates could not reach even 1% after the third pore volume, thus the flushing experiment was terminated.

4.4.1.2. Dissolution performance of 40% ethanol solution at low flow rate (20⁰C). Based on the ternary phase diagram of toluene-ethanol-water system, flushing with 40% ethanol solution was also performed at moderate flow rate. It was expected that the removal performance would not be high, as in the ternary phase diagram of toluene-ethanol-water system at 40% ethanol content, the overall system remained under the miscibility curve. The results generated complied with this assumption, which can also be seen in Figure 4.5. The effluent was collected at 40mL vials and only at the end of the fourth pore volume cloudiness was observed. As seen from the cumulative toluene recovery data in Figure 4.6, only 6% of toluene was removed from the system via 40% ethanol solution and this was accomplished just after the completion of four pore volumes. The GC analysis results showed that the effluent concentrations hardly reached 5000 mg/L (Figure 4.7).

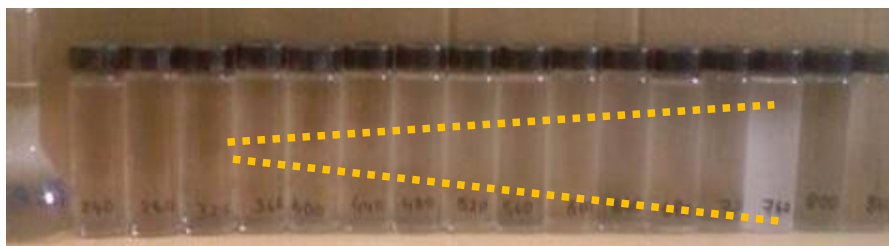


Figure 4.5. The samples collected during flushing with 40% ethanol solution at low flow rate (20⁰C).

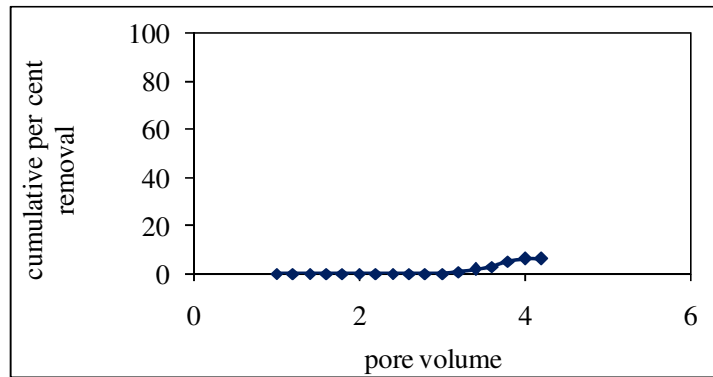


Figure 4.6. The cumulative toluene removal with 40% ethanol flushing at low flow rate (20°C).

The samples collected did not contain any free phase toluene but the cloudiness started by the end of the second pore volume and a slightly cloudy sample was found when the 760 mL of effluent was collected. After 760 mL, the samples again became transparent and the highest concentrations were found at these region.

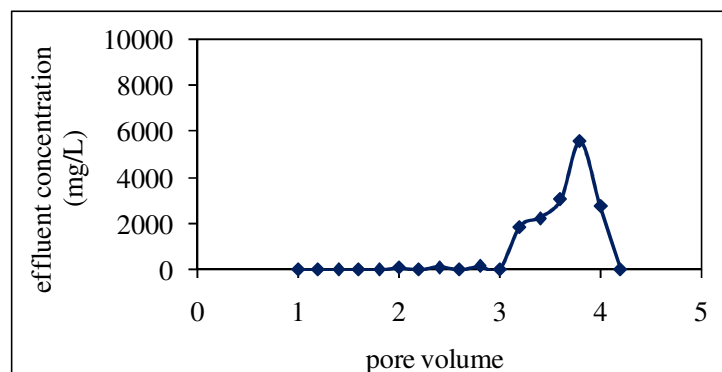


Figure 4.7. The effluent toluene concentration profiles with 40% ethanol flushing at low flow rate (20°C).

Free phase removal was not observed but as the color predictions were not applicable due to transparent sample, thus all samples were diluted to minimize underestimations that could be accompanied with colorless free phase presence in the vials.

The movement of the toluene bank is presented with respect to completed pore volumes in Figure 4.8. As can be seen from these photographs, toluene was dissolved in the lower regions of the column where it contacted the ethanol flood, but the local ethanol concentrations could not be sufficient to move the bank upwards. On the other hand, when compared with the toluene movement in flushing with 20% ethanol solution, solubilization was far enhanced.

After the completion of the introduction of the first pore volume a small pool of toluene (red circle in the first photograph in Figure 4.8) was noticed above the bank and at the end of the second pore volume the pool was no more visible. This was attributed to the movement of the pool in the middle of the column. The highest concentrations reached by the 760 mL was most probably due to the removal of this pool from the system in dissolved phase.

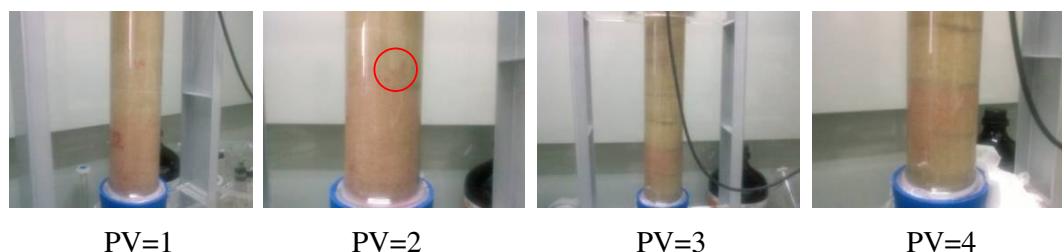


Figure 4.8. The movement of the dyed toluene during flushing with 40% ethanol solution at low flow rate (20⁰C).

4.4.1.3. Dissolution performance of 60% ethanol solution at low flow rate (20⁰C). Toluene (10g) was introduced to the column and the average flow rate was 3.17 mL/min during the flushing of 5 pore volumes of 60% (by weight) ethanol solution. At the end of the flushing of the first pore volume, the effluent was observed to be cloudy. After the first pore volume, the color of the effluent started to turn red (Figure 4.9). The cloudy effluent was left to stabilize for a few hours to enable separation of the phases and at the end of that period, red toluene drops became visible at the top of the vials. After this point, the toluene concentration in the effluent started to increase dramatically and the rate of toluene removal from the system reached the maximum level in the beginning of the second pore volume. This sharp increase can also be seen in Figure 4.10 and 4.11.

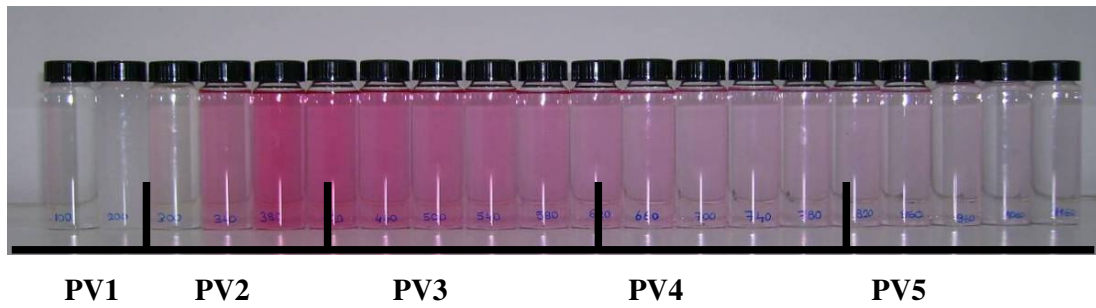


Figure 4.9. The samples collected during flushing with 60% ethanol solution at low flow rate (20°C).

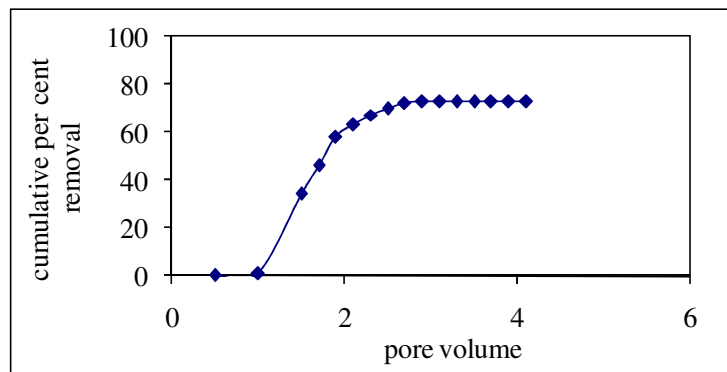


Figure 4.10. The cumulative toluene removal with 60% ethanol flushing at low flow rate (20°C).

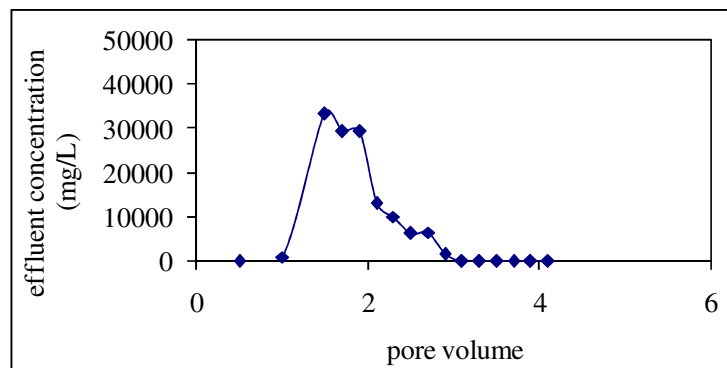


Figure 4.11. The effluent toluene concentration profiles with 60% ethanol flushing at low flow rate (20°C).

During the experiment, the flow rate varied slightly. Just after the injection of the toluene, the flow rate decreased slightly. The dissolution of toluene was observed on the outer parts of the glass column as can be seen in Figure 4.12. As the toluene started to move as a bank upwards, the flow rate reached its initial level gradually.

As the first pore volume is flushed through the column, the toluene started to move upwards very homogeneously. After 2 pore volumes left the system, the lower parts of the column, which previously had pale pink color, started to be cleaned by the ethanol solution. This cleaning became more obvious at the end of the 3rd pore volume where only the middle regions had pink color.

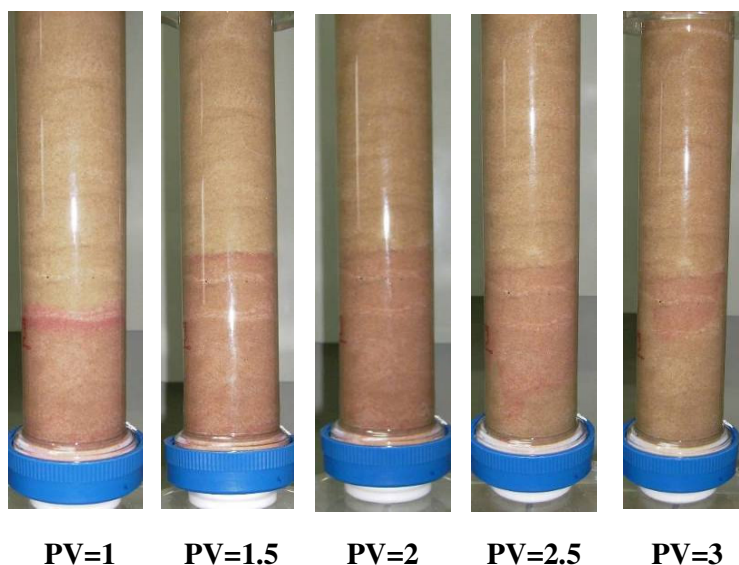


Figure 4.12. The movement of dyed toluene in the column during flushing with 60% ethanol solution at low flow rate (20°C).

4.4.1.4. Dissolution performance of 100% ethanol solution at low flow rate (20°C). The Flushing experiments were repeated with pure ethanol in this run. Since the ethanol content was maximum, most of the toluene was expected to leave the system in very short time. Cloudiness was observed in the last quarter of the first pore volume and free phase toluene started to leave the system by 170 mL.

As can be seen from Figure 4.13, a remarkable free phase toluene recovery was achieved in the 180 mL vial. It was concluded that both the initiation of toluene movement and accompanying dissolution mechanisms were realized with the introduction of pure phase ethanol. In vial 220 mL, three layers were observed which shows that toluene left the system at three different compositions – densities. The densities of the layers were sufficiently different so that layers were visible by the naked eye. Furthermore, the three layers were present in the same vial, it can be accepted that the density changes were very sudden, which caused the presence of three distinct phases in the same vial.

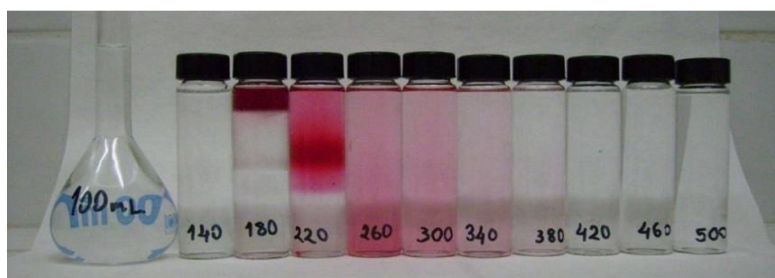


Figure 4.13. The samples collected during flushing with pure ethanol solution at low flow rate (20°C).

The toluene bank movement in the column also verified the fast recovery which is presented in Figure 4.14. Toluene moved upwards as a bank and no toluene was observed in the column after the completion of the third pore volume.

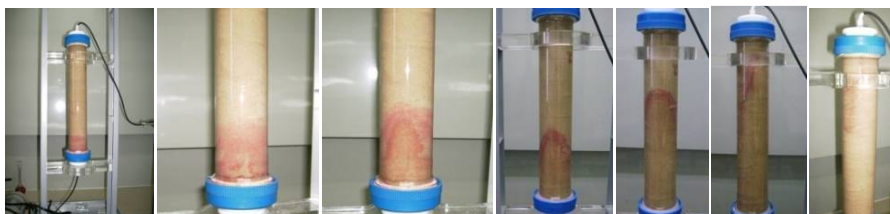


Figure 4.14. The movement of the dyed toluene during flushing with pure ethanol solution at low flow rate (20°C).

Flow rate of an average of 3.4 mL/min also contributed to the effective contact of flushing solution with toluene in the sand pack. Since the flushing solution had better contact with toluene while moving upwards in the sandpack, most of the toluene was recovered in the first two pore volumes. The third pore volume was more like a polishing step, active in removing the residuals. The cumulative toluene removal with 100% ethanol flushing at low flow rate is presented in Figure 4.15.

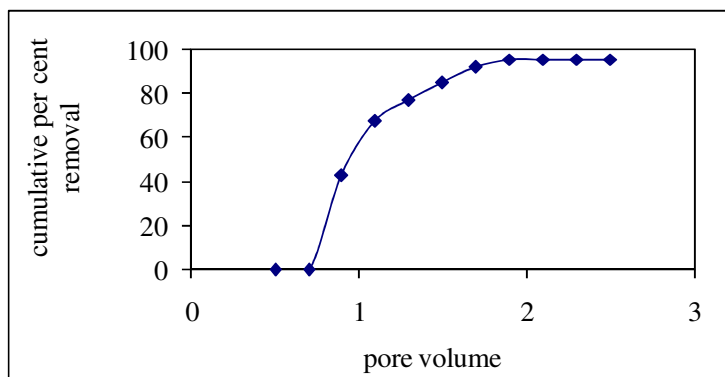


Figure 4.15. The cumulative toluene removal with 100% ethanol flushing at low flow rate (20°C).

The cumulative recovery rate profiles were as expected and a percent recovery of 95.53 were achieved with the completion of the second pore volume. The highest toluene concentration was reached at the last quarter of the first pore volume (Figure 4.16).

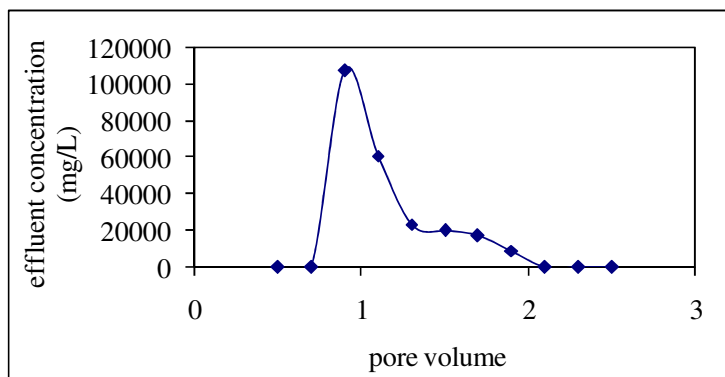


Figure 4.16. The effluent toluene concentration profiles with 100% ethanol flushing at low flow rate (20°C).

4.4.2. Dissolution Performance of Ethanol Solutions at High Flow Rate (20°C)

Flushing solutions with 60 and 100% ethanol content were repeated with high flow rate to investigate if the contact time was a significant variable in the recovery performance.

4.4.2.1. Dissolution performance of 60% ethanol solution at high flow rate (20°C). The effect of the flow rate of the flushing solution was investigated in this part of the study. The flow rate was around 7 mL/min, twice the flow rate used in the previous experiments. The column packing, NAPL injection and sample collection was similar to what was used in the previous experiments. The samples collected are given in Figure 4.17 and the toluene removal is shown in Figures 4.18 and 4.19.

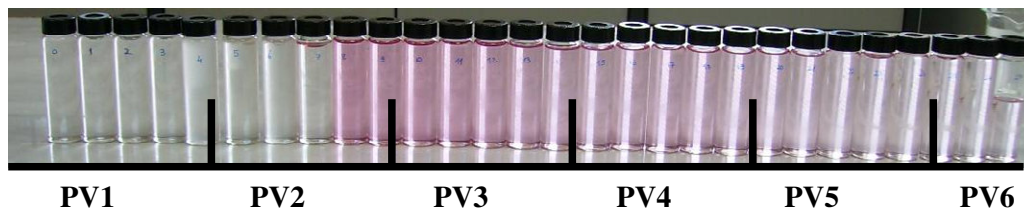


Figure 4.17. The samples collected during flushing with 60% ethanol solution at low flow rate (20°C).

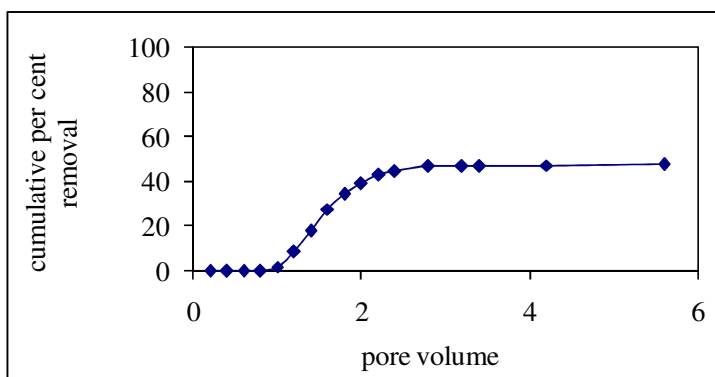


Figure 4.18. The cumulative toluene removal with 60% ethanol flushing at high flow rate (20°C).

When the toluene removal patterns are compared with the case where 60% ethanol solution was used in flushing, the case with high flow rate resulted in less removal after five pore volumes (Figure 4.18) and this was attributed to the low contact times of the ethanol solution with the toluene in the sandpack. This resulted in lower effluent toluene concentrations in the collected samples (Figure 4.19). The lower NAPL recovery suggests multiphase equilibrium between the toluene and the flushing solution was not achieved.

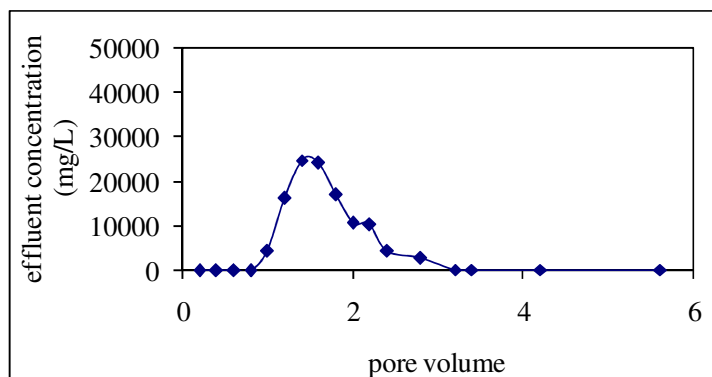


Figure 4.19. The effluent toluene concentration profiles with 60% ethanol flushing at high flow rate (20⁰C).

The red color of the samples were observed in the second part of the second pore volume in the case with low flow rate, whereas this red color could be seen in the last vial of the second pore volume in the case with high flow rate. It was also noticed that the intensity of the red color was kept in a narrow range in the case with low flow rate when compared with the case with high flow rate where the red color was seen in less intensity but in more vials.

4.4.2.2. Dissolution performance of 100% ethanol solution at high flow rate (20⁰C). The flushing experiment was conducted with pure ethanol as the solvent and the samples in Figure 4.20 were collected. The cloudy sample with pure phase toluene on top can be seen in the second vial, after which a vial with very dark colored toluene was filled. The pure phase toluene accumulated on the top of the sandpack and when the collected amount reached a full drop it separated from the sand and left the system (Figure 4.21).



Figure 4.20. The samples collected during flushing with pure ethanol solution at high flow rate (20°C).

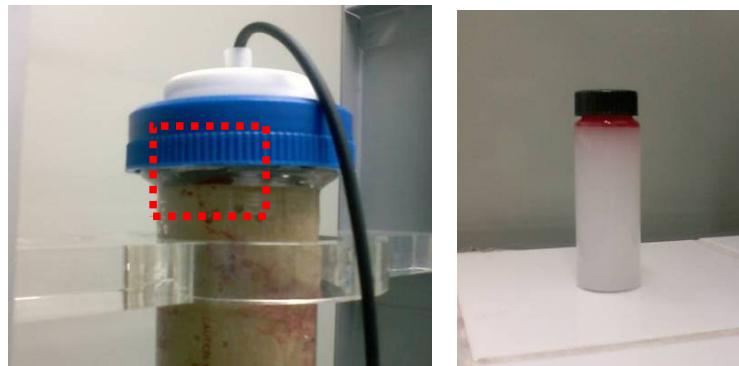


Figure 4.21. The accumulation of the free phase toluene at the top of the soil column and in the effluent collection vial.

When the color of the vials are compared with the vials in case with the same flushing composition applied at low flow rate, it is obvious that the removal was diminished due to the fast flushing which caused limited solubilization. The high flow rate also minimized the contact between the flushing solution and toluene, thus the maximum toluene concentration reached at the effluent was 69736 mg/L at the end of the third pore volume. The cumulative toluene removal with 100% ethanol flushing at high flow rate is presented in Figure 4.22, whereas the effluent toluene concentration profiles with 100% ethanol flushing at high flow rate is given in Figure 4.23.

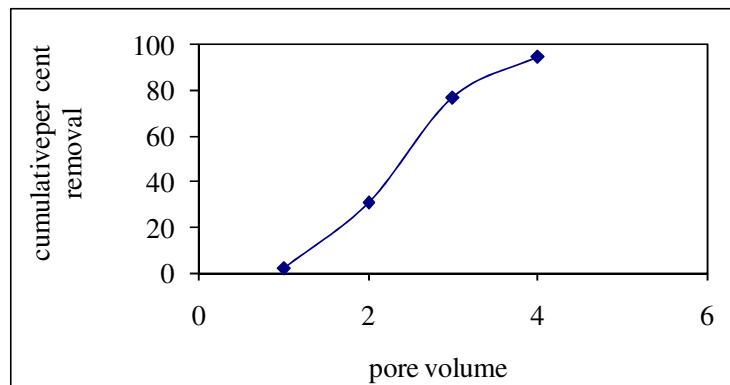


Figure 4.22. The cumulative toluene removal with 100% ethanol flushing at high flow rate (20°C).

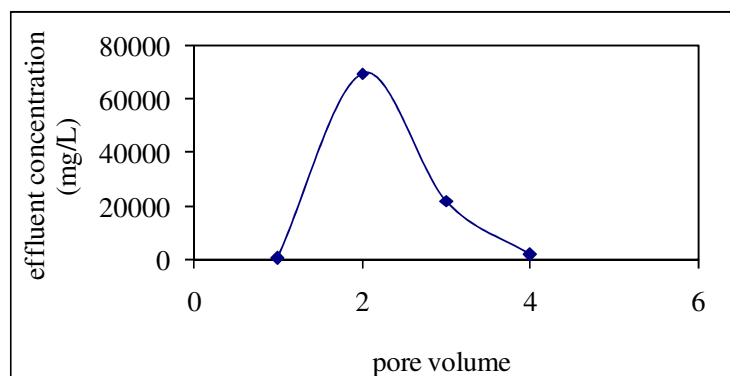


Figure 4.23. The effluent toluene concentration profiles with 100% ethanol flushing at high flow rate (20°C).

The toluene bank movement was initiated with the contact of ethanol. The homogeneous horizontal bank was immediately formed and started to rise in the column which can be easily seen in Figure 4.24. On the other hand, a toluene pool was noticed in the very bottom of the sandpack. This pool started to solubilize with the continuation of the injection and became invisible by the end of the second pore volume.

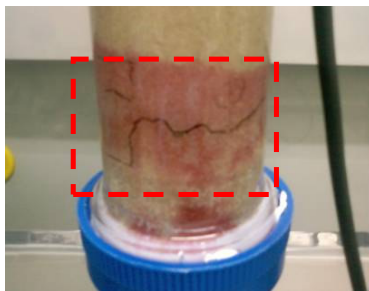


Figure 4.24. The movement of the toluene bank during flushing with pure ethanol.

4.4.3. Dissolution Performance of Ethanol Solutions with Intermittent Flow Rate (20°C)

The flushing experiments showed that the flow rate was directly affecting the performance of the application. The contact period between the contaminant and the flushing solution was minimized during flushing with high flow rate, whereas the recoveries were also not completed in cases where 60 and 100% ethanol containing flushing solutions were used. Therefore, an intermittent flow case was performed to investigate the effect of increase in contact times. The flow sequence employed was a two step flushing operation. The flushing solution was introduced to the system for 30 minutes and afterwards the flow was terminated for 15 minutes. This two step mode was continued for 4 pore volumes. The average flow rate used for 30 minutes flushing was 3.5 mL/min which was similar to the low flow rate experiments conducted in the previous section. The samples collected during flushing with 40% ethanol solution at intermittent flow rate is presented in Figure 4.25.



Figure 4.25. The samples collected during flushing with 40% ethanol solution at intermittent flow rate (20°C).

The experimental results showed that flushing at intermittent flow rate increased the recovery rates through more contact. The cumulative percent recovery reached almost 14% whereas the maximum toluene recovery for 40% ethanol solution at low flow rate was only 7%. This shows that by only increasing the contact time by shutting the flow the efficiency may be increased significantly. The cumulative toluene removal and the effluent toluene concentration profiles with 40% ethanol solution at intermittent flow rate are presented in Figures 4.26 and 4.27, respectively. As can be seen from Figure 4.27, the toluene concentrations increased at some periods, which could be due to the increased contact times.

The implications of these results for field applications is that establishing sufficient contact time between the flushing solution and the NAPL is a key parameter influencing the system efficiency. By increasing the contact time, the same efficiency can be achieved with lower cosolvent concentration in the flushing solution. However, given that heterogeneity and complexity of real systems, it is always expected that the system efficiency would be lower in the field than in laboratory scale experiments.

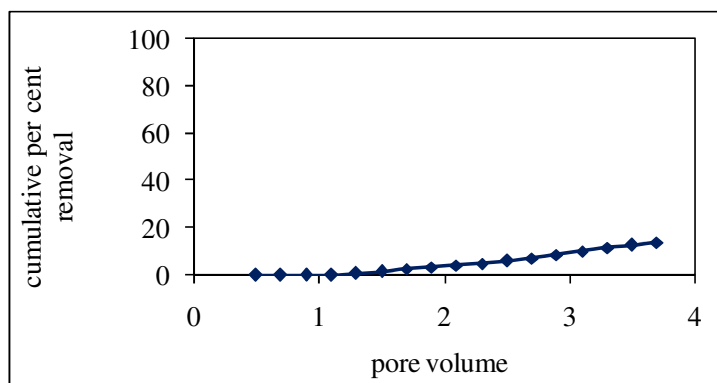


Figure 4.26. The cumulative toluene removal with 40% ethanol flushing at intermittent flow rate (20⁰C).

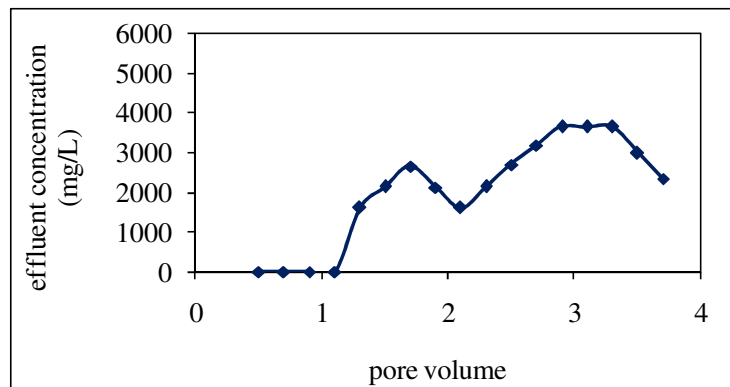


Figure 4.27. The effluent toluene concentration profiles with 40% ethanol solution at intermittent flow rate (20⁰C).

4.5. Conclusions

Toluene recovery performances were evaluated with respect to ethanol contents in the flushing solutions and flow rates that the flushing solutions are injected into the sand pack. Significant recovery of the NAPL was observed for the 60% and 100% ethanol content in the flushing solution. This is an expected result because the peak point on the toluene-water-ethanol ternary phase diagram (Figure 3.24) was about 50%. By exceeding this critical point, significant mobilization of the NAPL occurs.

A comparison of the cumulative toluene removal performances of different ethanol solutions is presented in Figure 4.28. When the breakthrough curves of toluene with different flushing solutions are compared, it is easily seen that the recovery efficiencies increase with increasing ethanol contents. Although the per cent recoveries increased with the ethanol content, the recoveries were comparable for 20 and 40% ethanol solutions. This result can again be explained by examining the ternary phase diagram which shows that for ethanol content less than 50%, enhanced solubilization of the NAPL occurs, but this enhanced solubility remains low.

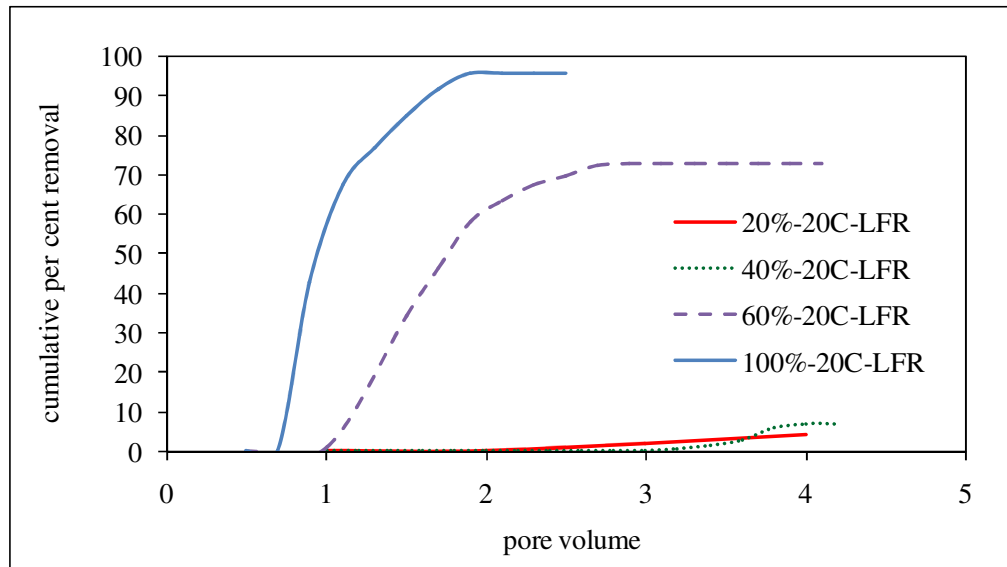


Figure 4.28. Comparison of the cumulative toluene removal performances of different ethanol solutions at low flow rate (20°C).

The initiation of the breakthrough curves were also evaluated as this indicates the movement of the solubilized toluene in the sandpack. The results agree with the expectations as the fastest initiation was observed with 100% ethanol solution.

The time needed for the cumulative mass recovered curve to reach steady state is indicative of the pore volumes needed to reach maximum recovery rates. As stated in the previous sections, in-situ flushing is a recovery alternative and the separation of the components in the effluent must be necessary to treat these wastewater. The effluent toluene concentrations with respect to pore volumes injected are presented in Figure 4.29. When the effluent concentrations are compared, it can be noticed that the toluene in the effluent for the 100% case was far greater than the other three cases. This is attributed to the higher solubilization potential of the flushing solution. A sharp and rapid increase in the effluent concentration is observed for this case, with very high recovery rates. This can be accepted as the best performance, but in field applications the cost and environmental issues of pumping pure ethanol must be evaluated together with the recovery performance in decision making.

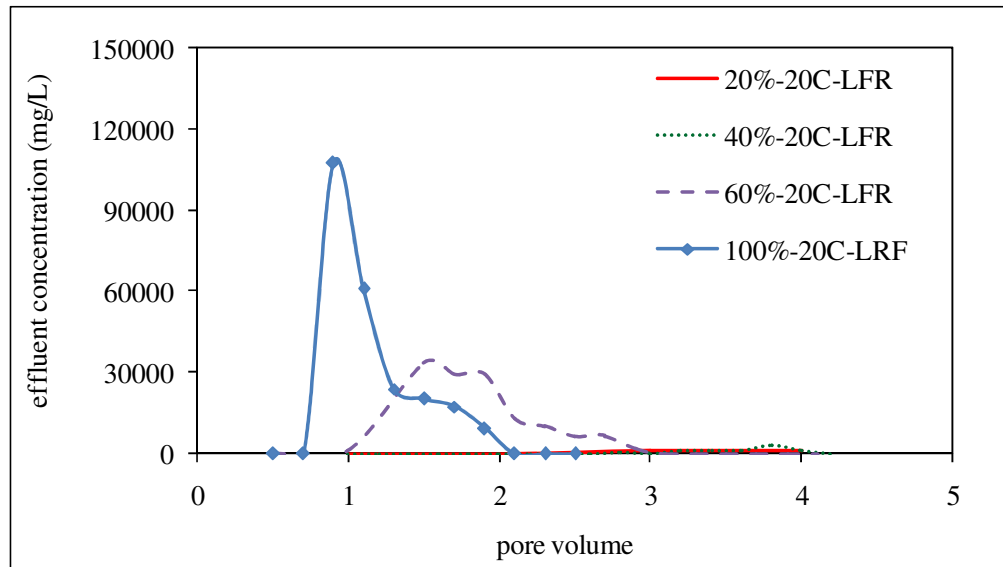


Figure 4.29. Comparison of the effluent toluene concentrations of different ethanol solutions at low flow rate (20⁰C).

As the recovery rates are directly related to the groundwater velocity of the flushing solution, flushing performances of the 60 and 100% ethanol solutions were investigated. The comparison of the cumulative toluene removal performances of different ethanol solutions at different flow rates are presented in Figure 4.30. The main purpose for using different flow rates is to investigate the effect of contact times on the solubilization potential of the flushing solution. As the cumulative per cent removals of the same flushing solutions at different flow rates are compared, it is observed that the recoveries were higher when low flow rates are applied. It was also noticed that the initiation of the breakthrough was faster in the 100% ethanol solutions at low flow rate compared to the same ethanol composition at high flow rate. The initiation of mass in the effluent are relatively similar for both flow rates. This can be attributed to the synergistic effect of the high ethanol content and the high contact times in the 100% case.

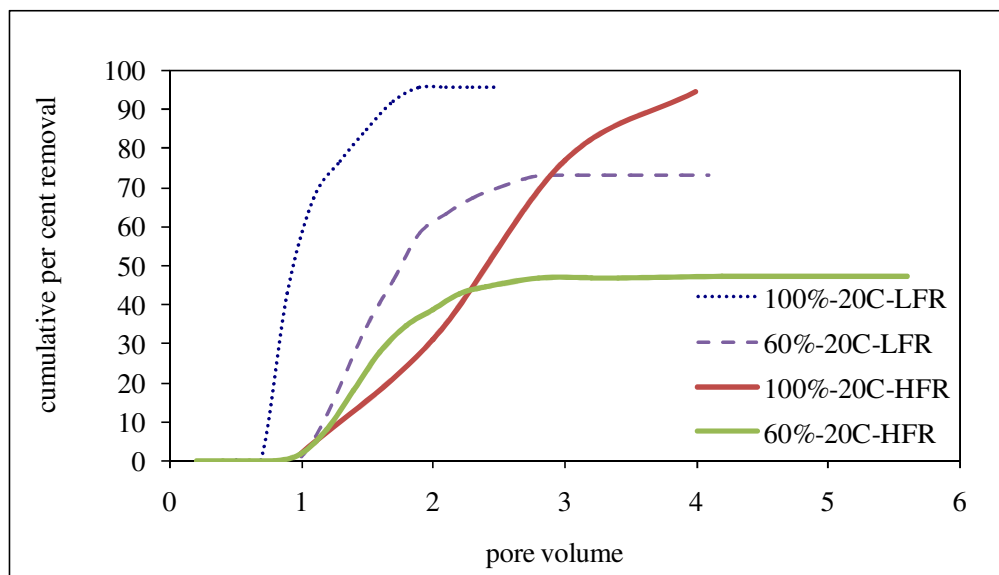


Figure 4.30. Comparison of the cumulative toluene removal performances of different ethanol solutions at different flow rates (20°C).

The effluent toluene concentrations with respect to pore volumes injected at different flow rates are presented in Figure 4.31. The effluent concentration profiles of the flushing solutions with 60% ethanol in different flow rates were very close. For the case with 100% ethanol, the profiles appear to be significantly different with much higher peak concentrations for the case with lower flow rate.

The impact of contact time between the NAPL and flushing solution was examined further using an intermittent flow rate. This flow regime resulted in slightly increased recoveries through more contact. For 40% ethanol solution, the cumulative percent recovery reached almost 14% whereas the maximum toluene recovery for at low flow rate was only 7% as presented in Figure 4.32. This shows that by only increasing the contact time by shutting the flow the efficiency can be increased almost twofold. The effluent toluene concentration profiles, on the other hand, were quite similar with an exception in the pore volume they were recorded. When the breakthrough curves for 40% ethanol solution flushing with low flow rate is compared with the 40% ethanol solution with 40% ethanol solution at intermittent flow rate, it was observed that the introduction of toluene in the effluent was quicker with the intermittent flow case. The comparison of the effluent

toluene concentrations of 40% ethanol solutions at different flow rates (20°C) is presented in Figure 4.33.

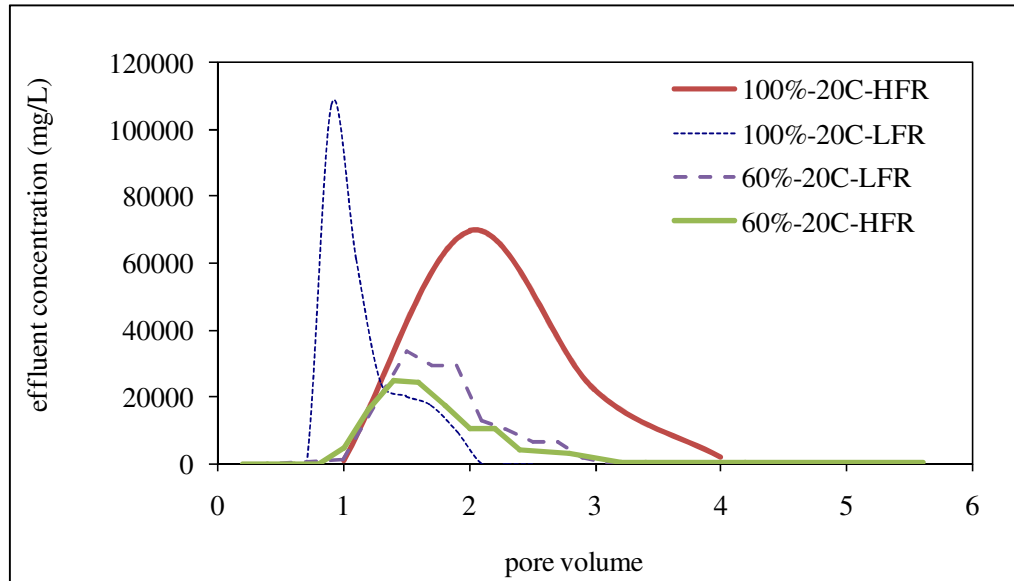


Figure 4.31. Comparison of the effluent toluene concentrations of different ethanol solutions at different flow rates (20°C).

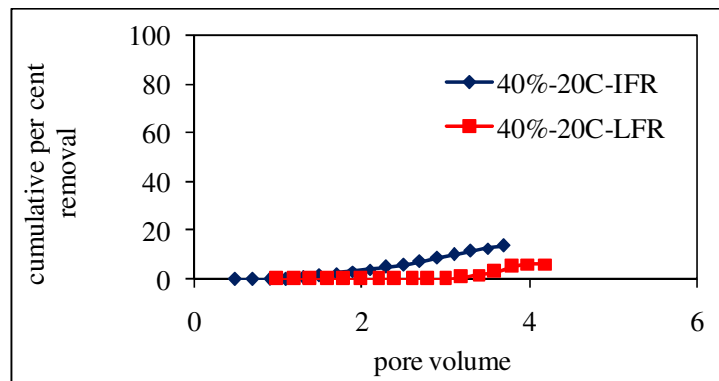


Figure 4.32. Comparison of the cumulative toluene removal performances of 40% ethanol solutions at different flow rates (20°C).

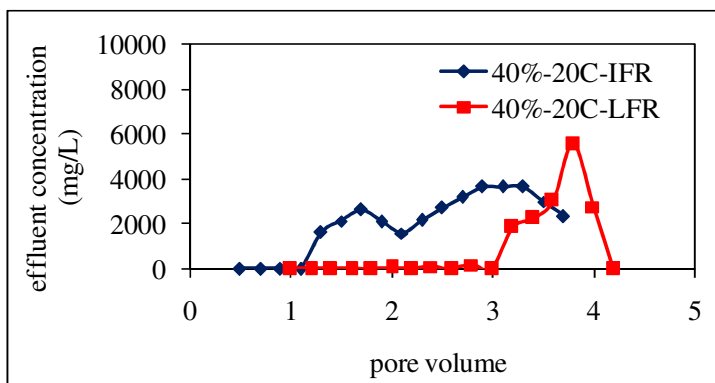


Figure 4.33. Comparison of the effluent toluene concentrations of 40% ethanol solutions at different flow rates (20°C).

The final toluene removal performances of different ethanol solutions at different flow rates are compared for 20°C in Figure 4.34. It was expected that the removal efficiencies would not exceed a certain value at ethanol contents below 50% as the ternary phase diagrams generated both experimentally and numerically showed that the minimum ethanol content should be 50-55% for one phase behavior. This expectation was proven with the sharp increase between 40 and 60% cases.

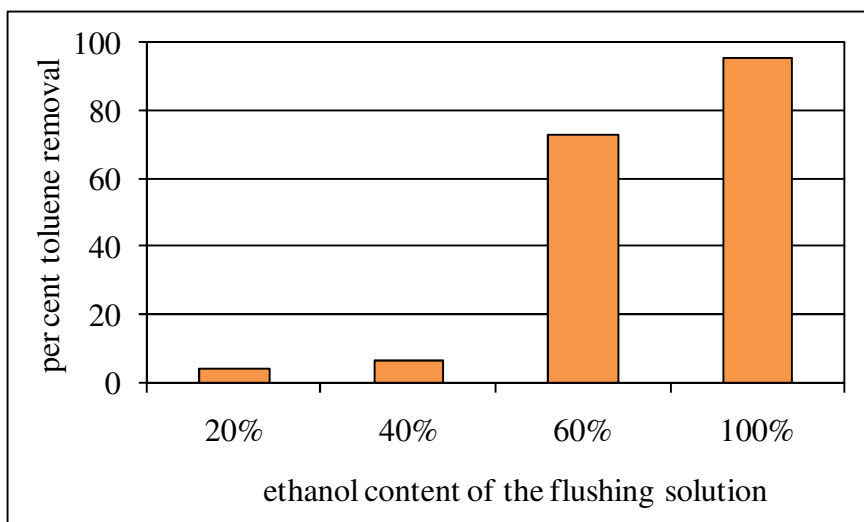


Figure 4.34. Comparison of the final toluene removal performances of different ethanol solutions at different flow rates (20°C).

When the recoveries of 20% and 40% ethanol contents are compared, it was noticed that only a little enhancement was accomplished in the 40% case. The increase in the recovery was most beneficial with 60% case as the 100% ethanol case was not practical in most applications due to the potential problems that might occur such as adverse effects on the microbiological balance of the subsurface and high costs of the chemicals used.

The flow rate was found to be affecting the contact rate and the performance of the experiments. The final toluene removal performances of different ethanol solutions at high and low flow rates are compared in Figure 4.35. The effect of flow rate was more easily noticed in the case with 60% ethanol content, whereas the results of the 100% ethanol cases also verified the impact of flow rate on the recovery performance of the experiments.

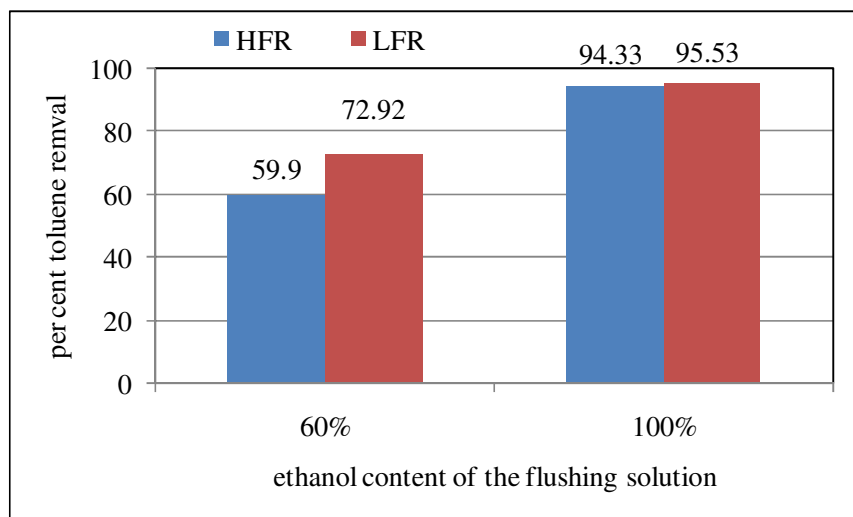


Figure 4.35. Comparison of the final toluene removal performances of different ethanol solutions at high and low flow rates (20°C).

The effect of intermittent flow was also shown comparatively in Figure 4.36 for low flow rates and at 40% ethanol content in the flushing solution. The toluene removal was almost doubled in the case with intermittent flow rate and this result was one of the promising findings in the research as only with the manipulation of flow rate the performance can be enhanced.

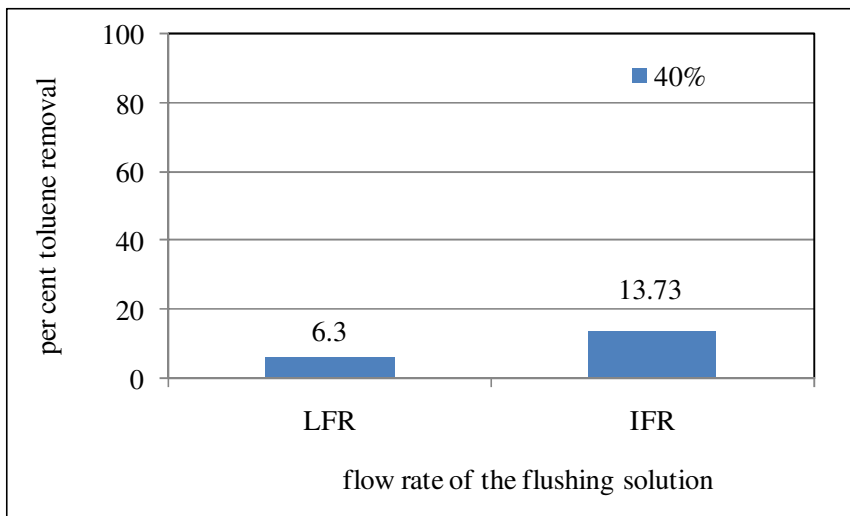


Figure 4.36. Comparison of the final toluene removal performances of 40% ethanol solution at low and intermittent flow rates (20°C).

The overall comparison of the results of the experiments showed that the ethanol content plays an important role in the percent recoveries. However, the removal performance may be increased by manipulation of the flow rate to increase contact time between the contaminant and the flushing solution. The results also indicated that the ethanol content must be close to the region where the miscibility curve is located in the ternary phase diagrams to produce significant solubilization of the NAPL mass. Even higher ethanol contents would be needed in field applications because of the heterogeneity and complexity of real systems.

5. EFFECT OF TEMPERATURE ON THE PERFORMANCE OF CHEMICAL AGENT FLUSHING

It was discussed in Section 4.2 that one of the important operational parameters controlling NAPL recovery through chemical agent flushing is temperature. This chapter describes the potential increase in system performance when the temperature of the flushing solution is increased. Section 5.1 discusses the impact of temperature on the physical and chemical properties of the NAPL flushing solution system. Section 5.2 describes studies involving thermal remediation of porous media contaminated with NAPL. Section 5.3 describes the experimental set up used in this part of the study. Results of the column experiments with thermal enhancements are presented in Section 5.4 .

5.1. Theory

Innovative in-situ recovery techniques are increasingly being evaluated for use at many sites due to the limitations of the conventional techniques. The ineffectiveness of conventional methods attribute to the low solubilities of NAPLs, mass transfer limitations and site heterogeneity (Lunn and Kueper, 1996). Thermal enhancements received great attention due to the benefits recognized (Davis and Lien, 1993). The benefits of thermal enhancements have been discussed in the remediation community over the past several years, with much of the attention centered on the ability of the methods to achieve adequate source removal to reach strict remediation objectives (U.S. Army Corps of Engineers, 2006). The origins of the thermal treatment technologies can be traced back to the oil industry. Steam injection has been applied in the field to enhance the recovery of high gravity oils. Electrical resistance heating has its origins in the petroleum industry, where it was developed to heat oil sands and oil shales to enhance oil recovery.

Flushing based techniques rely solely on the flow of liquids to deliver reagents or to remove dissolved contaminants. These techniques are dependent on the permeability of the media and permeability vary over many orders of magnitude in the subsurface (Bedient et al., 1999). As a result of this limitation liquid diffusion into and out of zones of low

permeability often is hindered in terms of delivering the reagents. The efficiency of thermal enhancements depend on the conduction of heat which is governed by the thermal conductivity distribution and the thermal gradient (U.S. Army Corps of Engineers, 2006). However, the conduction of heat in the subsurface is relatively slow as these materials are generally good insulators. Therefore, efficiency of the thermal treatment depends on the economical and effective delivery of heat into the subsurface.

Heating the contaminated system through addition of hot water, steam, or soil heating using heat blankets, thermal wells, or low frequency electrical heating is a common and proven alternative for traditional remediation methods (Heron, 1998). There are several mechanisms by which heat can be transferred into the subsurface to heat the targeted zone, including direct conduction of heat away from heaters placed in trenches or wells (thermal conductive heating), electrical resistivity heating of the subsurface by passing electrical currents through the soil and steam injection or steam enhanced extraction (Oostrom et al., 2006) .

Thermal treatment has been applied in past mainly to soils that have been excavated and these soils were then incinerated to release and/or destroy the contaminants. However, excavation of contaminated soils was found to be impractical and costly when the contamination occurs at great depths or covers a large area. As an alternative heat-based in-situ remediation methods were proposed especially in areas where excavation was not possible. In many instances, heat based in-situ remediation techniques have been found to be cost effective compared to the excavation and incineration option or other remediation techniques.

Steam, hot air and hot water injection rely on the contact between the injected fluid and the NAPL for heat transfer and recovery. The use of hot air in the field is limited due to the low heat capacity of $1 \text{ kJ/kg}^{\circ}\text{C}$. On the other hand, the heat capacity of steam is four times that of hot air. The high heat of evaporation of steam together with the higher heat capacity makes it more reliable in field applications (Davis and Lien, 1993).

Heat transfer is much faster than aqueous diffusion in porous media. Vaporization of NAPLs and removal from hydraulically inaccessible zones is rapid during thermal

remediation compared to conventional fluid delivery technologies. By increasing the temperature in groundwater systems, the controls of several physical forces responsible for NAPL entrapment are minimized and NAPL removal becomes more efficient (Imhoff et al., 1995). The efficiency of thermal remediation methods can be explained by a variety of factors such as:

- increased volatility of contaminants
- rapid mass transfer
- rapid diffusion and evaporation
- enhanced biological destruction
- heating of impermeable soils
- lower viscosity of water and contaminants
- faster chemical reactions

The main target in thermal remediation methods is to introduce heat to the media to overcome difficulties related to the capillary forces. The process should be monitored properly in order to control the heating flux (power input) in each location in field. These efforts necessitate good engineering practice.

It is essential to understand the properties of organic contaminants that effect their recovery in order to understand how heat can enhance a remediation process. In general, when an organic chemical is heated, its density is reduced, its vapor pressure is increased, its adsorption onto solid phases or absorption into soil organic matter is decreased and its molecular diffusion in the aqueous and gaseous phase is increased (Davis and Lien, 1993; Atkins, 1998). For DNAPLs such as creosote, the density changes can cause a DNAPL to become less dense than water, aiding in its recovery as an LNAPL.

On the other hand, the viscosity of the organic liquid decreases as the temperature increases, but the viscosity of gases increases with temperature. The overall effect of the introduction of heat depends mostly on the properties of the contaminant and the mechanism limiting the removal rate of the contaminant. As the increase in temperature causes expansion of liquids, there occurs a reduction in the interaction between molecules and this reduces the viscosity.

The effect of temperature on solubility is dependent on the chemical. At elevated temperatures, the interactions between constituents are reduced, thus, the net effect of temperature on solubility depends on which interactions are effected to the greatest extent (Davis and Lien, 1993).

The overall effect of thermal enhancements on the recovery of contaminants from the subsurface is somehow unpredictable. The thermal expansion of a liquid with its accompanying decrease in viscosity will allow the heated liquid to flow more readily. Expansion promotes movement of the fluids out of the pore through vaporization of the liquid to the gas phase. Meanwhile, the diffusion of contaminants increases as the temperature increases in both the aqueous and gaseous phases and this helps to move contaminants from areas of low permeability to areas of high permeability.

5.2. Useful Concepts in Thermal Treatment

There are some useful parameters used in the thermal applications such as boiling point, Henry's law constant and octanol-water partition coefficient.

5.2.1. Boiling Point

Boiling point of a liquid mixture is the temperature at which its total vapor pressure is equal to atmospheric pressure (U.S. Army Corps of Engineers, 2006) and is important in deciding the best thermal practice to be applied. The chemicals with low boiling points generally have a lower heat of vaporization. Therefore, these contaminants are relatively easy to volatilize. On the other hand, compounds with higher boiling points have lower vapor pressures at ambient temperatures and higher heat of vaporization. Thus, the energy required to move chemicals with high boiling points to gaseous phase is more.

The contaminants with the lowest boiling points generally have a lower heat of vaporization, thus these contaminants are relatively easy to volatilize. Laboratory experiments have shown that vaporization of even highly volatile compounds can cause a measurable decrease in the temperature of the system.

The total vapor pressure is the sum of partial pressures of all of the components of the mixture, therefore, the boiling point of the mixture can be achieved at a lower temperature than any of the boiling points of any of the separate components. This temperature is called the eutectic point of the azeotropic mixture and many contaminants can be easily removed in vapor at steam temperatures, even if their boiling temperatures are greater than 100°C (U.S. Army Corps of Engineers, 2006). Table 5.1 presents the eutectic boiling points of some NAPL mixtures.

Table 5.1. The eutectic boiling points of some NAPL mixtures (U.S. Army Corps of Engineers, 2006).

NAPL Mixture	Component Boiling Points (°C)	Co-Distillation Point (eutectic point) (°C)
Benzene - Water	80.1 - 100	69.4
Carbon Tetrachloride - Water	76.8 - 100	66.8
Chlorobenzene - Water	132 - 100	56.3
Chloroform - Water	61.2 - 100	56.3
1,2 Dichloroethane - Water	83.5 - 100	72.0
Dichloromethane - Water	40.1 - 100	<39.9
1,4 Dioxane - Water	101.3 - 100	87.8
Etylbenzene - Water	136.2 - 100	92.0
Hexane - Water	69.0 - 100	61.6
Styrene - Water	145.2 - 100	93.9
Tetrachloroethene - Water	121 - 100	88.5
Toluene - Water	110.6 - 100	85.0
1,1,2-Trichloroethane - Water	113.7 - 100	86.0
Trichloroethene - Water	87.1 - 100	73.1
Xylene - Water	139.1 - 100	94.5

5.2.2. Henry's Law Constant

Henry's law constants can also be used to determine the behaviour of the compound and the law is limited to dilute solutions.

$$P_a = x_a \cdot H_a \quad (5.1)$$

where P_a is the partial pressure of chemical a, x_a is the mole fraction of chemical a in solution and H_c is the Henry's law constant. Henry's law constants are function of the aqueous solubility and vapor pressure of the compound. When the Henry's law constant is high, the compound prefers to partition to the air phase (Atkins, 1998).

5.2.3. Octanol-Water Partition (K_{ow}) Coefficient

The octanol-water partition coefficient is defined as the ratio of the equilibrium concentration (expressed as C in Equation 5.2.) of a dissolved substance in a system containing two immiscible solvents (Lyman et al., 1990).

$$K_{ow} = \frac{C_{octanol}}{C_{water}} \quad (5.2)$$

K_{ow} has become a key parameter in environmental studies that focus on the fate of organic chemicals and it has been found to be related to water solubility, adsorption coefficients and bioconcentration factors for aquatic life (Lyman et al., 1990).

The partition coefficient is a parameter used to determine the hydrophobicity of a compound. The hydrophobicity of a compound increases with the K_{ow} (Logan, 1999). The alcohols have low but significant octanol/water partition coefficients K_{ow} between 24 and 240 resulting in NAPL/water partition coefficients between 1 and 22 (Setarge et al., 1999).

5.3. Remediation at Elevated Temperatures

Hot water flushing historically has been used in the petroleum industry to improve recoveries of viscous oils by enhancing oil mobility (Imhoff et al., 1995). This remediation technique is typically designed to mobilize NAPLs with high free-phase residual saturations, but can be expected to increase NAPL solubilization rates as well as aqueous solubility. Hot water injection generally recovers contaminants only in the liquid phase. However, it has been reported by Imhoff et al. (1995) that over the temperature range of 20 to 80⁰C, the NAPL/aqueous interfacial tension decreases by only 7%, which at typical NAPL residual saturations is not sufficient to induce mobilization. Therefore, the most effective method of NAPL removal from hot water flushing is likely through solubilization. Water solubility increases for organic contaminants at elevated temperatures, while dissolution rates increase by factors of two to five, leading to faster NAPL dissolution and removal (Sleep and Ma, 1997).

The air-water interfacial tension is known to decrease with increasing temperature, however it was stated in the report prepared by U.S. Army Corps of Engineers (2006) that temperature has only a minor effect on oil-water interfacial tensions.

Steam injection method has been investigated in 1D and 2D experiments by many researchers such as Gudbjerg et al. (2004), Kaslusky and Udell (2002) and Schmidt et al. (2002). During steam injection NAPLs vaporize soil vapor extraction is required to remove the vapour from the zone. She and Sleep (1999) reported that the method is especially advantageous in heterogeneous porous media. The researchers investigated the mechanisms in the removal of DNAPLs from a saturated layered porous medium system by steam injection. She and Sleep (1999) concluded that steam should be injected below the contaminated zone to ensure that a condensation front of DNAPL does not occur on the lower edge of a steam. Since the exact location of the contaminated area is not known properly in most of the cases, this will be difficult to achieve in the field (Schmidt et al., 2002). Gudbjerg et al. (2004) also conducted steam injection experiments to remove TCE captured on a fine sand layer situated below the water table. In the experiments boiling induced by heat conduction caused the free TCE to vaporize but the dissolved TCE was not removed by steam injection. It was underlined in the results that if pooled TCE exhibits

a pressure approaching the entry pressure of the underlying material, a reduction in surface tension due to the increase in temperature may cause downward migration of the DNAPL.

Thermal treatment is a field scale alternative that has been widely investigated (U.S. Army Corps of Engineers, 2006). However, there are some points that have to be addressed during management. As the movement of the contamination in the subsurface is enhanced via thermal treatment methods, there is always a risk of contaminant spreading but through engineered controls these risks are manageable.

The use of heat in recovery of the contaminants also has the potential to affect the biological community within the treated volume and impacts may extend outward from this zone due to the conduction of heat to surrounding soils.

Dewatering associated with thermal remediation is another potential problem that may result in consolidation of the soils. Changes in moisture content may affect the bearing strength of soils, threatening foundation stability.

The solubility of many materials is modified by temperature, which may increase the dissolved solids, including silica, or may cause others to precipitate near the treated zone. These impacts are generally unavoidable unless steps are taken to prevent groundwater contact with hot and warm soils, or unless groundwater does not naturally contact warmed soil. NAPL often undergoes significant physical change at elevated temperatures, many of which enhance mobility. If migration is not controlled adequately by the design of the recovery system, the NAPL may migrate away from the treated zone.

5.4. Experimental Set-up

The same glass column was used in the determination of the effect of thermal enhancements. An insulation tape was wrapped around the column and the system was heated to temperatures around 50°C. Meanwhile the temperature of the flushing solutions were also heated to temperatures around 50°C by immersing the bottle containing the solution in a preheated water bath to enable the temperature of the effluent to be stable at

temperatures between 30-40°C. The insulated column is presented in Figure 5.1. During stabilization of the target temperatures, the effluent temperature was checked in every 30 minutes and necessary adjustments in both the water bath and the insulation tape were made to have effluent with 30-40°C.

The flushing experiment with 60% ethanol was also repeated at 5°C to investigate the effect of very low temperatures which can be a more reliable case in field. The flushing solution was feed to the system at 5°C and the column was covered with cooling bands. The effluent temperatures recorded were in the range of 10-12°C. The photograph of the cooled column setup is given in Figure 5.2.

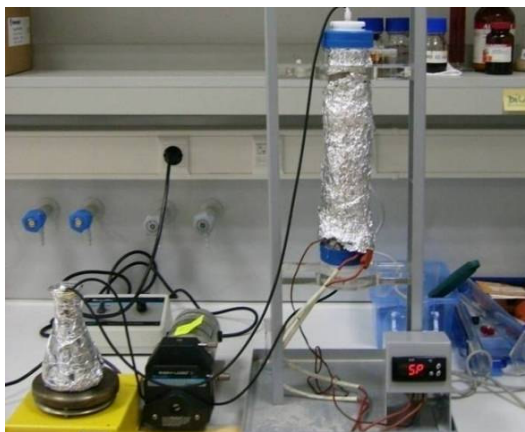


Figure 5.1. The insulated column (heated).



Figure 5.2. The insulated column (cooled).

5.5. Results and Discussion

The effect of thermal enhancements on the recovery efficiencies of ethanol solutions at different concentrations was investigated. Ethanol solutions of 20, 40 and 60% were prepared by mass and the results of the flushing runs were presented in this section.

5.5.1. Dissolution Performance of 20% Ethanol Solution at 40⁰C (Low Flow Rate)

The flushing experiment was conducted with 20% ethanol as the solvent and the samples collected during the experiment were given in Figure 5.3. The cloudy appearance in the vials was observed around 200mL with the completion of the first pore volume. The pure phase toluene was not observed in the vials which contribute to the removal of toluene only in dissolved form. It was expected that the concentrations of the toluene in the effluent could not exceed the solubility values. When compared with the performance of 20% ethanol solution at 20⁰C, the cloudiness was observed faster and the effluent concentration increase was steeper. The cumulative toluene removal and the effluent toluene concentration profiles with 20% ethanol solution at 40⁰C are presented at Figures 5.4 and 5.5 respectively.



Figure 5.3. The samples collected during flushing with 20% ethanol solution at 40⁰C (low flow rate).

The effluent concentrations reached a maximum around 2000 mg/L after the 3rd pore volume, thus the flushing experiment was terminated. The removal of toluene from the system was limited with the low ethanol concentrations and the only benefit observed was the quick response associated with the introduction of heat.

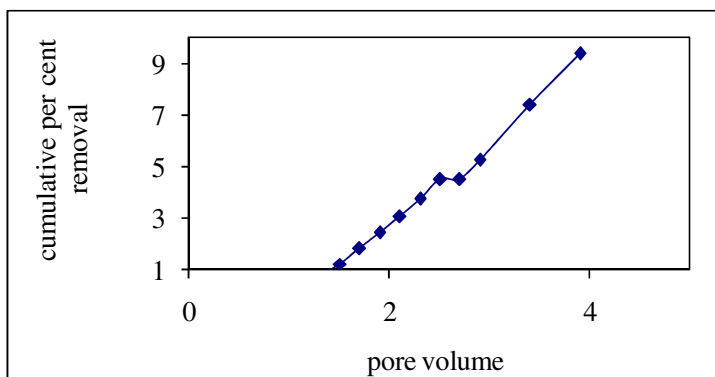


Figure 5.4. The cumulative toluene removal with 20% ethanol flushing at 40°C (low flow rate).

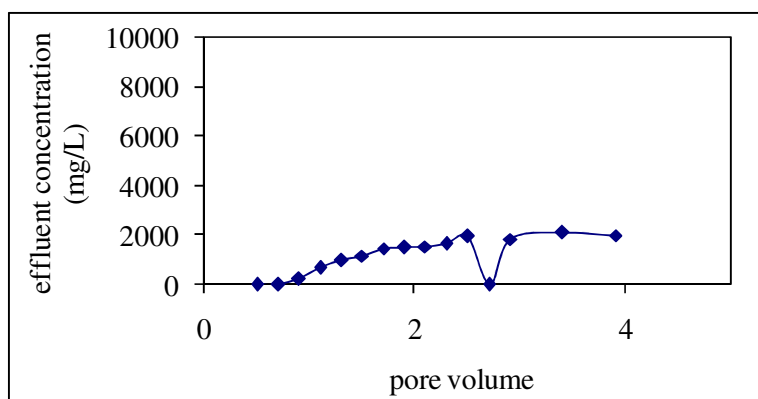


Figure 5.5. The effluent toluene concentration profiles with 20% ethanol flushing at 40°C (low flow rate).

5.5.2. Dissolution Performance of 40% Ethanol Solution at 40°C (Low Flow Rate)

Toluene was introduced to the column and the average flow rate was recorded as 3.43 mL/min during the flushing of 5 pore volumes of 40% ethanol solution. The effluent was observed to become cloudy after the introduction of 160 mL of the flushing solution and after the completion of the first pore volume the effluent was completely cloudy with no free phase till the 500 mL. After 500 mL, free phase toluene started to leave the system and this can be seen in Figure 5.6 and 5.7. The red color of toluene leaving the system was noticed easier by the 600 mL and cloudiness of the effluent started to diminish by 700 mL.

The samples collected were completely transparent after 720 mL. The cumulative recoveries and the effluent concentration profiles are presented at Figures 5.8 and 5.9 respectively for 40% ethanol solution at 40°C.

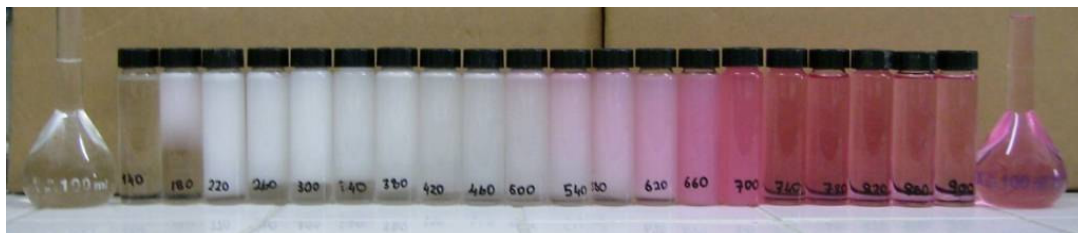


Figure 5.6. The samples collected during flushing with 40% ethanol solution at 40°C (low flow rate).

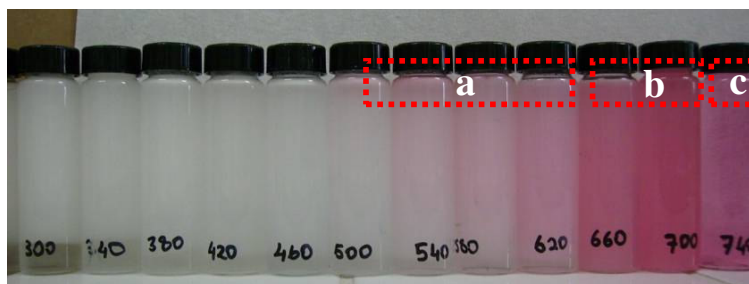


Figure 5.7. The phases of toluene removal with 40% ethanol solution at 40°C (low flow rate).

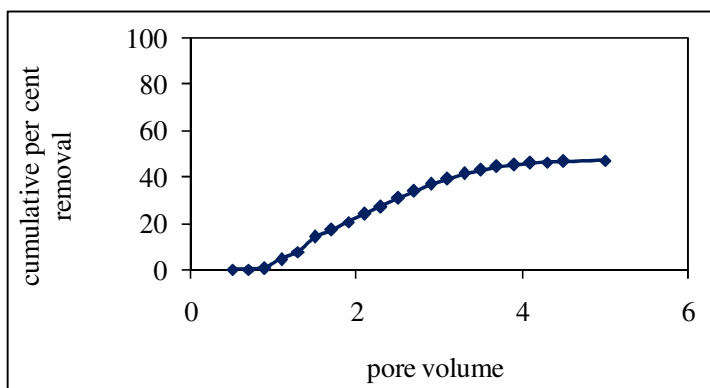


Figure 5.8. The cumulative toluene removal with 40% ethanol flushing at 40°C (low flow rate).

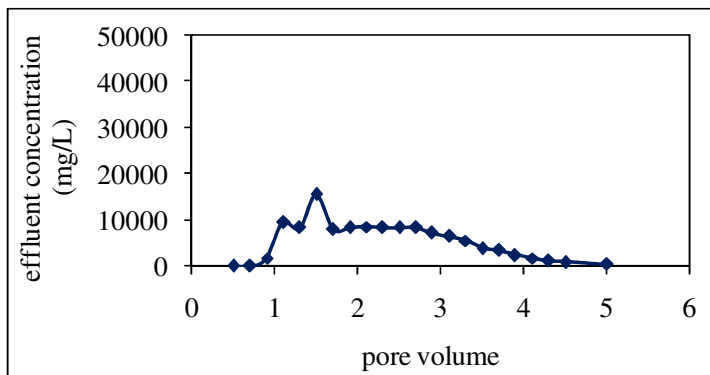


Figure 5.9. The effluent toluene concentration profiles with 40% ethanol flushing at 40°C (low flow rate).

5.5.3. Dissolution Performance of 60% Ethanol Solution at 40°C (Low Flow Rate)

The removal performance of 60% ethanol solution for 10 g of toluene injected upwards in a saturated sandpack was investigated at 40°C. Free phase toluene breakthrough was at 180 mL and layers of toluene were collected in vials 240-320 mL. After 320 mL, the homogeneous samples with decreasing color intensity were observed. The highest effluent toluene concentrations were around 30000 mg/L which was recorded at the end of the second pore volume. The cumulative toluene removal with 60% ethanol flushing at 40°C is presented in Figure 5.10.

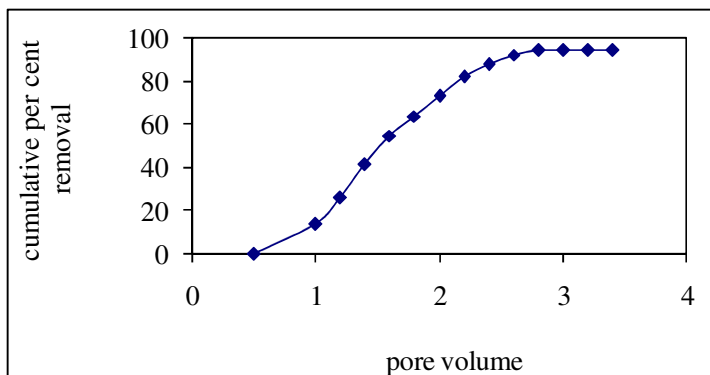


Figure 5.10. The cumulative toluene removal with 60% ethanol flushing at 40°C (low flow rate).

The final recovery was 88.17%, most of which was collected in three pore volumes. Toluene concentrations in the effluent started to decrease after the second pore volume which can be seen in Figures 5.11 and 5.12.

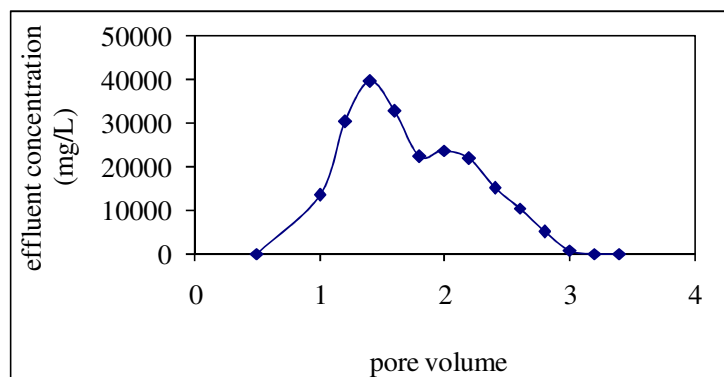


Figure 5.11. The effluent toluene concentration profiles with 60% ethanol flushing at 40°C (low flow rate).



Figure 5.12. The samples collected during flushing with 60% ethanol solution at 40°C (low flow rate).

5.5.4. Dissolution Performance of 60% Ethanol Solution at 10°C (Low Flow rate)

The flushing experiment with 60% ethanol solution was repeated at 10°C to investigate the relation of temperature with the recovery performance. 10°C was chosen as the average subsurface temperature reported was around 10°C (Fetter, 1994). The temperature of the flushing solution and the column was controlled throughout the experiment to minimize temperature changes which could interfere with the recovery efficiencies. The recovery efficiency was around 70% in flushing experiment with 60% ethanol solution at room temperature whereas, the recovery was only 39.8% when the

experiment was conducted at 10⁰C. This shows that the recoveries will be lower when the flushing runs are conducted at low temperatures. The cumulative recoveries and the effluent concentration profiles are presented at Figures 5.13 and 5.14 respectively for 60% ethanol solution at 10⁰C.

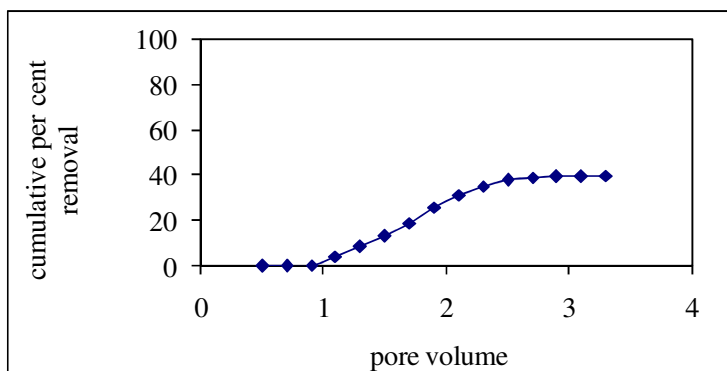


Figure 5.13. The cumulative toluene removal with 60% ethanol flushing at 10⁰C (low flow rate).

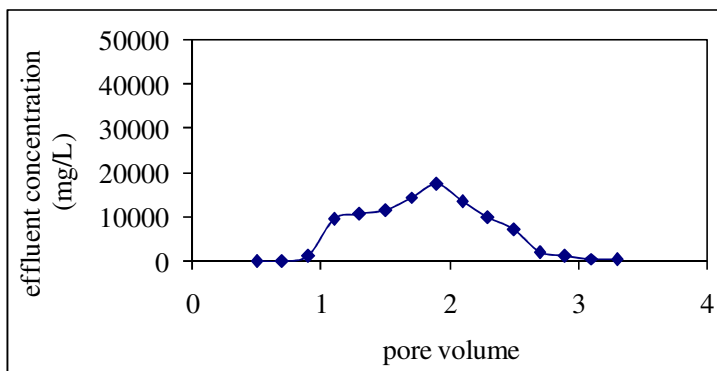


Figure 5.14. The effluent toluene concentration profiles with 60% ethanol flushing at 10⁰C (low flow rate).

The samples collected during flushing complied with the GC results, showing that the recovery was realized during second and third pore volume. The color comparisons for the sample vials also showed that limited toluene removal was accomplished when compared with the samples collected during 60% ethanol solution at higher temperatures.



Figure 5.15. The samples collected during flushing with 60% ethanol solution at 10°C (low flow rate).

5.6. Conclusions

In order to investigate the impact of thermal enhancements on the recovery efficiencies of contaminants from soil packs, different flushing scenarios were conducted. Thermally enhanced experiments provided better recovery efficiencies compared to the experiments conducted at lower temperatures. This was attributed to the fact that through enhanced solubilization and minimization of forces limiting movement of the contaminant, recoveries were accelerated. Comparison of the cumulative toluene removal performances and effluent toluene concentration profiles of different ethanol solutions at different temperatures are presented in Figures 5.16 and 5.17, respectively. The cumulative toluene removal percentages are compared in Figure 5.18.

For the case with 20% ethanol content, the increase in the temperature of the injected solution produced little impact because the 20% ethanol was too small to cause any substantial increase in the solubilization even at the higher temperature. However, the impact of thermal enhancements on the 40% ethanol solutions was more apparent as the recoveries were increased from 5 to nearly 35%.

A similarly large enhancement was observed for the case with 60% ethanol content at 40°C in comparison to the case conducted at 20°C. At 20°C, the toluene mass recovered was about 70% compared to 88% at 40°C.

The results of the flushing experiment with 60% ethanol solution at 10⁰C showed that the recovery efficiency decreased to around 40%. This points out to the importance of maintaining the temperature in the any laboratory scale evaluation close to what would be encountered in the field for more consistent evaluation of the real system.

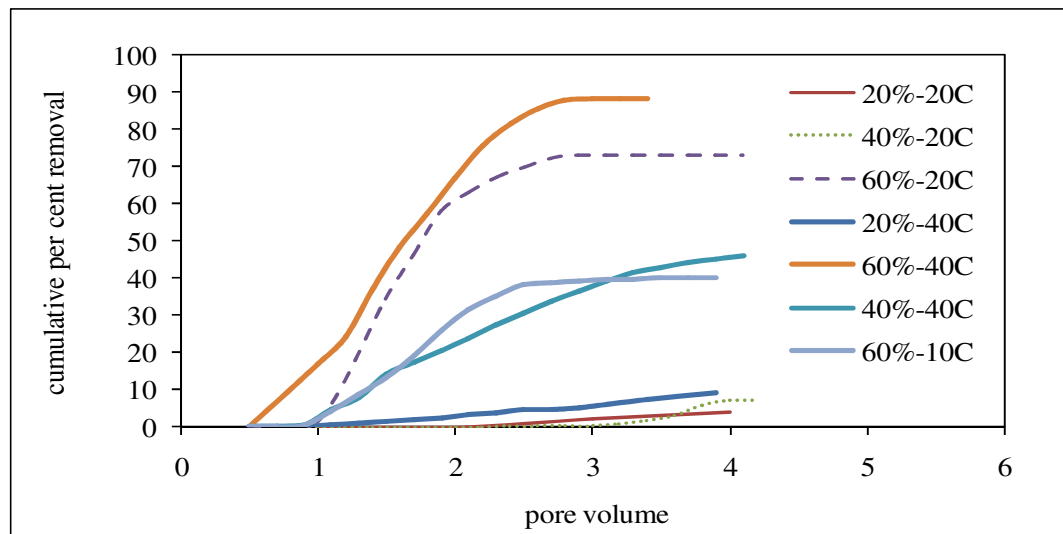


Figure 5.16. Comparison of the cumulative toluene removal performances of different ethanol solutions at different temperatures (low flow rate).

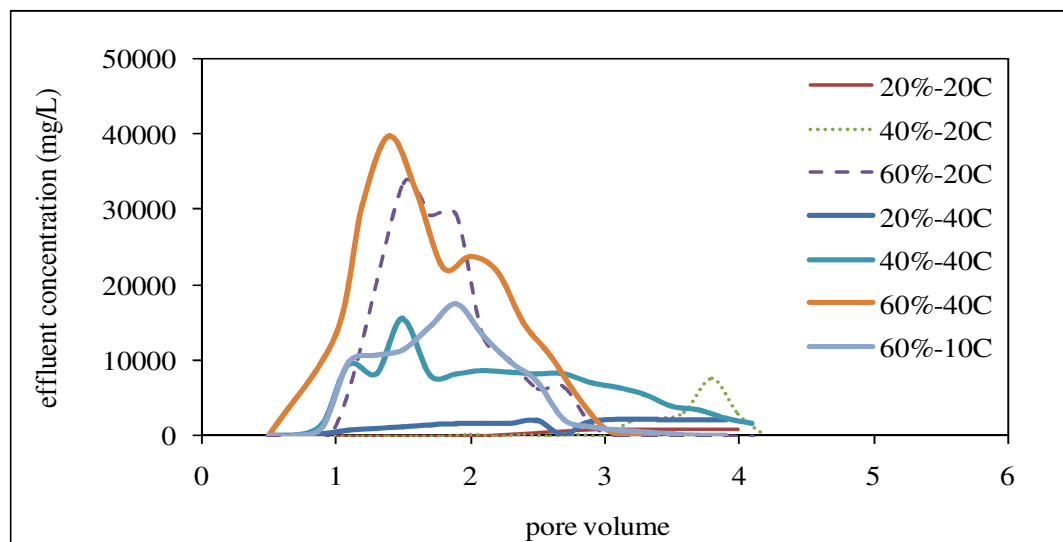


Figure 5.17. Comparison of the effluent toluene concentration profiles with different ethanol solutions at different temperatures (low flow rate).

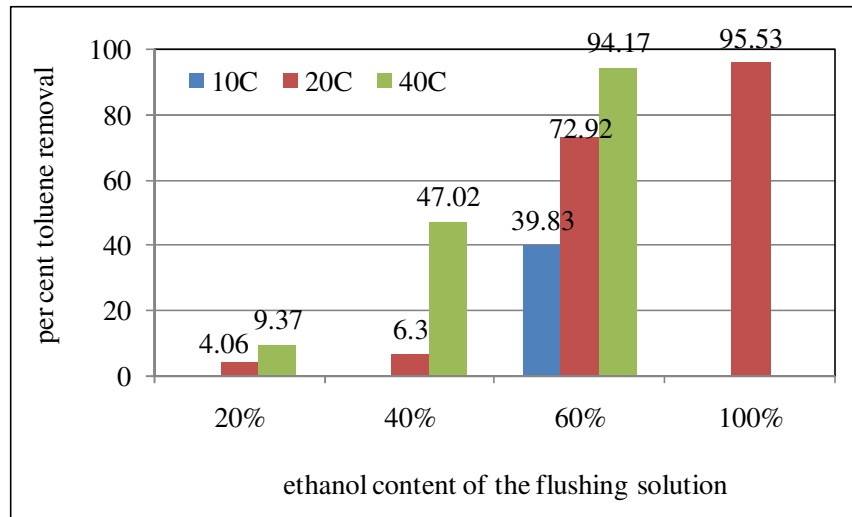


Figure 5.18. Comparison of the final toluene removal performances with different ethanol solutions and different temperatures (low flow rate).

6. FINAL CONCLUSIONS AND RECOMMENDATIONS FOR FUTURE RESEARCHES

The presence of organic compounds contaminants in the form of nonaqueous phase liquids (NAPL) in the subsurface is one of the most challenging environmental problems. Due to their unique properties, namely low biodegradability, low solubility and high interfacial tension, these compounds tend to persist in the subsurface for decades and perhaps centuries.

One of the most promising groundwater remediation technologies is the use of chemical agents such as surfactants or alcohols for their enhanced solubilization and mobility and ultimately removal from the porous media. Prior to conducting any expensive pilot tests or field work, it is important to develop inexpensive means for the rapid evaluation of the effectiveness of different chemical agents and the operating parameters of the system. In this study two bench scale experimental procedures were considered:

- ternary phase diagrams for the description of the multiphase behaviour of the system
- one-dimensional sand-packed column experiments for the testing of the evaluation of different operating parameters, namely chemical content of the flushing solution, flow velocity and regime, and temperature.

In addition, a computer program that computes the multiphase mole fractions at equilibrium was developed.

The target NAPLs that were considered in this study are toluene and 1,2-dichlorobenzene. These contaminants are widely used in industry and as components of gasoline. Both are highly toxic to the environment and human health.

The main findings of the present study are listed in the following pages. These are followed by recommendations for future research efforts.

Phase Behavior and Equilibrium

- Experimental methods developed to observe the ternary phase behavior indicate that alcohols, in particular ethanol, are effective in solubilizing the model NAPLs. However, the effectiveness of alcohols is enhanced when used together with surfactants, provided that the surfactants can be added to the system efficiently.
- Among the three surfactants considered, Triton X100 was the most favorable surfactant in the titrations and caused less problems in the introduction to the vials.
- The results for the interfacial tension measurements showed that the highest interfacial tensions were measured on the right side of the ternary phase diagram around 100% toluene. As the composition of the two phase mixture moved towards the water-ethanol axis, the interfacial tensions decreased.
- The interfacial tensions decreased more near the ethanol-toluene axis while moving upwards towards the 100% ethanol point. Since the phase compositions become close in the present phases, the interfacial tension becomes very small and this decrease is very rapid in the region where the plait point is located compared to other areas.
- Ternary phase diagrams that may be used as reference in chemically enhanced remediation activities are contaminant-specific. The results provide important preliminary data for the enhancement of the model contaminants in the subsurface.

Effect of Chemical Agent Content in Flushing Solutions

- Concentration profiles collected from the one-dimensional column experiments performed with toluene as the NAPL and ethanol as the solubilizing agent showed that an increase in recovery performances was achieved through increase in chemical agent content.
- Although the per cent recoveries increased with the ethanol content, the recoveries were only marginally higher for the case with 40% ethanol content (6% recovery after four pore volumes) than the case with 20% (4% recovery after four pore volume). These results are consistent with the results of the ternary phase behavior which predicted very little NAPL solubilization at these two ethanol contents.
- The expectations for enhanced dissolution were met in flushing with 60% ethanol, this is consistent with the ternary phase diagram results which show that the peak

point of the miscibility curve is close to 50% ethanol and this ethanol content must be approached or exceeded to produce effective solubilization of the NAPL.

Effect of Flow Rate

- The groundwater velocity, because of its direct influence on the contact time, was also found to play a significant role in the efficiency of the NAPL recovered.
- The initiation of the breakthrough was faster in the 100% ethanol solutions at low flow rate compared to the same ethanol composition at high flow rate. The initiation was relatively similar at 60% ethanol solutions at low and high flow rates.
- The effluent concentration profiles of the flushing solutions with 60% ethanol in different flow rates were very close, whereas the contact time seems to be more effective in the peak toluene concentrations for the flushing cases with pure ethanol.
- The use of intermittent flow rate to increase the contact time between the resident NAPL and the flushing solution can be an important factor in increasing NAPL recovery. For example, for the case of 40% ethanol in the flushing solution, NAPL recovery was about 14% at intermittent flow rate compared to 7% at low flow rate, an increase by a factor of 2.

Effect of Thermal Enhancements

- Thermally enhanced experiments provided better recovery efficiencies compared to the experiments conducted at lower temperatures. This was attributed to the fact that heat enhances solubilization and minimizes the forces limiting movement of the contaminant, namely IFT and viscosity.
- The recovery in flushing experiments with 20% ethanol was only marginally enhanced when the temperature of the flushing solution was 40⁰C, due to the local equilibrium concentrations. On the other hand, increasing the flushing solution temperature to 40⁰C resulted in a significant increase in the recovered NAPL, from 5 to nearly 35%.

- Breakthrough curves collected from the thermally enhanced dissolution experiments revealed that with the 60% ethanol in the flushing solution, the recoveries were more satisfactory when combined with the heat enhancements.

Recommendations on Future Studies

Based on the experimental work conducted in this study, future extensions may focus on the following issues:

- treatment of produced fluids - recycling of the chemical agents: In-situ chemical flushing would produce large volumes of water. Effective means for NAPL agent recovery would be needed.
- performance of alcohol flushing in the presence of mixed contaminants: The present experiments considered only one NAPL at a time. In real cases, multiple contaminants can be present which would significantly complicate the system and influence the recovery effectiveness.
- evaluation of alternatives for chemical agent solution delivery schemes: For example, one could consider pulsed, forward/backward etc. injection schemes.
- impact of combined chemical agent utilization on the performance of flushing operation: The results of the ternary phase diagram showed that promising results may be obtained through the use of multiple agents, either simultaneously or sequentially.
- The results of thermal enhancements in conjunction with chemical flushing were quite promising. This could be expanded to other NAPLs, possibly DNAPLs where thermal manipulation of the density may also be achieved.
- All the above experiments were conducted in one-dimensional columns containing fairly uniform porous media. In reality, soil heterogeneity is a salient characteristic of practically all geological units. The above experiments could be expanded to more complex setups such as two-dimensional tanks and, ultimately, field scale experiments.

REFERENCES

- Abdul, A.S., Gibson, T.L., Rai, D.N., 1990. Laboratory studies of the flow of some organic solvents and their aqueous solutions through bentonite and kaolin clays. *Ground Water*, 25, 524–533.
- Abriola, L.M., Dekker, T.J. and Pennell, K.D., 1993. Surfactant-enhanced solubilization of residual dodecane in soil columns: 2. Mathematical modeling. *Environmental Science and Technology*, 27, 12, 2341–2351.
- Adamson, D.T., McDade, J.M., Hughes, J.B., 2003. Inoculation of a DNAPL source zone to initiate reductive dechlorination of PCE. *Environmental Science and Technology*, 37, 11, 2525-2533.
- Anwar, A.H.M.F., Tien, T. H.; Inoue, Y., Takagi, F., 2003. Mass transfer correlation for nonaqueous phase liquid volatilization in porous media. *Environmental Science and Technology*, 37, 7, 1277-1283.
- ASTM D 2434-68, 2000. Standard Test Method for Permeability of Granular Solid (Constant Head), West Conshohocken, PA, USA.
- Ataie-Ashtiani, B., Hassanizadeh, S.M., Oostrom, M., Celia, M.A., White, M.D., 2001. Effective parameters for two-phase flow in a porous medium with periodic heterogeneities. *Journal of Contaminant Hydrology*, 49, 87-109.
- Atkins, P., 1998. *Physical Chemistry*. Freeman, New York, NY.
- Bai, G., Brusseau, M.L., Miller, R.M., 1997. Biosurfactant enhanced removal of residual hydrocarbon from soil. *Journal of Contaminant Hydrology*, 25, 157-170.
- Bear, J., 1972. *Dynamics of Fluids in Porous Media*, American Elsevier Publishing Co., New York.

Bedient, P.B., Rifai, H.S., Newell, C.J., 1999. Ground Water Contamination Transport and Remediation, Prentice Hall, Inc., USA.

Beitinger, E., 1998. Permeable Treatment Walls-Design, Constration, and Cost (542-R-98-003). NATO/CCMS Pilot Study, Committee on the Challenges of Modern Society USEPA.

Boving, T.B., Brusseau, M.L., 2000. Solubilization and removal of residual trichloroethene from porous media: Comparion of several solubilization agents. *Journal of Contaminant Hydrology*, 42, 51-67.

Bradford, S.A., Phelan, T.J., Abriola, L.M., 2000. Dissolution of residual tetrachloroethylene in fractional wettability porous media: correlation development and application. *Journal of Contaminant Hydrology*, 45, 35–61.

Brandes, D., 1992. Effect of Phase Behaviour on Residual DNAPL Displacement from Porous Media by Alcohol Flooding. Masters Dissertation, Clemson University, USA.

Brusseau, M.L., Wang, X., Hu, Q., 1994. Enhanced transport of low-polarity organic compounds through soil by cyclodextrin. *Environmental Science and Technology*, 28, 952–956.

Burden, F.R., Forstner, U., McKelvie, I., 2002. *Environmental Monitoring Handbook*, McGraw Hill, p 677.

Butler, E.C., Hayes, K.F., 1997. Micellar solubilization of non-aqueous phase liquid contaminants by nonionic surfactant mixtures: Effects of sorption, partitioning and mixing. *Water Resources*, 32, 5, 1345-1354.

Butler, E.C., Hayes, K.F., 1998. Effects of solution composition and pH on the reductive dechlorination of hexachloroethane by iron sulfide. *Environmental Science and Technology*, 32, 1276–1284.

Carey, M.A., Fretwell, B.A., Mosley, N.G., Smith, J.W.N., 2002. Guidance on the use of Permeable Reactive Barriers for Remediating Contaminated Groundwater. National Groundwater & Contaminated Land Centre report NC/01/51, Environment Agency, Bristol, UK.

Cassidy, N.J., 2007. Evaluating LNAPL contamination using GPR signal attenuation analysis and dielectric property measurements: Practical implications for hydrological studies. *Journal of Contaminant Hydrology*, 94, 1-2, 49-75.

Chevalier, L.R., Petersen, J.R., 1999. Literature review of 2-D laboratory experiments in NAPL flow, transport and remediation. *Journal of Soil Contamination*, 8, 1, 149-167.

Chevalier, L.R., Fonte, J.M., 2000. Correlation model to predict residual immiscible organic contaminants in sandy soils. *Journal of Hazardous Materials*, B72, 39-52.

Chiou, C.T., Kile, D.E., Brinton, T.I., Malcolm, R.L., Leenheer, J.A., MacCarthy P., 1987. A comparison of water solubility enhancements of organic solutes by aquatic humic materials and commercial humic acids. *Environmental Science and Technology*, 21, 1231-1234.

Choy, B., Reible, D.D., 1996. UNIFAC Activity Coefficient Calculator Version 3.0, <http://www.hsrcssw.org/ssw-downloads.html>.

Christ, J.A., Abriola, L.M., 2007. Modeling metabolic reductive dechlorination in dense non-aqueous phase liquid source-zones. *Advances in Water Resources*, 30, 6-7, 1547-1561.

Chu, W., Chan, K.H., 2003. The mechanisms of the surfactant-aided soil washing system for hydrophobic and partial hydrophobic organics. *The Science of the Total Environment*, 307, 83-92.

Cohen, R.M., Mercer, J.W., 1993. DNAPL Site Evaluation, C. K. Smoley / CRC Press, Boca Raton, Florida.

Conrad, S.H., Glass, R.J., Peplinski, W.J., 2002. Bench-scale visualization of DNAPL remediation processes in analog heterogeneous aquifers: Surfactant floods and in situ oxidation using permanganate. *Journal of Contaminant Hydrology*, 58, 13–49.

Cowell, M.A., Kibbey, T.C.G., Zimmerman, J.B., Hayes, K.F., 2000. Partitioning of ethoxylated nonionic surfactants in water/NAPL systems : Effects of surfactant and NAPL properties. *Environmental Science and Technology*, 34, 1583-1588.

Culligan, K.A., Wildenschild, D., Christensen, B.S.B., Gray, W.G., Rivers, M.L., 2006. Pore-scale characteristics of multiphase flow in porous media: A comparison of air–water and oil–water experiments. *Advances in Water Resources*, 29, 2, 227-238,

Davis, E.L., Lien, B.K., 1993. Laboratory study on the use of hot water to recover light oily wastes from sands (600/R-93/021). R.S. Kerr Environmental Research Laboratory, Ada, Oklahoma.

Dekker, T.J., Abriola, L.M., 2000. The influence of field-scale heterogeneity on the infiltration and entrapment of dense nonaqueous phase liquids in saturated formations. *Journal of Contaminant Hydrology*, 42, 187-218.

Dev, H.J., Bridges, G., Sresty, J., Enk, N., Mshaiel, A, Love, M., 1989. Radio frequency enhanced decontamination of soils contaminated with halogenated hydrocarbons (600/2-89/008). USEPA, Cincinnati, Ohio, USA.

Dwarakanath, V., Kostarelos, K., Pope, G.A., Shotts, D., Wade, W.H., 1999. Anionic surfactant remediation of soil columns contaminated by nonaqueous phase liquids. *Journal of Contaminant Hydrology*, 38, 4, 465–488.

Edwards, D.A., Adeel, Z., Luthy, R.G., 1994. Distribution of nonionic surfactant and phenanthrene in a sediment/aqueous system. *Environmental Science and Technology*, 28, 8, 1550–1560.

Fredenslund, A.A., Jones, R.L., Prausnitz, J.M., 1975. Group-contribution estimation of activity coefficients in nonideal liquid mixtures. *AIChE Journal*, 21, 1086-1099.

Falta, R.W., Brame, S.E., Lee, C.M., Coates, J.T., Wright C., Price, S., Haskell, P., Roeder, E., 1996. A field test of NAPL removal by high molecular weight alcohol injection. *Proceedings of the Symposium on NAPLs in the Subsurface Environment: Assessment and Remediation*, American Society of Civil Engineers, Washington, D.C., 257-268.

Falta, R.W., 1998. Using phase diagrams to predict the performance of cosolvent floods for NAPL remediation. *Ground Water Monitoring and Remediation*, 18, 3, 94–102.

Fawcett, W.R., 2001. *Liquids, Solutions, and Interfaces : From Classical Macroscopic Descriptions to Modern Microscopic Details*. Oxford University Press, Incorporated, Cary, NC, USA.

Fetter, C.W., 1994. *Applied Hydrogeology; Third Edition*. Prentice-Hall, Inc. , Englewood Cliffs, NJ.

Fontenot, M.M., Vigil, R.D., 2002. Pore-scale study of nonaqueous phase liquid dissolution in porous media using laser-induced fluorescence. *Journal of Colloid and Interface Science*, 247, 2, 481–489.

Fountain, J.C., Waddell-Sheets, C., Lagowski, A., Taylor, C., Frazier, D., Byrne, M., 1995. Enhanced Removal of Dense Non-aqueous Phase Liquids Using Surfactants: Capabilities and Limitations from Field Trials, *Surfactant Enhanced Subsurface Remediation – Emerging Technologies*, ACS Symposium Series, American Chemical Society, Washington, DC, 177–190.

Fountain, J.C., Starr, R.C., Middleton, T., Beikirch, M., Taylor, C., Hodge, D., 1996. A controlled field test of surfactant enhanced aquifer remediation. *Journal of Ground Water*, 34, 5, 910-916.

Freeze, R.A., Cherry, J.A., 1979. *Groundwater*. Prentice-Hall, Englewood Cliffs, NJ.

Fu, X., Imhoff, P.T., 2002. Mobilization of small DNAPL pools formed by capillary entrapment. *Journal of Contaminant Hydrology*, 56, 137-158.

Geller, J.T., Hunt, J.R., 1993. Mass-transfer from nonaqueous phase organic liquids in water-saturated porous-media. *Water Resources Research*, 29, 4, 833-845.

Golfinopoulos, S.K., Lekkas, T.D., Nikolaou, A.D., 2001. Comparison of methods for the determination of volatile organic compounds in drinking water. *Chemosphere*, 45, 275-284.

Grubb, D.G., Sitar, N., 1999. Mobilization of trichloroethene during ethanol flooding in uniform and layered sand packs under confined conditions. *Water Resources Research*, 35, 11, 3275-3289.

Gudbjerg, J., Sonnenborg, T.O., Jensen, K.H., 2004. Remediation of NAPL below the water table by steam-induced heat conduction. *Journal of Contaminant Hydrology*, 72, 207-225.

Haley, J.L., Hanson, B., Enfield, C., Glass, J., 1991. Evaluating the effectiveness of groundwater extraction systems. *Ground Water Monitoring and Review*. 11, 1, 119-124.

Hansen, H.K., Rasmussen, P., Fredenslund, A., Schiller, M., Gmehling, J., 1991. Vapor-liquid equilibria by UNIFAC group contribution: 5. Revision and extension. *Industrial Engineering and Chemical Resources*, 30, 2352-2355.

Harjo, B., Ng, K.M., 2004. Visualization of high-dimensional liquid-liquid equilibrium phase diagrams. *Industrial Engineering and Chemical Resources*, 43, 14, 3566 -3576.

Harwell, J.H., Sabatini, D.A., Knox, R.C., 1999. Surfactants for ground water remediation. *Colloids and Surfaces-A*. 151, 255-268.

Hayase, K., Tsubota, H., 1983. Sedimentary humic and fulvic acid as surface active substances. *Geochimica et Cosmochimica Acta*, 47, 947-952.

Heron, G., Van Zutphen, M., Christensen, T.H., Enfield, C.G., 1998. Soil heating for enhanced remediation of chlorinated solvents: A laboratory study on resistive heating and vapor extraction in a silty, low permeable soil contaminated with trichloroethylene. *Environmental Science and Technology*, 32, 1474-1481.

Helmig, R., 2003. Multiphase flow, transport and bioremediation in the subsurface. Seminar Notes, University of Stuttgart, Germany.

Hofstee, C., Ziegler, C.G., Trötschler, O., Braun, J., 2003. Removal of DNAPL contamination from the saturated zone by the combined effect of vertical upward flushing and density reduction. *Journal of Contaminant Hydrology*, 67, 61-78.

Illangasekare, T.H., Ramsey, J.L., Jensen, K.H., Butts, M.B., 1995a. Experimental study of movement and distribution of dense organic contaminants in heterogeneous aquifers. *Journal of Contaminant Hydrology*, 20, 1-25.

Illangasekare, T.H., Armbruster, E.J., Yates, D.N., 1995b. Non-aqueous phase fluids in heterogeneous aquifers: Experimental study. *Journal of Environmental Engineering*, 121, 8, 571-79.

Imhoff, P.T., Gleyzer, S.N., McBride, J.F., Vancho, L.A., Okuda, I., Miller, C.T., 1995. Cosolvent enhanced remediation of residual reuse nonaqueous phase liquids—Experimental investigation. *Environmental Science and Technology*, 29, 8, 1966–1976.

ITRC, 2005. *Permeable Reactive Barriers: Lessons Learnt/New Directions*, 444 North Capitol Street, NW, Suite 445, Washington, DC 20001.

Jafvert, C.T., 1996. Surfactants and cosolvents. Technology Evaluation Report, TE-96-02, Ground-Water Remediation Technologies Analysis Center, USA.

Jawitz, J.W., Annable, M.D., Rao, P.S.C., Rhue, R.D., 1998. Field implementation of a Winsor type I surfactant/alcohol mixture for in-situ solubilization of a complex LNAPL as a single-phase microemulsion. *Environmental Science and Technology*, 32, 523–530.

Jawitz, J.W., Dai, D., Rao, P.S.C., Annable, M.D., Rhue, R.D., 2003. Rate-limited solubilization of multicomponent nonaqueous-phase liquid by flushing with cosolvents and surfactant: modeling data from laboratory and field experiment, *Environmental Science and Technology*, 37, 1983–1991.

Jeong, S.W., Corapcioglu, M.Y., 2003. A micromodel analysis of factors influencing NAPL removal by surfactant foam flooding. *Journal of Contaminant Hydrology*, 60, 77-96.

Jia, C., Shing, K., Yortsos, Y.C., 1999. Visualization and simulation of non-aqueous phase liquids solubilization in pore networks. *Journal of Contaminant Hydrology*, 35, 363–387.

Jin, M., Delshad, M., Dwarakanath, V., McKinney, D.C., Pope, G.A., Sepehrnoori, K., Tilburg, C.E., 1995. Partitioning tracer test for detection, estimation, and remediation performance assessment of subsurface nonaqueous phase liquids. *Water Resources Research*, 31, 5, 1201–1211.

Johnson, V.P., John, W.W., 1999. PCE solubilization and mobilization by commercial humic acid. *Journal of Contaminant Hydrology*, 35, 343–362.

Johnson-Logan, L.R., Broshears, R.E., Klaine, S.J., 1992. Partitioning behaviour and the mobility of chlordane in groundwater. *Environmental Science and Technology*, 26, 2234-2239.

Jones, D.A., Lelyveld, T.P., Mavrofidis, S.D., Kingman, S.W., Miles, N.J., 2002. Microwave heating applications in environmental engineering - a review. *Resources, Conservation and Recycling*, 34, 2, 75-90.

Kanga, S.H., Bonner, J.S., Page, C.A., Mills, M.A., Autenrieth, R.L., 1997. Solubilization of naphthalene and methyl-substituted naphthalene's from crude oil using biosurfactants. *Environmental Science and Technology*, 31, 556-561.

Kaslusky, S.F., Udell, K.S., 2002. A theoretical model of air and steam co-injection to prevent the downward migration of DNAPLs during steam enhanced extraction *Journal of Contaminant Hydrology*, 55, 213–223.

Kechavarzi C., Soga, K. Wiart, P., 2000. Multispectral image analysis method to determine dynamic fluid saturation distribution in two-dimensional three-fluid phase flow laboratory experiments. *Journal of Contaminant Hydrology*, 46, 265-293.

Kelly, S.J., 2002. Field-scale demonstration of a permeable reactive barrier treatment system: Nitrate as a terminal electron acceptor, PhD Dissertation, Royal Military College of Canada.

Khachikian, C., Harmon, T.C., 2000. Nonaqueous phase liquid dissolution in porous media: Current state of knowledge and research needs. *Transport in Porous Media*, 38, 1-2, 3-28.

Kile, D.E., Chiou, C.T., 1989. Water solubility enhancements of DDT and trichlorobenzene by some surfactants below and above the critical micelle concentration. *Environmental Science and Technology*, 23, 7, 832-838.

Kim, T.J., Chrysikopoulos, C.V., 1999. Mass transfer correlations for nonaqueous phase liquid pool dissolution in saturated porous media. *Water Resources Research*, 35, 2, 449-459.

Ko, S., Schlautman, M.A., Carraway, E.R., 1998. Partitioning of hydrophobic organic compounds to sorbed surfactants. 1. Experimental studies. *Environmental Science and Technology*, 32, 18, 2769–2775.

Kostarelos, K., Pope, G.A., Rouse, B.A., Shook, G.M., 1998. A new concept: The use of neutrally buoyant microemulsion for DNAPL remediation. *Journal of Contaminant Hydrology*, 34, 383-397.

Lake, L.W., 1989. *Enhanced Oil Recovery*. Prentice-Hall, Englewood Cliffs, NJ, 550 pp.

Lee, S.L., Zhai, X., Lee, J., 2007. INDOT Guidance Document for In-Situ Soil Flushing. Purdue University, FHWA/IN/JTRP-2006/28.

Lee, K.Y., Peters, C.A., 2004. UNIFAC modeling of cosolvent phase partitioning in nonaqueous phase liquid–water systems. *Journal of Environmental Engineering*, 130, 4, 478–483.

Lehr, J. H. (Ed.), 2004. *Wiley's Remediation Technologies Handbook : Major Contaminant Chemicals and Chemical Groups*, John Wiley & Sons, Incorporated, Hoboken, NJ, USA.

Lenhard, R.J., Johnson, T.G., Parker, J.C., 1993. Experimental observations of nonaqueous phase liquid subsurface movement. *Journal of Contaminant Hydrology*, 12, 79–101.

Lighty, J.S., Silcox, G.D., Pershing, D.W., Cundy, V.A., Linz, D.G., 1968. Fundamentals for the thermal remediation of contaminated soil, particle and bed desorption models. *Environmental Science and Technology*, 24(1), 750-757.

Liu, Q., Dong, M., Zhou, W., Ayub, M., Zhang, Y.P., Huang, S., 2004. Improved oil recovery by adsorption–desorption in chemical flooding. *Journal of Petroleum Science and Engineering*, 43, 1-2, 75-86.

Logan, B.E., 1999. *Environmental Transport Processes*, Wiley, New York.

Lowe, D.F., Oubre, C.L., Ward, C.H., 1999. *Surfactants and Cosolvents for NAPL Remediation: A Technology Practices Manual*, Lewis Publishers, Boca Raton.

Lunn, S.R.D., Kueper, B.H., 1996. Removal of DNAPL pools using upward gradient ethanol floods. In “Non-aqueous Phase Liquids (NAPLs) in the Subsurface Environment: Assessment and Remediation – Proceedings of the Specialty Conference”. ASCE National Convention, Washington, November 12-13, pp. 345-356.

Lunn, S.R.D., Kueper, B.H., 1999. Manipulation of density and viscosity for the optimization of DNAPL recovery by alcohol flooding. *Journal of Contaminant Hydrology*, 38, 427-445.

Lyman, W.J., Reehl, W.F., Rosenblatt, D.H., 1990. *Handbook of Chemical Property Estimation Methods*, McGraw-Hill Book Company, USA.

Mackay, D.M., Cherry, J.A., 1989. Groundwater contamination: pump-and-treat remediation. *Environmental Science and Technology*, 23, 16, 630–636.

Magnussen, T., Rasmussen, P., Fredenslund, A.A., 1981. UNIFAC parameter table for prediction of liquid-liquid equilibriums. *Industrial Engineering Chemistry: Process Design*, 20, 331.

Martel, R., Gelinias, P.J., Desnoyers, J.E., 1998. Aquifer washing by micellar solutions: 1. Optimization of alcohol-surfactant-solvent solutions. *Journal of Contaminant Hydrology*, 29, 319-346.

Martel, R., Hébert, A., Lefebvre, R., Gélinais, P., Gabriel, U., 2004. Displacement and sweep efficiencies in a DNAPL recovery test using micellar and polymer solutions injected in a five-spot pattern. *Journal of Contaminant Hydrology*, 75, 1-2, 1-29.

Mason, A., Kueper, B.H., 1996. Numerical simulation of surfactant-enhanced solubilization of pooled DNAPL. *Environmental Science and Technology*, 30, 11, 3205–3215.

McCray, J.E., 1998. *Enhanced Dissolution of Multiple-Component Nonaqueous Phase Organic Liquids in Porous Media Using Cyclodextrin: Theoretical, Laboratory, and Field Investigations*, Ph.D. Dissertation, The University of Arizona.

McCray, J.E., Boving, T., Brusseau, M.L., 2000. Cyclodextrin-enhanced solubilization of hydrophobic organic compounds with implications for aquifer remediation. *Ground Water Monitoring and Remediation*, 20, 1, 94–103.

Miller, C.T., Poirier-McNeill, M.M., Mayer, A.S., 1990. Dissolution of trapped nonaqueous phase liquids: mass transfer characteristics. *Water Resources Research*, 26, 11, 2783–2796.

Minogue, M., 2008. What connects regulatory governance to poverty?. *The Quarterly Review of Economics and Finance*, 48, 2, 189-201.

Montgomery, J.H., 1995. *Groundwater chemicals desk reference*, CRC Press, Boca Raton, USA.

Mulligan, C.N., Yong, R.N., Gibbs, B.F., 2001. Surfactant-enhanced remediation of contaminated soil: a review. *Engineering Geology*, 60, 371-380.

National Research Council, 1997. *Innovations in Ground Water and Soil Cleanup*. National Academy Press, Washington, DC.

National Research Council, 1999. *Groundwater and Soil Cleanup: Improving Management of Persistent Contaminants*, National Academies Press.

National Research Council, 2004. *Contaminants in the Subsurface: Source Zone Assessment and Remediation*, National Academies Press.

NATO/CCMS, 2003. *Evaluation of Demonstrated and Emerging Technologies for the Treatment and Clean up of Contaminated Land and Groundwater (Phase III): 2002 Annual Report (542-R-02-010)*. NATO/CCMS Pilot Study, USEPA.

Newell, C.J., Acree, S.D., Ross, R.R., Huling, S.G., 1995. *Light Nonaqueous Phase Liquids*, Ground Water Issue (540/S-95/500), Office of Research and Development, USA.

Nobre, M.M.M., Nobre, R.C.M., 2004. Soil vapor extraction of chlorinated solvents at an industrial site in Brazil. *Journal of Hazardous Materials*, 110, 1-3, 119-127.

Official Gazette, 1991. *Regulation for the Control of Solid Wastes*, Ankara.

Official Gazette, 1995. Regulation for the Control of Hazardous Waste, Ankara.

Palmer, C.D., Fish, W., 1992. Chemical Enhancements to Pump-and-Treat Remediation (540/S-92/001). U.S. Environmental Protection Agency, USA.

Palomino, A.M., Grubb, D.G., 2004. Recovery of dodecane, octane and toluene spills in sandpacks using ethanol. *Journal of Hazardous Materials*, 110, 39–51.

Pan, C., Dalla, E., Franzosi, D., Miller, C.T., 2007. Pore-scale simulation of entrapped non-aqueous phase liquid dissolution. *Advances in Water Resources*, 30, 3, 623–640.

Pankow, J.F., Cherry, J.A., 1996. Dense Chlorinated Solvents and other DNAPLs in Ground Water, Waterloo Press, Portland, Oregon.

Parker, S.P. (Ed.), 2003. Dictionary of Chemistry, McGraw-Hill Companies, Blacklick, OH, USA.

Pennell, K.D., Abriola, L.M., Weber, W.J., 1993. Surfactant-enhanced solubilization of residual dodecane in soil columns: 1. Experimental investigation. *Environmental Science and Technology*, 27, 2332–2340.

Pennell, K.D., Pope, G.A., Abriola, L.M., 1996. Influence of viscous and buoyancy forces on the mobilization of residual tetrachloroethylene during surfactant flushing. *Environmental Science and Technology*, 30, 4, 1328–1335.

Pennell, K.D., Adinolfi, A.M., Abriola, L.M., Diallo, M.S., 1997. Solubilization of dodecane, tetrachloroethylene, and 1,2-dichlorobenzene in micellar solutions of ethoxylated nonionic surfactants. *Environmental Science and Technology*, 31, 5, 1382–1389.

Perry, R.H., Green, D., 1984. Perry's Chemical Engineering Handbook, 6th. Edition, McGraw-Hill, USA.

Peters, C.A., Luthy, R.G., 1993. Coal tar dissolution in watermiscible solvents: Experimental evaluation. *Environmental Science and Technology*, 27, 13, 2831–2843.

Pope, G.A., Wade, W.H., 1995. Lessons from Enhanced Oil Recovery Research for Surfactant Aquifer Remediation. *Surfactant-Enhanced subsurface Remediation*, ACS Symposium Series, American Chemistry Society, Washington, DC.

Pope, G.A., 2003. *Surfactant Enhanced Aquifer Remediation*. Center for Petroleum and Geosystems Engineering, The University of Texas at Austin, USA.

Poppendieck, D.G., Loehr, R. C., Webster, M. T., 1999. Predicting hydrocarbon removal from thermally enhanced soil vapor extraction systems: 1. Laboratory studies. *Journal of Hazardous Materials*, 81-93.

Powers, S.E., Loureiro, C.O., Abriola, L.M., Weber Jr., W.J., 1991. Theoretical study of the significance of nonequilibrium dissolution of nonaqueous phase liquids in subsurface systems. *Water Resources Research*, 27, 4, 463–477.

Prak, D.J.L., Pritchard, P.H., 2002. Solubilization of polycyclic aromatic hydrocarbon mixtures in micellar nonionic surfactant solutions. *Water Resources*, 36, 3463–3472.

Ramsburg, C.A., Pennell, K.D., 2002. Density-modified displacement for dense nonaqueous-phase liquid source zone remediation: Density conversion using a partitioning alcohol. *Environmental Science and Technology*, 36, 9, 2082–2087.

Rahbeh, M. E., Mohtar, R. H., 2007. Application of multiphase transport models to field remediation by air sparging and soil vapor extraction. *Journal of Hazardous Materials*, 143, 1-2, 156-170.

Reddi, L.N., Nichols, J., Korfiatis, G.P., 1998. Bench-scale investigation on vibrorecovery of NAPL ganglia from sands. *Journal of Environmental Engineering*, 124, 9, 897-901.

Reid, V.W., Longman, G.F., Heinerth, E., 1967. Determination of anionic active detergents by two phase titration. *Tenside*, 4, 9, 292–304.

Reitsma, S., Kueper, B. H., 1998. Non-equilibrium alcohol flooding model for immiscible phase remediation: 1. Equation development. *Advances in Water Resources*, 21, 8, 649-662.

Ritter, K., Odziemkowski, M.S., Gillham, R.W., 2002. An in situ study of the role of surface films on granular iron in the permeable iron wall technology. *Journal of Contaminant Hydrology*, 55, 87-111.

Robert, T., Martel, R., Conrad, S.H., Lefebvre, R., Gabriel, U., 2006. Visualization of TCE recovery mechanisms using surfactant-polymer solutions in a two-dimensional heterogeneous sand model. *Journal of Contaminant Hydrology*, 86, 3-31.

Roeder, E., 1998. Phase density modifications for the remediation of DNAPLs by cosolvent flooding utilizing separate phase mobilization. Ph.D. Thesis, Clemson University, Clemson, USA.

Roeder, E., Falta, R.W., 2001. Modeling unstable alcohol flooding of DNAPL-contaminated columns. *Advances in Water Resources*, 24, 803-819.

Roeder, E., Falta, R.W., Lee, C.M., Coates, J.T., 2001. DNAPL to LNAPL transitions during horizontal cosolvent flooding. *GWMR*, Winter, 77-88.

Rosen, M.J., 1978. *Surfactants and Interracial Phenomena*, John Wiley and Sons, New York.

Roy, D., Kommalapati, R.R., Mandava, S.S., Valsarai, K.T., Constant, V.D., 1997. Soil washing potential of a natural surfactant. *Environmental Science and Technology*, 31, 670-675.

RTDF, 2005. The Basics: Understanding the behaviour of light nonaqueous phase liquids (LNAPLs) in the subsurface. www.rtdf.org/public/napl/.

Saba, T., Illangasekare, T.H., Ewing, J., 2001. Investigation of surfactant-enhanced dissolution of entrapped nonaqueous phase liquid chemicals in a two-dimensional groundwater flow field. *Journal of Contaminant Hydrology*, 51, 1-2, 63–82.

Sabatini, D.A., Knox, R.C., Tucker, E.E., Puls, R.W., 1997. Environmental Research Brief. Innovative Measures for Subsurface Chromium Remediation: Source Zone, Concentrated Plume, and Dilute Plume (600-S-97-005), National Risk Management Research Laboratory, Ada, OK 74820.

Sahloul, N.A., Ioannidis, M.A., Chatzis, I., 2002. Dissolution of residual non-aqueous phase liquids in porous media: Pore-scale mechanisms and mass transfer rates. *Advances in Water Resources*, 25, 1, 33–49.

Sawyer, C.S., Kamakoti, M., 1998. Optimal flow rates and well locations for soil vapour extraction design. *Journal of Contaminant Hydrology*, 32, 1, 63–76.

Schmidt, R., Gudbjerg, J., Sonnenborg, T.O., Jensen, K.H., 2002. Removal of NAPLs from the unsaturated zone using steam: Prevention of downward migration by injecting mixtures of steam and air. *Journal of Contaminant Hydrology*, 55, 233–260.

Schmoll, O., Howard, G., Chilton, J., Chorus, J., 2006. Protecting Groundwater for Health: Managing the Quality of Drinking Water Sources. World Health Organization, IWA Publishing.

Schroth, M.H., Istok, J.D., Ahearn, S.J., Sekler, J.S., 1995. Geometry and position of light nonaqueous-phase liquid lenses in water-wetted porous media. *Journal of Contaminant Hydrology*, 19, 269-287.

Schwille, F., 1988. Dense Chlorinated Solvents in Porous and Fractured Media: Model Experiments. Lewis Publishers, Boca Raton, Florida.

Seader, J.D., Henley, E.J., 1999. *Separation Process Principles*, John Wiley and Sons, New York.

Seagren, E.A., Rittmann, B.E., Valocchi, A.J., 2002. Bioenhancement of NAPL pool dissolution: experimental evaluation. *Journal of Contaminant Hydrology*, 55, 1-2, 57-85.

Setarge, B., Danzer, J.I., Klein, R., Grathwohl, P., 1999. Partitioning and interfacial tracers to characterize nonaqueous phase liquids (NAPLs) in natural aquifer material. *Physics and Chemistry of the Earth, Part B: Hydrology, Oceans and Atmosphere*, 24, 6, 501-510.

Shah, F.H., Hadim, H.D., Korfiatis, G.P., 1995. Laboratory studies of air stripping of VOC-contaminated soils. *Journal of Soil Contamination*, 4, 1, 93-109.

She, H.Y., Sleep, B.E., 1999. Removal of perchloroethylene from a layered soil system by steam flushing. *Ground Water Monitoring and Remediation*, 19, 70-77.

Shiau, B.J., Sabatini, D.A., Harwell, J.H., 2000. Chlorinated solvent removal using food grade surfactants: column studies. *Journal of Environmental Engineering*, 611-621.

Simunek, J., van Genuchten, M.T., Sejna, M., Toride, N., Leij, F.J., 1999. *The STANMOD Computer Software for Evaluating Solute Transport in Porous Media Using Analytical Solutions of Convection-Dispersion Equation, Versions 1.0 and 2.0*, U.S. Salinity Laboratory, USDA, ARS, Riverside, California.

Sleep, B.E., Ma, Y., 1997. Thermal variation of organic fluid properties and impact on thermal remediation feasibility. *Journal of Soil Contamination*, 6, 3, 281-306.

Staples, C.A., Geiselmann, S.J., 1998. Cosolvent influences on organic solute retardation factors. *Ground Water*, 26, 2, 192-198.

St-Pierre, C., Martel, R., Gabriel, U., Lefebvre, R., Robert, T., Hawari, J., 2004. TCE recovery mechanisms using micellar and alcohol solutions: phase diagrams and sand column experiments. *Journal of Contaminant Hydrology*, 71, 155-192.

Suchomel, E.J., 2006. Partial mass recovery from DNAPL source zones: Contaminant mass flux reductions and reductive dechlorination of residual DNAPL. PhD Dissertation, Georgia Institute of Technology, USA.

Szektli, J., 1998. Introduction and general overview of cyclodextrin chemistry. *Chemical Reviews*, 98, 1743-1753.

Theodoropoulou, M., Karoutsos, V., Tsakiroglou, C., 2001. Investigation of the contamination of fractured formations by non-Newtonian oil pollutants. *Environmental Forensics*, 2, 321-334.

Thibodeaux, L.J., 1995. *Environmental Chemodynamics*. John Wiley and Sons, Inc., USA.

Travis, C.C., Doty, C.B., 1990. Can contaminated aquifers at superfund sites be remediated?. *Environmental Science and Technology*, 24, 10, 1464–1466.

Tuck, D.M., Iversen, G.M., Prikle, W.A., 2003. Organic dye effects on dense nonaqueous phase liquids (DNAPL) entry pressure in water saturated porous media. *Water Resources Research*, 39, 8, 1207-1214.

UNEP, 2006. *Challenges to International Waters – Regional Assessments in a Global Perspective*, Nairobi, Kenya.

U.S. Army Corps of Engineers, 2006. *Design: In-situ Thermal Remediation*. USA Department of Defence Publications, USA.

U.S. Environmental Protection Agency, 2000. *Engineered Approaches to In Situ Bioremediation of Chlorinated Solvents: Fundamentals and Field Applications (542-R-00-008)*. Office of Solid Waste and Emergency Response, Technology Innovation Office, Washington, DC.

Van Dijke, M. I. J., Van Der Zee, S., 1997. A similarity solution for oil lens redistribution including capillary forces and oil entrapment. *Transport in Porous Media*, 29, 99-125.

Vayenas, D.V., Michalopoulou, E., Constantinides, G.N., 2002. Visualization experiments of biodegradation in porous media and calculation of the biodegradation rate. *Advances in Water Resources*, 25, 2, 203-219.

Verschueren, K. 1983. *Handbook of Environmental Data on Organic Chemicals*, Second Edition, Van Nostrand Reinhold.

Walker, R.C., Hofstee, C., Dane, J. H., Hill, W. E., 1998. Surfactant enhanced removal of PCE in a partially saturated, stratified porous medium. *Journal of Contaminant Hydrology*, 34, 31-46.

Wang, P., Dwarakanath, V., Rouse, B.A., Pope, G.A., Sepehmoori, K., 1998. Partition coefficients for alcohol tracers between nonaqueous-phase liquids and water from UNIFAC-solubility method. *Advances in Water Resources*, 21, 171–181.

Webster, G.R.B., Muldrew, D.H., Graham, J.J., Sarna, L.P., Muir, D.C.G., 1986. Dissolved organic matter mediated aquatic transport of chlorinated dioxins. *Chemosphere*, 15, 9, 1379–1386.

West, C. C., Harwell, J. H., 1992. Surfactants and subsurface remediation. *Environmental Science and Technology*, 26, 12, 2324–2330.

Winsor, P.A., 1968. Binary and multicomponent solutions of amphiphilic compounds. *Chemical Reviews*, 68, 1.

Zhao, B., Zhu, L., Yang, K., 2006. Reducing partitioning loss and enhancing solubilization by mixing sodium dodecylbenzene sulfonate with Triton X-100 in DNAPL/water systems. *Chemosphere*, 62, 772–779.

Zhou, M., Rhue, R.D., 2000. Screening commercial surfactants suitable for remediating DNAPL source zones by solubilization. *Environmental Science and Technology*, 34, 1985-1990.

Zarur, A.J., Mehenti, N.Z., Heibel, A.T., Ying, J.Y., 2000. Phase behaviour, structure and applications of reverse microemulsions stabilized by nonionic surfactants. *Langmuir*, 16, 9168-9176.

Zhong, L.R., Mayer, A.S., Pope, G.A., 2003. The effects of surfactant formulation on nonequilibrium NAPL solubilization. *Journal of Contaminant Hydrology*, 60, 1–2, 55–75.

Zimmerman, J.B., Kibbey, T.C.G., Cowell, M.A., Hayes, K.F., 1999. Partitioning of ethoxylated nonionic surfactants into non-aqueous organic liquids: Influence on solubilization behaviour. *Environmental Science and Technology*, 33, 169-176.

Internet References

- <http://ntp.niehs.nih.gov>, U.S. Department of Health and Human Services, National Toxicology Programme, 2007.
- http://esc.syrres.com/ABC/HSDB_pp.htm, Syracuse Research Corporation Web Site, HSDB Chemical and Physical Properties of Ethyl Benzene, 2008.
- <http://www.petrochemistry.net/>, APPE – Association of Petrochemicals Producers in Europe, 2008.
- <http://www.shellchemicals.com>, Shell Chemicals Web Site, 2008.
- <http://www.metrohm.co.uk>, Metrohm Company Web Site, 2006.
- <http://www.cheresources.com>, The Chemical Engineers' Resource Page, 2008.
- <http://www.geodelft.co.uk/LNAPL.htm>, GeoDelft, “Risk Management”, 2004.
- http://www.chemiway.co.jp/en/data/03_m19.html, Chemiway Maruzen Petrochemicals, Product Data Sheets, 2008.
- <http://www.karlyoder.com>, Molecular structure of 1,2-dichlorobenzene, 2007.
- <http://www.tennoji-h.oku.ed.jp>, Molecular structure of toluene, 2007.
- <http://www.kruss.de>, KRUSS GmbH Official Web Site, 2006.

APPENDIX A

FORTRAN COMPUTER PROGRAM FOR THE DETERMINATION OF THE TERNARY PHASE DIAGRAMS

```

c constructs ternary phase diagrams from UNIFAC output
c Feb 26, 2007
C with LiNEAR interpolation
c implicit double precision (a-h,o-z)
      parameter (N=3,ndata=11,ninta=101,nintn=101)
      common fff,xaw,gn(ndata,ndata),ga(ndata,ndata),gw(ndata,ndata)

c interpolated activity coefficient (NOT used in the minimization of F)

      Dimension xa(ninta),xn(nintn),
&   gamman(ninta,nintn),gammaa(ninta,nintn),gammaw(ninta,nintn)

c variables used in the BCPOL subroutine
      REAL FVALUE, X(N), XGUESS(N),XLB(N), XUB(N)

      EXTERNAL BCPOL, FCN
c      EXTERNAL DBCPOL, FCN

c variables used in the BCONF subroutine
c      DIMENSION XSCALE(N),IPARAM(N),RPARAM(N)
c      *****

c List of parameters
c      ndata: no mole fractions in the input file (from UNIFAC)
c      ninta: no of interpolated data- agent
c      nintn: no of interpolated data- napl
c      gn,ga,gw: activity coef. data from UNIFAC- input
c      gamman,gammaa,gammaw: interpolated activity coef. data
c      xa,xn: interpolated agent and napl mole fractions
c      three unknowns are: x(1)=xww, x(2)=xan, x(3)=xwn

c      DATA XSCALE/1.0,1.0,1.0/
c      *****

c read activity data
      open (3,file="input.dat",status="old")
      open(4,file="guess.dat",status="old")
      open (7,file="act1.out",status="unknown")
      open (8,file="act2.out",status="unknown")
      open (9,file="act3.out",status="unknown")
      open (15,file="ternary.out",status="unknown")

      read(3,*) dummy
      do 10 j=1,ndata
      read (3,*)dummy,(gn(i,j),i=1,ndata)
10  continue
      do 12 j=1,ndata
      read (3,*)dummy,(ga(i,j),i=1,ndata)
12  continue
      do 14 j=1,ndata
      read (3,*)dummy,(gw(i,j),i=1,ndata)
14  continue
c      *****
c interpolation

```

```

do 20 i=1,ninta
  do 25 j=1,nintn
    xa(i)=0.001*float(i-1)
    xn(j)=0.001*float(j-1)
    if(xa(i)+xn(j).gt.1.00001)goto 20
    do 30 ii=1,ndata
      if(xa(i).ge.0.1*float(ii-1).and.xa(i).lt.0.1*float(ii))then
        goto 31
      endif
    30 continue
    31 do 35 jj=1,ndata
      if(xn(j).ge.0.1*float(jj-1).and.xn(j).lt.0.1*float(jj))then
        goto 36
      endif
    35 continue
    36 if(gn(ii+1,jj+1).ge.0.)then
      c interpolate gamma napl
      a1=gn(ii,jj)+(gn(ii,jj+1)-gn(ii,jj))/0.1*(xn(j)-0.1*float(jj-1))
      a2=gn(ii+1,jj)+(gn(ii+1,jj+1)-gn(ii+1,jj))/0.1*
      & (xn(j)-0.1*float(jj-1))
      gamman(i,j)=a1+(a2-a1)/0.1*(xa(i)-0.1*float(ii-1))
      c interpolate gamma agent
      a1=ga(ii,jj)+(ga(ii,jj+1)-ga(ii,jj))/0.1*(xn(j)-0.1*float(jj-1))
      a2=ga(ii+1,jj)+(ga(ii+1,jj+1)-ga(ii+1,jj))/0.1*
      & (xn(j)-0.1*float(jj-1))
      gammaa(i,j)=a1+(a2-a1)/0.1*(xa(i)-0.1*float(ii-1))
      c interpolate gamma water
      a1=gw(ii,jj)+(gw(ii,jj+1)-gw(ii,jj))/0.1*(xn(j)-0.1*float(jj-1))
      a2=gw(ii+1,jj)+(gw(ii+1,jj+1)-gw(ii+1,jj))/0.1*
      & (xn(j)-0.1*float(jj-1))
      gammaw(i,j)=a1+(a2-a1)/0.1*(xa(i)-0.1*float(ii-1))
      else
      c interpolate gamma napl
      a1=gn(ii,jj)+(gn(ii,jj+1)-gn(ii,jj))/0.1*(xn(j)-0.1*float(jj-1))
      a2=gn(ii+1,jj)+(gn(ii,jj+1)-gn(ii+1,jj))/0.1*
      & (xn(j)-0.1*float(jj-1))
      gamman(i,j)=a1+(a2-a1)/(0.1-(xn(j)-0.1*float(jj-1)))*
      & (xa(i)-0.1*float(ii-1))
      c interpolate gamma agent
      a1=ga(ii,jj)+(ga(ii,jj+1)-ga(ii,jj))/0.1*(xn(j)-0.1*float(jj-1))
      a2=ga(ii+1,jj)+(ga(ii,jj+1)-ga(ii+1,jj))/0.1*
      & (xn(j)-0.1*float(jj-1))
      gammaa(i,j)=a1+(a2-a1)/(0.1-(xn(j)-0.1*float(jj-1)))*
      & (xa(i)-0.1*float(ii-1))
      c interpolate gamma water
      a1=gw(ii,jj)+(gw(ii,jj+1)-gw(ii,jj))/0.1*(xn(j)-0.1*float(jj-1))
      a2=gw(ii+1,jj)+(gw(ii,jj+1)-gw(ii+1,jj))/0.1*
      & (xn(j)-0.1*float(jj-1))
      gammaw(i,j)=a1+(a2-a1)/(0.1-(xn(j)-0.1*float(jj-1)))*
      & (xa(i)-0.1*float(ii-1))
    endif
  25 continue
20 continue

c write interpolated data
  do 100 j=1,101
    write(7,101)(gamman(i,j),i=1,101)
    write(8,101)(gammaa(i,j),i=1,101)
    write(9,101)(gammaw(i,j),i=1,101)
101 format(200f12.4)
100 continue
  write(*,*) 'interpolation complete'

c *****
c unknowns
c xnw

```

```

c      xnn
c      xww
c      xwn
c      xan
c      xaw

c  read initial guesses and upper/lower bounds
  read(4,*)npoint
    ncount=1
999  read(4,*)xaw,(xguess(i),i=1,N)
    read(4,*)(xub(i),i=1,N)
    read(4,*)(xlb(i),i=1,N)
    write(*,*) xaw
c  *****
c  minimization of F function
    IBYTE=0
    FTOL=1.0E-05
    MAXFCN=1000
c  IPARAM(1)=0
c  FSCALE=1.0
    CALL BCPOL(FCN,N,XGUESS,IBYTE,XLB,XUB,FTOL,MAXFCN,X,FVALUE)
c  CALL DBCPOL(FCN,N,XGUESS,IBYTE,XLB,XUB,FTOL,MAXFCN,X,FVALUE)

c  CALL DU4INF(IPARAM,RPARAM)
c  CALL DBCONF(FCN,N,XGUESS,IBYTE,XLB,XUB,XSCALE,FSCALE,IPARAM,
c  & RPARAM,X,FVALUE)
    xww=x(1)
    xan=x(2)
    xwn=x(3)
    xnw=1.-xaw-xww
    xnn=1.-xan-xwn
    if(ncount.eq.1)
&write(15,*)' xnw, xaw, xww, xnn,
& xan, xwn f
    write(15,102) xnw,xaw,xww,xnn,xan,xwn,fff
102  format(7f12.6)
    if(ncount.lt.npoint) then
      ncount=ncount+1
      goto 999
    endif
  stop
  END

  SUBROUTINE FCN(N,X,F)
c  implicit double precision (a-h,o-z)
  parameter (ndata=11)
  common fff,xaw,gn(ndata,ndata),ga(ndata,ndata),gw(ndata,ndata)
  INTEGER N
  REAL X(N),F
  xww=x(1)
  xan=x(2)
  xwn=x(3)
  xnw=1.-xaw-xww
  xnn=1.-xan-xwn
c  compute activity coef. for the aqueous phase from xaw and xnw using interpolation
  do 30 ii=1,ndata
    if(xaw.ge.0.1*float(ii-1).and.xaw.lt.0.1*float(ii))then
      goto 31
    endif
30  continue
31  do 35 jj=1,ndata
    if(xnw.ge.0.1*float(jj-1).and.xnw.lt.0.1*float(jj))then
      goto 36
    endif
35  continue
36  write(*,*)xaw,xnw,ii,jj

```

```

    if(gn(ii+1,jj+1).ge.0.)then
c   interpolate gamma napl
    a1=gn(ii,jj)+(gn(ii,jj+1)-gn(ii,jj))/0.1*(xnw-0.1*float(jj-1))
    a2=gn(ii+1,jj)+(gn(ii+1,jj+1)-gn(ii+1,jj))/0.1*
&   (xnw-0.1*float(jj-1))
        gnw=a1+(a2-a1)/0.1*(xaw-0.1*float(ii-1))
c   interpolate gamma agent
    a1=ga(ii,jj)+(ga(ii,jj+1)-ga(ii,jj))/0.1*(xnw-0.1*float(jj-1))
    a2=ga(ii+1,jj)+(ga(ii+1,jj+1)-ga(ii+1,jj))/0.1*
&   (xnw-0.1*float(jj-1))
        gaw=a1+(a2-a1)/0.1*(xaw-0.1*float(ii-1))
c   interpolate gamma water
    a1=gw(ii,jj)+(gw(ii,jj+1)-gw(ii,jj))/0.1*(xnw-0.1*float(jj-1))
    a2=gw(ii+1,jj)+(gw(ii+1,jj+1)-gw(ii+1,jj))/0.1*
&   (xnw-0.1*float(jj-1))
        gww=a1+(a2-a1)/0.1*(xaw-0.1*float(ii-1))
    else
c   interpolate gamma napl
    a1=gn(ii,jj)+(gn(ii,jj+1)-gn(ii,jj))/0.1*(xnw-0.1*float(jj-1))
    a2=gn(ii+1,jj)+(gn(ii,jj+1)-gn(ii+1,jj))/0.1*
&   (xnw-0.1*float(jj-1))
        gnw=a1+(a2-a1)/(0.1-(xnw-0.1*float(jj-1)))*(xaw-0.1*float(ii-1))
c   interpolate gamma agent
    a1=ga(ii,jj)+(ga(ii,jj+1)-ga(ii,jj))/0.1*(xnw-0.1*float(jj-1))
    a2=ga(ii+1,jj)+(ga(ii,jj+1)-ga(ii+1,jj))/0.1*
&   (xnw-0.1*float(jj-1))
        gaw=a1+(a2-a1)/(0.1-(xnw-0.1*float(jj-1)))*(xaw-0.1*float(ii-1))
c   interpolate gamma water
    a1=gw(ii,jj)+(gw(ii,jj+1)-gw(ii,jj))/0.1*(xnw-0.1*float(jj-1))
    a2=gw(ii+1,jj)+(gw(ii,jj+1)-gw(ii+1,jj))/0.1*
&   (xnw-0.1*float(jj-1))
        gww=a1+(a2-a1)/(0.1-(xnw-0.1*float(jj-1)))*(xaw-0.1*float(ii-1))
    endif

c   compute activity coef. for the napl phase from xan and xnn using interpolation
    do 40 ii=1,ndata
        if(xan.ge.0.1*float(ii-1).and.xan.lt.0.1*float(ii))then
            goto 41
        endif
40    continue
41    do 45 jj=1,ndata
        if(xnn.ge.0.1*float(jj-1).and.xnn.lt.0.1*float(jj))then
            goto 46
        endif
45    continue
46    if(gn(ii+1,jj+1).ge.0.)then
c   interpolate gamma napl
    a1=gn(ii,jj)+(gn(ii,jj+1)-gn(ii,jj))/0.1*(xnn-0.1*float(jj-1))
    a2=gn(ii+1,jj)+(gn(ii+1,jj+1)-gn(ii+1,jj))/0.1*
&   (xnn-0.1*float(jj-1))
        gnn=a1+(a2-a1)/0.1*(xan-0.1*float(ii-1))
c   interpolate gamma agent
    a1=ga(ii,jj)+(ga(ii,jj+1)-ga(ii,jj))/0.1*(xnn-0.1*float(jj-1))
    a2=ga(ii+1,jj)+(ga(ii+1,jj+1)-ga(ii+1,jj))/0.1*
&   (xnn-0.1*float(jj-1))
        gan=a1+(a2-a1)/0.1*(xan-0.1*float(ii-1))
c   interpolate gamma water
    a1=gw(ii,jj)+(gw(ii,jj+1)-gw(ii,jj))/0.1*(xnn-0.1*float(jj-1))
    a2=gw(ii+1,jj)+(gw(ii+1,jj+1)-gw(ii+1,jj))/0.1*
&   (xnn-0.1*float(jj-1))
        gwn=a1+(a2-a1)/0.1*(xan-0.1*float(ii-1))
    else
c   interpolate gamma napl
    a1=gn(ii,jj)+(gn(ii,jj+1)-gn(ii,jj))/0.1*(xnn-0.1*float(jj-1))
    a2=gn(ii+1,jj)+(gn(ii,jj+1)-gn(ii+1,jj))/0.1*

```



```


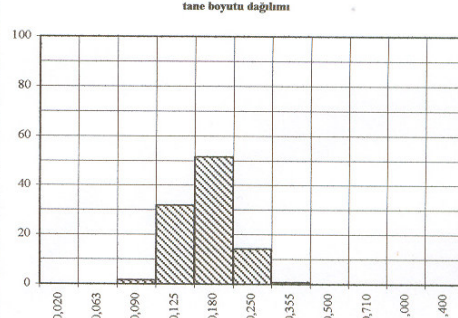
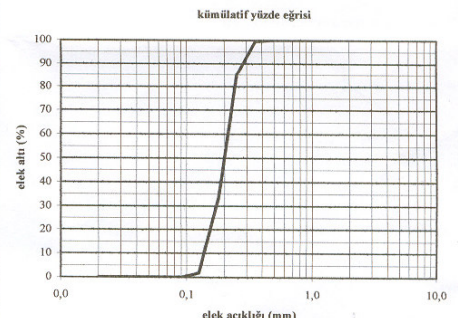

& (xnn-0.1*float(jj-1))
    gnn=a1+(a2-a1)/(0.1-(xnn-0.1*float(jj-1)))*(xan-0.1*float(ii-1))
c  interpolate gamma agent
a1=ga(ii,jj)+(ga(ii,jj+1)-ga(ii,jj))/0.1*(xnn-0.1*float(jj-1))
a2=ga(ii+1,jj)+(ga(ii,jj+1)-ga(ii+1,jj))/0.1*
& (xnn-0.1*float(jj-1))
    gan=a1+(a2-a1)/(0.1-(xnn-0.1*float(jj-1)))*(xan-0.1*float(ii-1))
c  interpolate gamma water
a1=gw(ii,jj)+(gw(ii,jj+1)-gw(ii,jj))/0.1*(xnn-0.1*float(jj-1))
a2=gw(ii+1,jj)+(gw(ii,jj+1)-gw(ii+1,jj))/0.1*
& (xnn-0.1*float(jj-1))
    gwn=a1+(a2-a1)/(0.1-(xnn-0.1*float(jj-1)))*(xan-0.1*float(ii-1))
endif

c  compute minimization function
F=abs(gaw*xaw-gan*xan)+abs(gww*xww-gwn*xwn)+abs(gnw*xnw-gnn*xnn)
fff=f
open (8,file="iterat.dat",status="unknown")
write(8,1)f,xnw,xaw,xww,gnw,gaw,gww,xnn,xan,xwn,gnn,gan,gwn
1  format (13e14.6)
    RETURN
    END

```

APPENDIX B

SILTAS SAND 60/70 USED IN THE COLUMN EXPERIMENTS

 SILTAS KUMLARI SAN. ve TIC. A.Ş.		Döküm Kumu Numune Kalite Kontrol Raporu				Ürün Adı	60/70 AFS
						Rapor No	KKG 02
						Üretim/Parti No	KKG06A6
						Müşteri	BOĞAZIÇI ÜNİVERSİTESİ
						Yasata Plaka No	
Mrk.Tel: (216) 335 70 08-09 - Faks: 335 71 57 Fabl.Tel: (216) 732 85 72 - Faks: 732 85 88 Fab2.Tel: (216) 731 35 98-99 - Faks: 731 35 88						Fabrika Çıkış Tarihi	05.07.2006
Sıra No	Muayene ve Deneyler	İlgili Standartlar					
1	Elek Analizi	TS 5426 / 5425					
	elek göz açıklığı (mm)	elek üstü a (gr)	elek üstü b (%)	elek altı c (%)	elek üstü küm	elek altı küm.	
			0,00	0,00	0,00	100,00	
	1,400	0,000	0,00	0,00	0,00	100,00	
	1,000	0,000	0,00	0,00	0,00	100,00	
	0,710	0,000	0,00	0,00	0,00	100,00	
	0,500	0,000	0,00	0,66	0,00	100,00	
	0,355	0,330	0,66	14,13	0,66	99,34	
	0,250	7,060	14,13	51,62	14,79	85,21	
	0,180	25,790	51,62	31,93	66,41	33,59	
	0,125	15,950	31,93	1,58	98,34	1,66	
	0,090	0,790	1,58	0,08	99,92	0,08	
	0,063	0,040	0,08	0,00	100,00	0,00	
	0,020	0,000	0,00	0,00	100,00	0,00	
	Toplam	49,96	100,00	100,00			
Tane Boyutu		Sonuçlar					
AFS		65,42					
Mikron		203,95					
2	Teorik Özgül Yüze (cm ² /g)	115,97					
3	Dağılım Katsayısı (S ₀ =Q ₁ /Q ₃)	1,41					
	Q ₁ (mm)	0,24					
	Q ₃ (mm)	0,17					
4	Ortalama Tane Büyükl. (Mk-M50)	0,20	50				
	2/3 Mk	0,14	5				
	4/3 Mk	0,27	89				
	Homojenlik Derecesi %	84					
 tane boyutu dağılımı							
 kümülatif yüzde eğrisi							
Sıra No	Muayene ve Deneyler	İlgili Standartlar	Sınır değerler	Sonuçlar		Numune İçindir.	
5	Gözle Muayene	TS 5426		1.Num	2.Num		
6	Bileşim	TS 2979					
	SiO ₂ %			98,6			
	Fe ₂ O ₃ %			0,23			
	CaO + MgO %			0,02+0,00			
	Na ₂ O + KO %			0,07+0,11			
	Al ₂ O ₃ %			0,54			
7	Kızdırma Kaybı %	TS 2980		0,25			
8	Sinterleşme Sıcaklığı °C	TS 5426		>1500		Müşteri Şartname No:	
9	Kil %	TS 5426				Yayın Tarihi:	
10	Rutubet %	TS 3084					
Deneyi Yapan			Onay				
K.K.Teknisyeni	İmza	Tarih	Saat	K.G.Müdürü	İmza	Tarih	
R.YÖRÜK		05/07/06	16:40	T YILDIZ		05/07/06	